Dissertation
submitted to the
Combined Faculties for the Natural Sciences and for Mathematics
of the Ruperto-Carola University of Heidelberg, Germany

for the degree of

Doctor of Natural Sciences

presented by

MSc. Sibgha Tahir

Born in Toba Tek Singh, Pakistan
Oral examination: 23.01.2018

CD40L-dependent von Willebrand factor-platelet string formation in the mouse microcirculation *in vivo*

Referees: Prof. Dr. Markus Hecker
Prof. Dr. Peter Angel

Dedication

To my loving parents and husband

Table of contents

List of Figures

List of Tables

List of Abbreviations

A disintegrin and metalloproteinase with a thrombospondin type 1 motif, member 13	ADAMTS13
ADAMTS13 knockout	ADAMTS13ko
Carboxy fluorescein diacetate	CFDA
Cluster of differentiation	CD
CD40 ligand	CD40L
Charge coupled device	CCD
Endothelial cell(s)	EC(s)
Interferon	IFN
Interleukin-1	IL-1
Intraperitoneal	IP
Intravenous	i.v
Kilo Dalton	kDa
MegaCD40ligand	MegaCD40L
Nitric oxide	NO
Platelet derived growth factor	PDGF
Prostacyclin	PGI_2
P-selectin glycoprotein ligand-1	PSGL-1
Quantum dot	Qdot
Reactive oxygen species	ROS
Smooth muscle cell(s)	SMC(s)
Standard error of the mean	SEM
Stromal cell-derived factor-1	SDF-1
Thrombozyten (thrombocyte) buffer	Tz-buffer
Thrombotic thrombocytopenic purpura	TTP
Transforming growth factor-β	TGF-β
Tumor necrosis factor-α	TNF-α
Tumor necrosis factor receptor	TNFR
Ultra-large von Willebrand factor	ULVWF

Vascular endothelial growth factor	VEGF
Von Willebrand factor	vWF
Weibel-Palade bodies	WPBs
Zinc fixative buffer	Zn-fixative buffer

1. Summary

Both physiological and pathophysiological vascular remodeling processes involve the crosstalk between vascular and immune cells. CD40 ligation on endothelial cells (EC) *in vitro* promotes the release and deposition of ultra-large von Willebrand factor (ULVWF) multimers on their surface. Platelets rapidly adhere, turn P-selectin positive and recruit circulating leukocytes, allowing their attachment to and subsequent diapedesis through the EC monolayer. ULVWF multimers are cleaved by the zinc metalloproteinase ADAMTS13. However, it is not yet known whether CD40-CD40L interactions play a role in microvessels *in vivo*. In particular, it is not known whether the shear stress dependency observed *in vitro* leads to ULVWF multimer-platelet string formation predominantly in arterioles being exposed to higher shear stress than venules, and whether these strings are formed in the presence of ADAMTS13.

We hypothesized that CD40L serves as potent stimulator of endothelial cell von Willebrand factor (vWF) release in the microcirculation *in vivo* which leads to formation of ULVWF multimers providing active binding sites for surveilling platelets and, secondarily, circulating leukocytes (see graphical summary Figure 1). To test this hypothesis, multiphoton-based live cell imaging in cremaster vessels of the mouse was used to study ULVWF multimer-platelet string formation and leukocyte-EC interaction *in vivo*. Carboxy fluorescein diacetate (CFDA) stained platelets were injected into the circulation of both wild type and ADAMTS13 knockout mice. Leukocytes were labeled using PE-conjugated anti-mouse CD45 antibody. Then ULVWF multimer-platelet string formation together with interaction of leukocytes was observed in the microvasculature of these animals before and after CD40L stimulation. The distribution of CD40 and vWF in the vasculature was observed by using Qdot-525 labeled anti-CD40 and Qdot-565 labeled anti-vWF antibodies, respectively.

Herein, it is reported that CD40L is a potent stimulator of vWF-dependent platelet string formation in the murine microcirculation *in vivo*. ULVWF multimer-platelet strings form

both in arterioles (mean diameter = 53 µm) and venules (mean diameter = 60 µm) after CD40L treatment *in vivo* but are clearly more prevalent in venules in spite of the lower shear stress there. However, in the presence of ADAMTS13 their number is kept rather low. The deficiency of ADAMTS13 enhances ULVWF multimer-platelet string formation following CD40L stimulation. Leukocyte extravasation is much more prominent in venules and boosted in the absence of ADAMTS13, namely following CD40L stimulation. Therefore, low ADAMTS13 plasma levels as observed in patients with coronary heart disease may contribute to the pro-thrombotic and pro-inflammatory state of the vessel wall. ULVWF multimers are preferentially observed in venules where they co-localize with both platelets and the endothelial cell CD40 receptor. Based on these observations, we propose that pro-inflammatory leukocyte extravasation preferentially takes place at sites of vWF-induced platelet adherence, a process which is elicited by platelet-CD40L stimulation of endothelial cells.

Graphical Summary

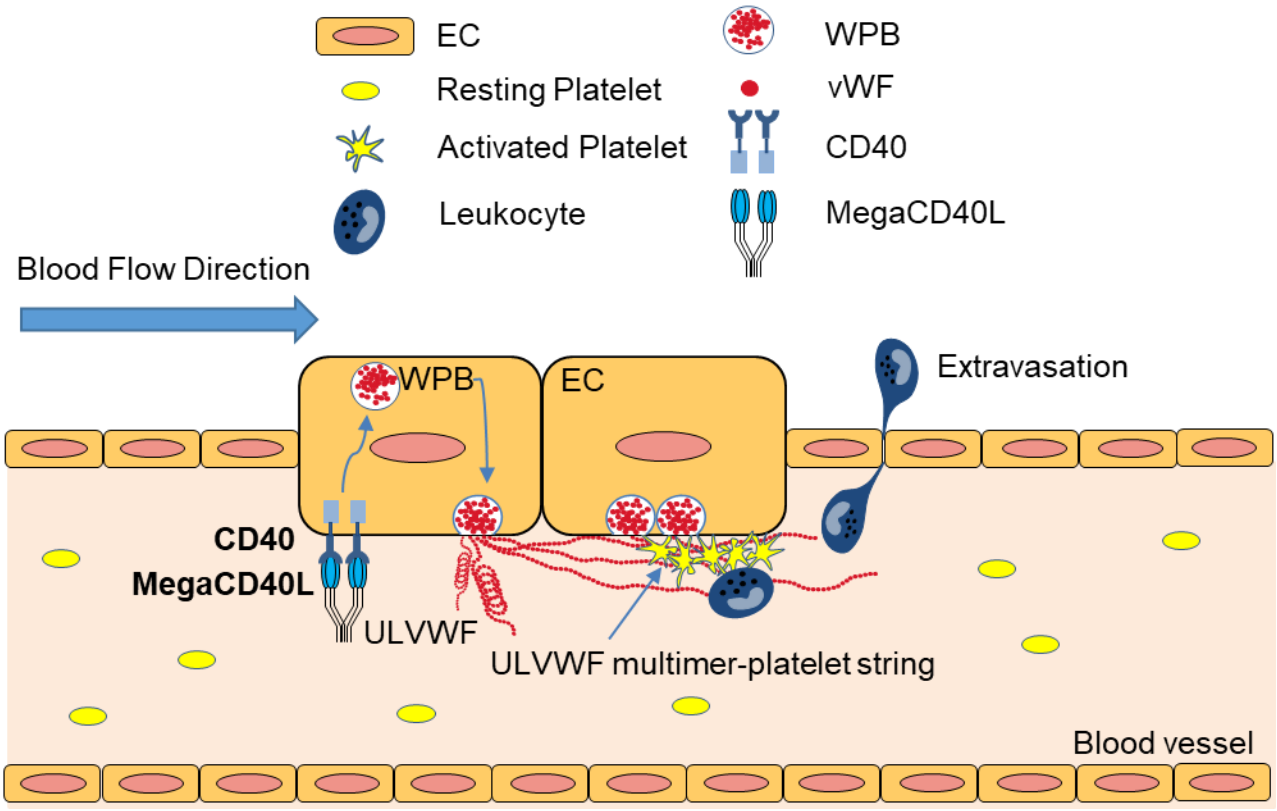

Figure 1: Graphical representation of CD40-CD40L mediated interactions. *CD40 ligation on ECs induces the release of vWF from Weibel-Palade body (WPB) stores that in turn leads to ULVWF multimer-platelet string formation on the luminal EC surface followed by leukocyte recruitment and their subsequent extravasation through the EC monolayer.*

Zusammenfassung

Sowohl physiologische als auch pathophysiologische vaskuläre Umbauprozesse beinhalten Interaktionen zwischen Gefäß- und Immunzellen. Die Bindung des CD40-Liganden (CD40L) an den CD40-Rezeptor auf Endothelzellen (EZ) *in vitro* fördert die Freisetzung und Ablagerung von ultralangen von Willebrand-Faktor (ULVWF) Multimeren auf ihrer luminalen Oberfläche. Blutplättchen haften hieran an, werden P-Selektin-positiv, rekrutieren zirkulierende Leukozyten und ermöglichen so deren Anhaftung an und die anschließende Diapedese durch die einschichtigen Endothelzellen. ULVWF-Multimere werden durch die Zinkmetalloproteinase ADAMTS13 gespalten. Bislang ist jedoch noch nicht bekannt, ob derartige CD40-CD40L-Interaktionen in Mikrogefäßen *in vivo* eine Rolle spielen. Insbesondere ist unbekannt, ob die *in vitro* beobachtete Schubspannungsabhängigkeit zu einer ULVWF Multimer-Blutplättchen-Komplexbildung vorwiegend in Arteriolen führt, da diese einer höheren Schubspannung ausgesetzt sind als Venolen, und ob diese Komplexbildung in Gegenwart von ADAMTS13 überhaupt stattfindet.

Der vorliegenden Doktorarbeit liegt die Hypothese zugrunde, dass CD40L als potenter Stimulus der vWF-Freisetzung in der Mikrozirkulation *in vivo* dient, was zur Bildung von ULVWF-Multimeren führt, die aktive Bindungsstellen für patrolierende Blutplättchen und sekundär zirkulierende Leukozyten darstellen. Um diese Hypothese zu testen, wurde eine Multiphoton-basierte Live-Zell-Bildgebung in Blutgefäßen des *M. cremaster* der Maus verwendet, um die ULVWF-Multimer/Blutplättchen-Komplexbildung bzw. die Leukozyten-EZ-Interaktion *in vivo* zu untersuchen. Carboxyfluoresceindiacetat (CFDA)-gefärbte Blutplättchen wurden in die Zirkulation von Wildtyp- und ADAMTS13-Knockout-Mäusen injiziert. Leukozyten wurden durch Verwendung von PE-konjugiertem anti-Maus-CD45-Antikörper markiert. Dann wurden in den Mikrogefäßen dieser Tiere vor und nach CD40L-Stimulation die Bildung von Plättchen-dekorierten vWF-Fäden zusammen mit der Wechselwirkung von Leukozyten beobachtet. Die Verteilung von CD40 und vWF im Gefäßsystem wurde durch den Einsatz von Qdot-525-markierten Anti-CD40 und Qdot-565-markierten Anti-vWF-Antikörpern untersucht.

Die vorliegende Doktorarbeit zeigt, dass CD40L ein starker Stimulus für die ULVWF-Multimer/Blutplättchen-Komplex- bzw. Fadenbildung in der Mikrozirkulation der Maus *in vivo* ist. ULVWF-Multimer/Blutplättchen-Fäden bilden sich *in vivo* nach CD40L-Zugabe sowohl in Arteriolen (mittlerer Durchmesser 53 µm) als auch in Venolen (mittlerer Durchmesser 60 µm), sind aber in Venolen weiter verbreitet, trotz der dort nachweislich niedrigeren Schubspannung. In Gegenwart von ADAMTS13 ist die Anzahl der nachweisbaren Fäden niedrig. In Abwesenheit von ADAMTS13 ist die ULVWF-Multimer/Blutplättchen-Fadenbildung nach CD40L-Stimulation deutlich gesteigert. Die Leukozyten-Extravasation ist in den Venolen deutlich erhöht und nimmt in Abwesenheit von ADAMTS13 nochmals zu, besonders nach CD40L-Stimulation. Daher können niedrige ADAMTS13-Plasmaspiegel, wie sie bei Patienten mit koronarer Herzkrankheit nachweisbar sind, zu dem prothrombotischen und proentzündlichen Zustand der Gefäßwand beitragen. ULVWF-Multimere konnten bevorzugt in Venen nachgewiesen werden, wo sie mit Blutplättchen-dekorierten Fäden und endothelialen CD40-Rezeptoren kolokalisieren. Basierend auf diesen Beobachtungen wird postuliert, dass die proinflammatorische Leukozyten-Extravasation bevorzugt an Stellen der vWF-induzierten Plättchen-Adhäsion stattfindet, die durch die Blutplättchen-CD40L-vermittelte Stimulation von Endothelzellen hervorgerufen wird.

2. Introduction

2.1 Vascular remodeling

The term vascular remodeling refers to the changes in blood vessel geometry that are occur in response to long term variations in blood hemodynamics or as a result of vascular injury caused by trauma and underlying cardiovascular risk factors. The kind and extent of vascular remodeling does not only depend on the type of stimuli but also on the location of blood vessels, e.g. the type of remodeling taking place in small resistance vessels is different from the one occurring in large conduit arteries (Mulvany 2002). Although the variations in hemodynamic forces are the principal cause of vascular remodeling in the majority of physiologic and pathologic conditions (Langille 1996), many pathophysiologic stimuli such as oxidative stress (Montezano and Touyz 2014), inflammation and apoptosis (Walsh et al. 2000) are major causes of vascular remodeling through inducing endothelial dysfunction. The mechanisms underlying these pathophysiologic processes are complex and involve a variety of cell types, chemokines and changes in extracellular matrix but their primary feature is the abnormal growth or proliferation of smooth muscle cells (SMCs) that might be caused by 1) increased endothelial permeability, 2) release of growth factors from platelets and/or monocytes, and 3) release of growth factors from endothelial cells (ECs) or SMCs themselves (Dzau et al. 2002; Owens 1989).

The blood vessels are mainly composed of ECs, SMCs and fibroblasts that interact with one another in an autocrine-paracrine fashion (Gibbons and Dzau 1994). Although all cells can participate in vascular remodeling, but the vascular endothelium due to its prime location in the blood vessel lumen plays an essential role in maintaining vascular function and homeostasis (Quyyumi 1998). The vascular endothelium not only serves as sensor for detecting humoral signals but also works as effector for eliciting biological responses leading to changes in structure (and function) of blood vessels.

The underlying process of vascular remodeling involves the complex and highly regulated events of:

a) Detection of hemodynamic changes/vessel injury by the cell sensors.
b) Transduction of signals within cells and between neighboring cells.
c) Synthesis and release of vasoactive substances that influence cell growth, proliferation, apoptosis, migration and changes to the extracellular matrix.
d) The resultant change in vessel geometry in response to cellular or non-cellular components.

Under normal physiological conditions, the endothelium is responsible for the maintenance of vascular tone and homeostasis through the release of vasodilators (e.g. nitric oxide (NO) and prostacyclin) and vasoconstrictors (e.g. thromboxane A_2, endothelin and free radicals). NO aids in vasodilation, downregulates pro-inflammatory and cell adhesion molecules, and inhibits proliferation and migration of SMCs hence contributing to maintaining vascular tone (Tousoulis et al. 2012; Drexler and Hornig 1999). While the endothelium-derived contractile factors increase intracellular calcium levels in SMCs, reactive oxygen species (ROS) and activation of cyclooxygenase-1 or 2 cause endothelium-dependent contractions that can be observed in numerous animal models of diabetes, hypertension and aging (Feletou et al. 2011). Endothelial dysfunction has been recognized as the doorstep to major cardiovascular events such as thrombus formation, atherosclerosis, myocardial infarction, stroke and peripheral artery disease (Cai and Harrison 2000; Eyries et al. 2004; Roquer et al. 2009). Cardiovascular risk factors play a major role in endothelial dysfunction causing oxidative stress that in turn leads to inactivation or degradation of NO. Thus activated, ECs produce large amounts of reactive oxygen species (ROS) that upregulate the transcription of pro-inflammatory and pro-thrombotic genes, chemokines and adhesion molecules resulting in microvascular dysfunction and enhanced leukocyte infiltration (Cai et al. 2003). The vascular remodeling which is initiated as an adaptive response (e.g. in arteriogenesis) may eventually become maladaptive (e.g. in atherosclerosis) and leads to impaired vascular functions.

2.2 Role of platelets in vascular remodeling

Platelets, also called thrombocytes, are anuclear disc-shaped cell fragments (2-4 µm) that are generated from bone marrow megakaryocytes by a process called thrombopoiesis and released into the circulation (Junt et al. 2007). Regardless of being anuclear, platelets are active moieties due to the presence of cell organelles (endoplasmic reticulum, mitochondria, Golgi apparatus), and are still able to synthesize proteins from mRNA. Under normal physiologic conditions, there are around 750 billion quiescent platelets circulating in human blood and patrolling for any endothelial damage in the vasculature. Upon encountering such an injury platelets become activated and come in to play their main role of maintaining a vascular barrier by attaching to the subendothelial matrix, namely collagen, aggregating and closing the wound by serving as a hemostatic plug to prevent bleeding (Ho-Tin-Noe et al. 2011).

Platelets contain alpha granules, dense granules and lysosomes. The alpha granules are large vesicles (200-400 nm) that store adhesion and repairing factors like von Willebrand factor (vWF), multimerin and factor V which are important for both platelet-platelet interactions and platelet-blood cells interactions. The dense granules are small platelet granules (150 nm) with non-protein constituents that are pro-aggregating factors like nucleotides (ADP, ATP), biogenic amines and bivalent cations. Lysosomes contain clearing factors with bactericidal activity (Rendu and Brohard-Bohn 2001; Hayward et al. 1995). Upon activation, the release of ADP, fibrinogen, fibronectin, serotonin and vWF from platelet granules, but namely synthesis and release of thromboxane A_2 leads to reversible and irreversible platelet aggregation, respectively. The platelet aggregate grows by associating with other platelets through fibrinogen binding to glycoprotein IIb/IIIa receptors. It is tethered to the subendothelial matrix through glycoprotein Ib-vWF and glycoprotein VI-collagen interactions.

Platelets are best known for their vital role in hemostasis but in addition they are equally important in vascular remodeling by linking hemostasis to inflammation (von Bruhl et al. 2012; Zarbock et al. 2007; Van Hinsbergh and Tasev 2015). Platelets have numerous cell surface receptors and adhesion molecules which on engaging activate intracellular signaling pathways resulting in the release of chemokines and cytokines that play a key

role in inflammation (Lam et al. 2015). Amongst them, CXCL4 (also called PF4) and CXCL7 (also called NAP-2) are the most abundant chemokines derived from platelets (Karshovska et al. 2013). Besides these, platelets express and release several other chemokines like CCL3, CCL5, CCL7, CXCL5, CXCL1, CXCL12 and MIF (Karshovska et al. 2013).

Vascular inflammation is a key process during remodeling of macrovascular (e.g. atherosclerosis, (Hansson et al. 2006))and microvascular (e.g. arteriogenesis (Liu et al. 2014) arterial blood vessels in the as well as in diabetes or as a consequence of arterial hypertension (Savoia and Schiffrin 2007; Schiffrin 2015), regardless of whether it constitutes an adaptive or maladaptive change, that is accompanied by platelet activation and amplified by their interaction with ECs and leukocytes (Fuentes et al. 2013). Platelets are not only involved in modulating inflammatory and immune responses but they are also considered equally important in thrombus formation upon plaque rupture and atherosclerosis progression (Lievens and von Hundelshausen 2011; Gawaz et al. 2005). Inflammation is a complex process that can be either protective or pathologic and its investigation may lead to identification of new therapeutic targets for controlling cardiovascular diseases.

Platelets also play a role in protecting developing vessels in the microcirculation and the lymphatics at sites of inflammation. Recently, the role of platelets in arteriogenesis has regained attention (Kahn 2015). Arteriogenesis refers to an increase in diameter of existing collateral arterioles in response to a blockade in the main feeding artery for which the collaterals serve as natural bypasses maintaining normal blood flow at least at rest (Deindl and Schaper 2005). Thus, platelet GPIbα has been found to facilitate platelet-EC interactions via integrin receptors that enable the recruitment of innate immune cells under conditions of high shear stress hence promoting arteriogenesis (Chandraratne et al. 2015). By secreting several of the aforementioned chemokines, cytokines and growth factor, namely Platelet derived growth factor (PDGF), platelets support remodeling of the collateral arterioles to small arteries.

In the hypoxic tissue, arteriogenesis mostly goes hand in hand with angiogenesis. Angiogenesis involves the sprouting of new blood vessels (Ribatti and Crivellato 2012).

Platelets can also produce pro-angiogenic mediators and assist in tissue repair and regeneration. There are extensive studies on the involvement of the hemostatic system in angiogenesis (Kisucka et al. 2006; Feng et al. 2011) where the presence of platelets has been found to stimulate angiogenesis followed by vessel maturation through releasing, e.g. transforming growth factor-β (TGF-β), PDGF, vascular endothelial growth factor (VEGF) and stromal cell-derived factor-1 (SDF-1). In addition, this has been attributed on the one hand to the deficiency of an antiangiogenic factor in platelets called thrombospondin-1, which regulates the balance between proangiogenic and antiangiogenic factors during neovascularization (Feng et al. 2011). On the other hand, thromboxane A_2 produced by activated platelets has been found to restore blood flow through thromboxane prostanoid receptor in a hind limb ischemia model by aiding in releasing platelet proangiogenic factors, thereby promoting angiogenesis and arteriogenesis (Amano et al. 2015).

Atherosclerosis, a chronic inflammation of large to medium-sized arteries at the typical predilection sites (branches, curvatures), is composed of asymmetric focal thickenings constituting lipid droplets, debris and immune cells (Hansson et al. 2006). It is characterized by the recruitment of platelets, monocytes and neutrophils to these developing lesions which is followed by infiltration of various subsets of T-cells as well as dendritic cells (Weber et al. 2008). Arterial bifurcations and curvatures serve as predilection sites for atherosclerosis due to blood flow disturbances causing endothelial dysfunction and subsequent leukocyte recruitment and infiltration of the vessel wall (Galkina and Ley 2009). In this context, platelets play a major role in the initiation of this process by interacting with the ECs through platelet GPIbα (which interacts with vWF and P-selectin) and GPIIb-IIIα (also called integrin $\alpha_{IIb}\beta_3$, which interacts with fibrinogen and vWF) that is followed by leukocyte recruitment (Massberg et al. 2002). Thrombin activated platelets secrete RANTES (also called CCL5) which is deposited on EC surface that triggers monocyte arrest hence spurring inflammation, neointima and ultimately plaque formation in the arterial vessel wall (von Hundelshausen et al. 2001). In addition, increased platelet CX3CR1 expression has been suggested to augment platelet-monocyte interaction through CX3CL1-CX3CR1 mediated platelet activation at sites of atherosclerosis (Postea et al. 2012). In this milieu, neutrophils release their

nuclear contents called neutrophil extracellular traps (NETs), composed of DNA and granule proteins containing neutrophil elastase, thereby exacerbating atherosclerotic lesion formation (Megens et al. 2012). However, the interaction between these immune cells still needs further investigation as it is ambiguous how they, especially monocytes, transmigrate through the EC barrier at atherosclerosis-prone sites.

2.3 Role of leukocytes in vascular inflammation and remodeling

Leukocyte infiltration has been found to be one of the hallmark events of vascular inflammation (Ley 1996). During vascular inflammation, platelets tend to adhere to the endothelium and serve as recruitment site for circulating pro-inflammatory leukocytes, such as neutrophils and monocytes, even at high shear stress of 20 and 40 dyn/cm^2 (Bernardo et al. 2005). Circulating leukocytes through their P-selectin glycoprotein ligand-1 (PSGL-1) interact with P-selectin on activated platelets (McEver 2001) which leads to ERK1/2MAPK-dependent conformational change in leukocyte integrins, hence promoting extravasation of leukocytes into the perivascular tissue (Zuchtriegel et al. 2016). In addition, platelets are also capable of forming platelet-leukocyte complexes in the circulation which have a high affinity for ECs and may thus expedite extravasation (Gawaz et al. 2005).

In the pathophysiologic condition of atherosclerosis, the monocytes soon after extravasation into the subintimal space acquire the properties of resident macrophages, by expressing scavenger receptors, take up preferentially oxidized LDL cholesterol particles and convert into foam cells. In addition, SMCs switch from a contractile to synthetic phenotype and generate significant amount of foam cells (Chaabane et al. 2014). These foam cells then form a fatty streak which is a hallmark of developing atherosclerotic lesions (Libby 2002; Libby and Aikawa 2002).

2.4 VWF contribution to vascular remodeling

2.4.1 Distribution of vWF

VWF, the largest multimeric glycoprotein present in plasma, is encoded by a gene on chromosome 12pter-p12 with a length of 180 kb and comprising 52 exons (McKusick

and Amberger 1993). It is mainly synthesized by ECs (Jaffe et al. 1974) where it is stored in specialized vesicles called Weibel-Palade bodies (WPBs) (Warhol and Sweet 1984). In addition, it is also synthesized in platelet precursors called megakaryocytes and stored in platelets' α-granules together with P-selectin (Kupinski and Miller 1985). In the vasculature, vWF can be found in three different pools namely (i) soluble plasma vWF (secreted from ECs and platelets upon activation), where ECs are the major source of plasma vWF, (ii) basement membrane vWF (deposited in the extracellular matrix) and (iii) cellular vWF (stored in ECs and platelet α-granules).

2.4.2 Structure of vWF

VWF circulates through the vasculature in multimeric form with the smallest dimer of 500 kDa that can multimerize through disulfide bonds up to an ultra-large molecule of 20,000 kDa (Wagner 1990). VWF comprises a multidomain structure that is essential for its regulatory function (Figure 2). The important domains of vWF and their respective binding partners are:

1) D'D3 - binding to clotting factor VIII
2) A1 - binding to platelet GPIbα
3) A2 - binding of ADAMTS13
4) A3 - binding to type I and III collagen
5) C1 - binding to platelet GPIIb-IIIα
6) C terminal CK domain - dimerizes vWF

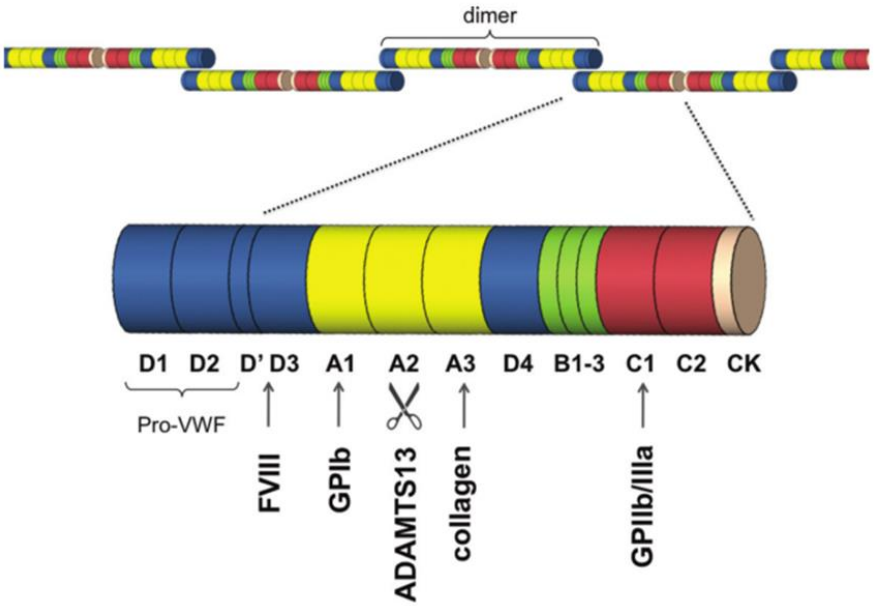

Figure 2: Schematic representation of dimeric vWF domains. *The important domains of vWF with their respective binding and cleavage sites are shown (De Meyer et al. 2012).*

2.4.3 VWF in vascular hemostasis and remodeling

VWF plays an important role in maintaining vascular hemostasis in two ways. Firstly, plasma vWF serves as a carrier molecule for clotting factor VIII in the blood thus enhancing its half-life by protecting it against proteolysis (Zimmerman et al. 1983). Secondly, it acts as a cross linker molecule that initiates the first interaction between non-activated circulating platelets and damaged endothelium during vascular injury (Federici 2003). Circulating vWF is present in a globular conformation where its A2 domain interacts with the A1 domain causing its blockade and unavailability of vWF for both GPIbα and proteolytic cleavage by ADAMTS13 (a disintegrin and metalloproteinase with a thrombospondin type 1 motif, member 13). Similarly, the secreted vWF also adopts the globular conformation which later on tends to form ultra-large vWF (ULVWF) multimers anchored to the luminal EC surface (Mourik et al. 2013). Upon vascular damage, endothelial vWF is released which binds to the exposed collagen via its A3 domain and the high shear rate in the vessel promotes

conformational changes that cause dissociation of the A1-A2 complex resulting in unfolding of the A1binding domain for platelet GPIbα. The A1 domain is exposed prior to the A2 domain, ensuring that vWF initiates/contributes to hemostasis before it is inactivated by ADAMTS13 (Aponte-Santamaria et al. 2015). The A1- GPIbα interaction allows the initial rolling and arrest of non-activated platelets on the endothelium followed by their firm adhesion on collagen via GPVI-$\alpha_2\beta_1$ integrin leading to platelet activation. Later on, vWF facilitates the aggregation of activated platelets at the injured site like fibrinogen by crosslinking neighboring platelets through their GPIIb-IIIα integrin receptors (Figure 3) (De Marco et al. 1986).

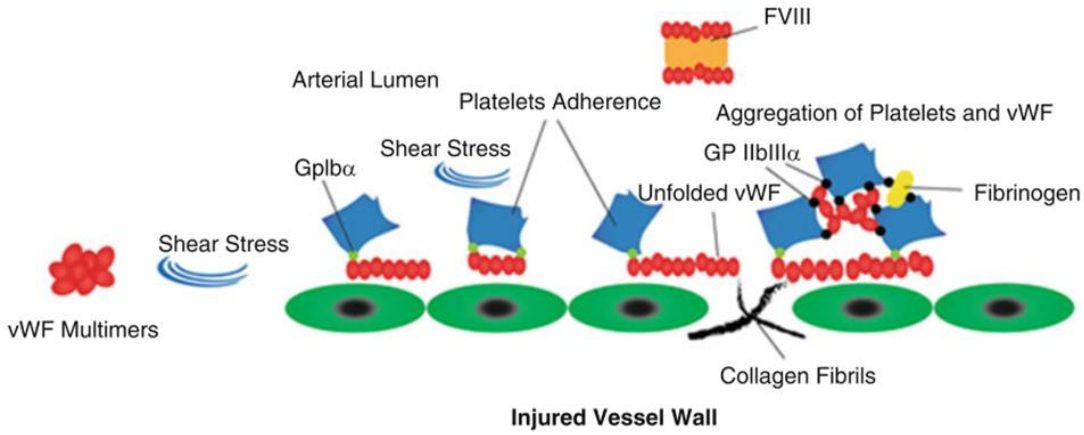

Figure 3: Schematic diagram showing functions of vWF. *VWF serves as a carrier of clotting factor VIII as well as a cross linker molecule between platelets (GPIbα) and the damaged endothelium (collagen in the subendothelial matrix) during vascular injury (Shahidi 2017).*

2.4.4 Regulation of vWF by ADAMTS13

The amount (and length) of the ULVWF multimers deposited on the EC surface is regulated by ADAMTS13 that cleaves the potentially hyperactive ULVWF multimers into inactive monomers thus preventing thrombosis and replenishing plasma vWF (Dong et al. 2003). Initially, ADAMTS13 was found to be synthesized in hepatic stellate cells (Zhou et al. 2005) but later on it was found to be synthesized and constitutively released by ECs (Turner et al. 2006; Tati et al. 2011).

The various domains of ADAMTS13 starting from the N-terminus are (Figure 4):

1) Ca^{+2} and Zn^{+2} dependent metalloprotease (MP)
2) Disintegrin like domain (Dis)
3) Thrombospondin-1 repeat (1)
4) Cysteine rich domain (Cys)
5) Spacer domain
6) Seven tandem repeats
7) Two CUB domains (CUB1 and CUB2)

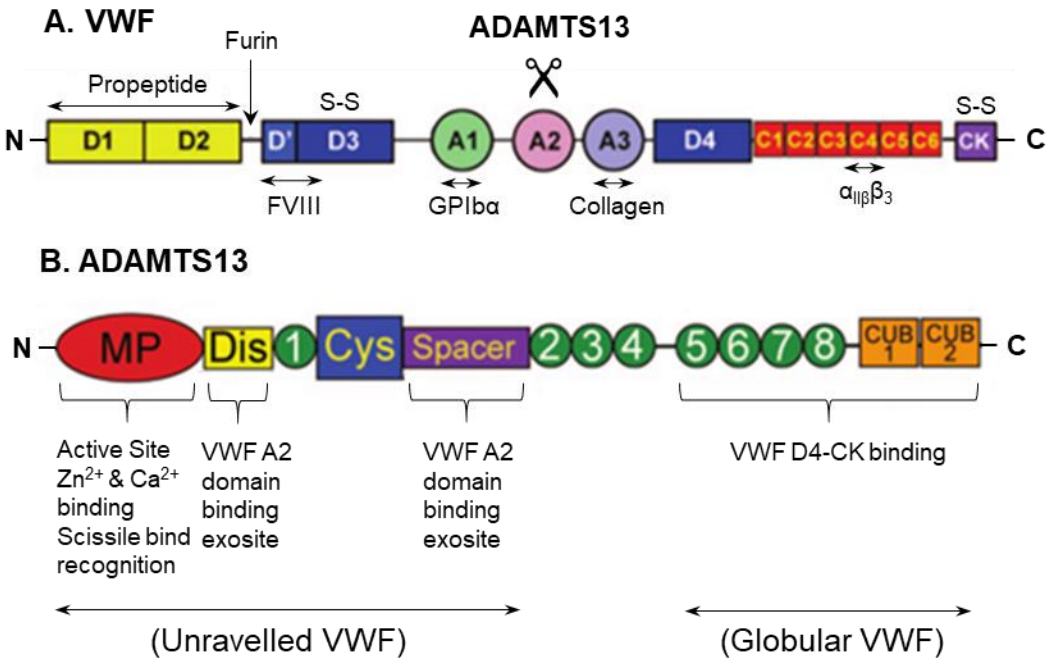

Figure 4: Inter-domain interactions between vWF and ADAMTS13. *Different domains of ADAMTS13* ***(B)*** *showing their association with respective vWF* ***(A)*** *domains during their globular and stretched states (Crawley and Scully 2013).*

ADAMTS13 carries out the cleavage of platelet-decorated ULVWF multimer strings *in vivo* (De Maeyer et al. 2010) and the cleavage is done at the Tyr1605-Met1606 bond in the A2 domain (Figure 5).

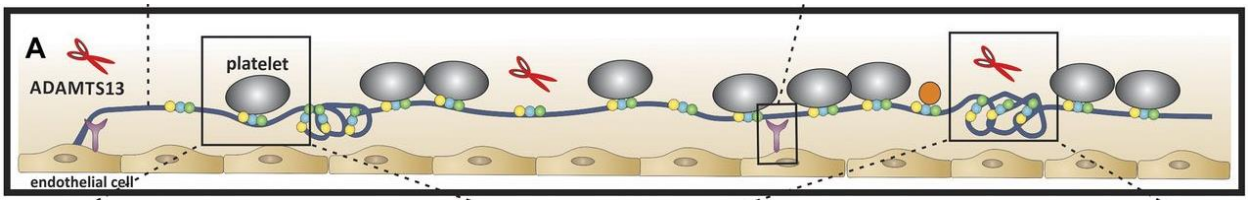

Figure 5: Model showing proteolytic activity of ADAMTS13. *Regulation of platelet-decorated ULVWF multimer strings on the EC surface by the proteolytic activity of ADAMTS13 that converts it into smaller fragments (De Ceunynck et al. 2013).*

Since long time, it was believed that ADAMTS13 is constitutively active in plasma and that the globular conformation of vWF hides the cleavage site preventing it from degradation. Recently, it has been shown that ADAMTS13 is conformationally activated by vWF via their various domains interactions. The spacer domain of ADAMTS13 is covered by its CUB1 domain, thus limiting the proteolytic activity of its catalytic site comprising the MP, Dis, 1, Cys and S domains. The initial low affinity interaction of vWF with ADAMTS13 via the D4-CK domains engages the TSP8-CUB2 domains, hence disrupting the CUB1-spacer domain interaction leading to ADAMTS13 activation (South et al. 2017).

Platelet vWF differs from plasma vWF in terms of forming higher molecular weight multimers and reduced N-linked sialylation that impart resistance against ADAMTS13 proteolysis, hence enabling platelet plug formation at sites of vascular injury (McGrath et al. 2013). In addition to ADAMTS13, activated leukocyte proteases (elastase, proteinase 3, cathepsin G, and matrix metalloproteinase 9) have been found to cleave synthetic vWF at or near the A2 domain of vWF (ADAMTS13 cleavage site), implicating a possible role of activated leukocytes in vWF regulation (Raife et al. 2009; Lancellotti et al. 2013; Tati et al. 2017).

An imbalance between ADAMTS13 activity and EC vWF release causes the formation of ULVWF multimers on the EC surface which in turn induces platelet adhesion and aggregation. Previously, low levels of ADAMTS13 were only associated with the thromboembolic complications of thrombotic thrombocytopenic purpura (TTP) (Zheng et al. 2001) but later studies have related both low levels of ADAMTS13 and high levels of

vWF to the occurrence of cardiovascular events (Bongers et al. 2009) including hypertension, thrombotic microangiopathies, arterial thrombosis, ischemic stroke, myocardial infarction and heart failure (Akyol et al. 2016; Dhanesha et al. 2016).

VWF plays a very important role in communication between circulating leukocytes and endothelium via adhered platelets and promotes leukocyte extravasation (Petri et al. 2010). Leukocytes are preferentially recruited to and extravasate in postcapillary venules (Bruce et al. 2014) which raises the question whether this is due to an exclusive release of vWF in venules and capillaries or whether there are any predilection sites for vWF release like, e.g. bifurcations. There is also limited information whether in the microcirculation *in vivo* the regions with visible ULVWF multimer-platelet strings have any influence on leukocyte extravasation and whether this is enhanced in the absence of ADAMTS13.

VWF also plays a vital role in vascular remodeling, both in arteriogenesis and angiogenesis, by facilitating leukocyte infiltration and blood flow recovery during post ischemic neovascularization (de Vries et al. 2017). Recently, ADAMTS13 and vWF have been found to play an antagonistic role in post ischemic vascular remodeling where the administration of recombinant ADAMTS13 in mice after stroke has been found to improve vascular repair and neovascularization (Xu et al. 2017).

2.4.5 Shear stress dependency of ULVWF multimer-platelet string formation

Following vascular injury platelets are capable of adhering to subendothelial vWF even under conditions of high shear stress. Fluid shear stress regulates ULVWF multimer-platelet strings in three distinct ways. Firstly, it facilitates the multimerization of vWF into ULVWF multimers deposited on the EC surface. Secondly, it enables the unfolding of ULVWF multimers thus exposing their binding domain A1 for platelet adhesion resulting in formation of ULVWF multimer-platelet strings. Thirdly, shear stress regulates the force dependent cleavage of ULVWF multimers by stretching the concatamers thereby exposing the cleavage domain A2 to ADAMTS13 (Kragh et al. 2014; Shim et al. 2008). It is still elusive though whether shear stress does play any role in vWF release and ULVWF multimer-platelet string formation *in vivo.* In the vasculature, shear stress varies

from arteries, arterioles, capillaries, venules and veins depending upon their morphology and physical dimensions. If shear stress helps in unwinding ULVWF multimers, it is also not known whether there are any difference in arterioles and venules in terms of the number of ULVWF multimer-platelet strings. *In vitro*, cleavage of ULVWF multimers on the EC surface has been reported at both arterial (20-50 dyn/cm^2) and venous (2.5 dyn/cm^2) levels of shear stress (Dong et al. 2002). If that was the case *in vivo*, too, it would raise the question which difference or not it will make on ULVWF multimer-platelet string formation in the absence of ADAMTS13.

2.5 Role of CD40-CD40L interactions in vascular remodeling

Among many pathways for initiating platelet-EC-leukocyte interactions, one important co-stimulation is CD40-CD40L interaction.

2.5.1 Distribution

CD40L (also called CD154 or gp39), a member of the tumor necrosis factor (TNF) family, is a 33 kDa type II transmembrane glycoprotein initially recognized as a cell surface trimer on T-cells (Foy et al. 1996). The initial studies suggested its molecular weight to be 39 kDa, hence named gp39, but most cell types have a 32-33 kDa cell surface protein. CD40L is predominantly expressed on activated CD4-positive T cells (Roy et al. 1993) and on platelets (Henn et al. 1998) while in a lesser amount on activated CD8-positive T cells, natural killer (NK) cells, monocytes, macrophages, basophils, mast cells (Gauchat et al. 1993) and activated eosinophils (Gauchat et al. 1995). In addition CD40L is also expressed on non-immune cells like ECs and SMCs (Mach et al. 1997).

CD40L is pre-formed in platelets and translocated to the surface upon activation. Extracellular proteases can cleave CD40L from the membrane of activated platelets yielding a functional polypeptide which is termed soluble CD40L (Choi et al. 2010). Elevated levels of soluble CD40L have been found in the plasma of patients suffering from cardiovascular disease(s) that predominantly involve platelets (Tousoulis et al. 2010; Varo et al. 2003).

CD40, a member of the tumor necrosis factor receptor (TNFR) superfamily, is a 48 kDa type I transmembrane protein initially recognized and characterized as a receptor on B-lymphocytes. It plays an important role both in humoral and cell-mediated immune responses (Vogel and Noelle 1998). CD40 is expressed not only on immune cells like B-lymphocytes, dendritic cells, follicular dendritic cells, granulocytes, monocytes, macrophages and platelets (Henn et al. 2001) but also on non-hematopoietic cells like ECs, epithelial cells, vascular SMCs, fibroblasts and neuronal cells (Hollenbaugh et al. 1995; Tan et al. 2002).

CD40 and CD40L due to their presence in soluble forms are also able to act in a paracrine and endocrine fashion. The abundance of CD40 on the vascular EC surface has been found to be heterogeneous in mice where it is expressed preferentially in capillaries, venules and veins but not in arteries or arterioles except in atherosclerotic animals where it is upregulated at the prototypic atherosclerosis predilection sites (Korff et al. 2007).

2.5.2 Mechanism of action in vascular remodeling

In the initiation and progression phase of vascular remodeling processes there exists a link between hemostasis and innate immunity but the underlying intercellular crosstalk still remains elusive. CD40L on platelets is highly regulated for initiating immune response despite constitutive CD40 co-expression on platelets. While ECs also strongly control the amount and functionality of CD40 present on their surface (Korff et al. 2007; Wagner et al. 2011), CD40 ligation triggers the downstream activation of TRAF6 followed by inositol-1,4,5 trisphosphate-mediated calcium mobilization. It has been shown by our group previously that this way CD40 ligation stimulates the release of vWF from the WPBs *in vitro* and causes its deposition as ULVWF multimers on the EC surface in the presence of flow (Moller et al. 2015). Platelets promptly adhere to these ULVWF multimers, translocate P-selectin on their surface and recruit circulating monocytes, hence facilitating their attachment to and successive diapedesis through the EC monolayer even under conditions of intermediate to high shear stress (Figure 6). In addition, CD40L stimulation of ECs evokes expression of the ligand itself on their surface (Wagner et al. 2004), (Danese et al. 2004). The interaction of CD40L on

platelets with CD40 on neighboring platelets in a thrombus leads to the cleavage of membrane bound CD40L, releasing the 18 kDa soluble form of CD40L that is capable of inducing only a weak pro-inflammatory reaction by ECs, hence regulating the overall pro-inflammatory response (Henn et al. 2001). Platelet CD40 has been shown to play a crucial role in the progression of pathophysiologic macrovascular remodeling by activation of ECs and leukocytes, thus resulting in leukocyte infiltration at atherosclerosis predilection sites (Gerdes et al. 2016). Patients with elevated levels of CD40L are at a higher risk of developing cardiovascular diseases according to clinical data (Garlichs et al. 2001). However, it is still not clear whether CD40L is a potent stimulus for vWF release in the microcirculation as well. Investigating CD40-CD40L interaction, the respective crosstalk between endothelial and immune cells, and the signaling pathways leading to their adherence, transmigration and differentiation, will enable us to better address the physiologic and pathophysiologic conditions of microvascular remodeling.

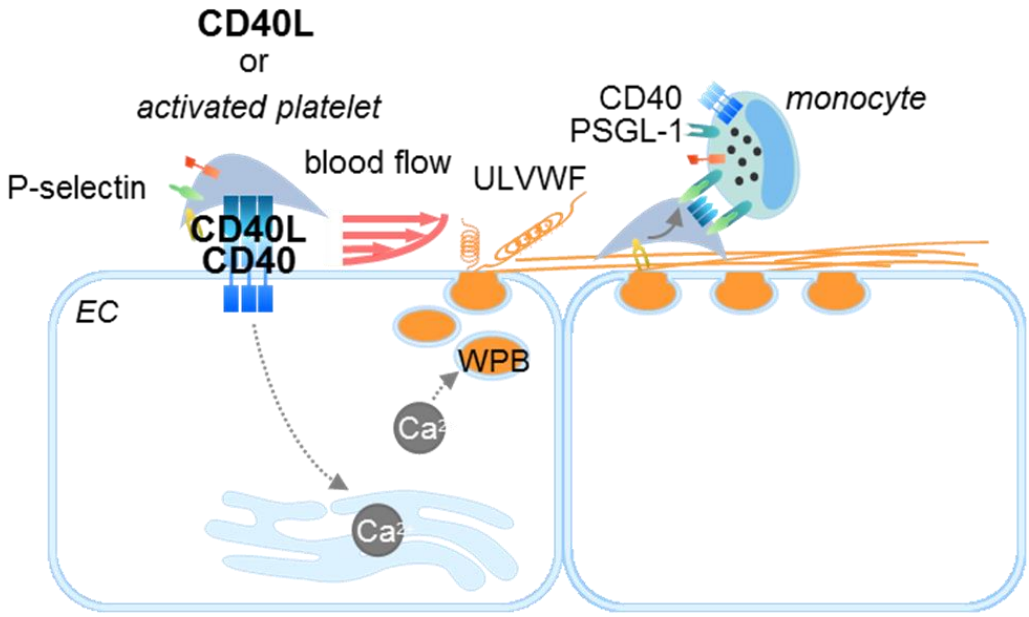

Figure 6: Workflow of ULVWF multimer-platelet mediated leukocyte recruitment to the vessel wall. *sCD40L or platelet CD40L binding to CD40 receptor on the EC surface induces the Ca^{2+}-dependent release of vWF which forms ULVWF multimers on the EC surface enabling binding and activation of platelets that in turn recruit circulating monocytes and enforce their adhesion via P-selectin-PSGL-1 interaction. Modified from (Moller et al. 2015).*

2.6 Purpose and investigated problem

Cardiovascular disease is the leading cause of death worldwide, accounting for 31 % of all global deaths according to the 2016 WHO report. ULVWF multimer-platelet mediated leukocyte extravasation is one of the hallmarks of vascular inflammation which serves as a doorstep to cardiovascular events. While we found previously that the CD40 pathway is important for vWF release *in vitro,* it is not yet known whether CD40-CD40L interactions play a role in thrombus formation and/or leukocyte diapedesis in microvessels *in vivo.* In addition, it is also not known whether the shear stress dependency observed *in vitro* preferentially leads to ULVWF multimer-platelet string formation in arterioles *in vivo* and whether these strings form at all in the presence of ADAMTS13.

The aims of the present study were to analyze in the microcirculation *in vivo:*

1. The role and effect of CD40L as a stimulus for vWF release and subsequent ULVWF multimer-platelet string formation.
2. The potential modulatory role of shear stress for vWF exposure and platelet adhesion.
3. The control of ULVWF multimer-platelet string formation by ADAMTS13.
4. The role of such strings in leukocyte extravasation.

Investigation of these new questions in the intact microcirculation is expected to advance our understanding about cellular dynamics in the initial steps of microvascular vascular remodeling and will potentially enable development of diagnostic and early therapy approaches for prevention and treatment of cardiovascular diseases.

3. Materials

3.1 Chemicals and reagents

Table 1: List of chemicals and reagents used

Chemical/reagent	Catalog No.	Supplier
5-Carboxy fluorescein diacetate (CFDA)	C1354	ThermoFisher Scientific
MegaCD40 ligand	ALX-522-110-C010	Enzo
Prostaglandin I_2.Na (Prostacyclin)	sc-201231	Santa Cruz Biotechnology
Isoflurane (Forene)	Ch-B:6044172	abbvie
Na-citrate	MEG 256001	Megro GmbH
Heparin-Natrium-25000-ratiopharm injektionslösung (5x5ml)	PZN3029843	Ratiopharm GmbH
Saline solution 0.9 % NaCl (10 ml)	B306175/01	Fresenius Kabi

3.2 Kits

Table 2: List of kits used

Kit Name	Catalog No.	Supplier
Alexa Fluor® 488 Antibody Labeling Kit	A20181	ThermoFisher Scientific

SiteClick™ Qdot® 525 Antibody Labeling Kit	S10449	ThermoFisher Scientific
SiteClick™ Qdot® 565 Antibody Labeling Kit	S10450	ThermoFisher Scientific

3.3 Antibodies

Table 3: Antibodies used in this study

Antibody	**Catalog No.**	**Supplier**
Alexa Fluor® 488 anti-mouse CD40 Antibody	102910	Biolegend
Alexa Fluor® 647 anti-mouse CD31 Antibody	102516	Biolegend
PE anti-mouse CD154 Antibody	106505	Biolegend
PE anti-mouse CD41 Antibody	133906	Biolegend
Alexa Fluor® 647 rat anti-mouse CD31Antibody	563608	BD Biosciences
PE anti-Mouse CD45 Antibody	12-0451-83	eBioscience
Von Willebrand Factor, Polyclonal, Unconjugated, Ig fraction.	A008202-2	Dako
CD40 Monoclonal Antibody	MA1-80627	ThermoFisher Scientific
Alexa Fluor 488 chicken anti-rat IgG	A-21470	ThermoFisher Scientific

Secondary Antibody		
Alexa Fluor 546 goat anti-rabbit IgG Secondary Antibody	A11010	ThermoFisher Scientific
FITC rat monoclonal anti-mouse CD40 Antibody	Ab22470	abcam

3.4 Consumables

Table 4: List of materials used in this study

Material	**Catalog No.**	**Supplier**
µ-Slide I 0.4 Luer ibiTreat: Flow chambers	80176	ibidi
Cover slips 18×18 mm, thickness 1	235503104	Wagner & munz
Confocal-UV-matrix	CONFO30	Micro Tech Lab
Glass slides (Menzel-Gläser Superfrost Plus)	4951PLUS4	ThermoScientific
Quick dry top coat	-	Essence
Silicone adhesive (hochviskos)	-	GE Bayer Silicones
Adhesive surgical tape	3M ID DH888843181	Durapore™
Fine Bore Polythene Tubing 0.288 mm ID, 0.61 mm OD	REF 800/100/100 LOT 243137	Smiths medical
Eye ointment Bepanthen (5 g)	81552983	BAYER

Surgical threads Metric 0.5 Metric 1	10A051000 10C103000	Pearsalls Limited
Surgical gloves (Latex free, powder free)	-	SEMPERCARE® nitrileskin[2]

3.5 Buffers

Table 5: List of buffers used

Buffers	**Purpose**	**Composition**	**Amount**
Thrombocyte buffer (Tz-buffer) (500 ml)	Platelet isolation	138 mM NaCl 2.7 mM KCl 12 mM $NaHCO_3$ 0.4 mM NaH_2PO_4 1 mM $MgCl_2 \times 6H_2O$ 5 mM D-Glucose 5 mM Hepes	4.03 g 0.1 g 0.5 g 0.03 g 0.1 g 0.45 g 0.6 g
The Tz-buffer was adjusted to a pH of 7.35 and was filtered under sterile conditions. Stored at 4 ^{o}C. Upon every use it was supplemented with 500 ng/ml of prostacyclin (PGI_2) (1 mg/ml stock, 1:2000).			
Zinc fixative buffer (1000 ml)	Tissue fixation	<u>0.1 M Tris (pH 7.4)</u> Tris Distilled water	 12.1 g 1000 ml

		Zinc-fixative 0.1M Tris buffer Calcium acetate Zinc acetate Zinc chloride	 1000 ml 0.5 g 5 g 5 g
Do not adjust the pH value further, it will cause zinc failure. The buffer was stored at room temperature.			

3.6 Anesthetics, analgesics and antidotes

Table 6: Various anesthetics, analgesics and antidotes used in this study

Category	**Dosage**	**Volume**
Anesthesia Ketamine Xylazine NaCl	 100 mg/kg 10 mg/kg 0.9 %	(For 1 ml solution) 100 µl 100 µl 800 µl
The amount of ketamine-xylazine anesthesia administered was 10 µl/g for male mouse which was maintained, after observing mouse reflexes, by the additional IP injection of 100 µl.		
Anesthesia Medetomidin Midazolam Fentanyl NaCl	 0.5 mg/kg 5 mg/kg 0.05 mg/kg 0.9 %	(For 4 ml solution) 160 µl 320 µl 320 µl 3200 µl

The amount of narcosis administered was 15 µl/g of mouse weight which was maintained, after observing mouse reflexes, by the additional IP injection of 100 µl.	
Category	**Dosage**
Antidote Flumazenil Atipamezol	 0.5 mg/kg 2.5 mg/kg
Analgesic Buprenorphin	 0.065 mg/kg

3.7 Equipments

Table 7: List of equipments used

Equipment	**Model**	**Supplier**
Two-photon excitation fluorescence microscope	TriM Scope	LaVision BioTec GmbH
Confocal microscope	TCS-SP5	Leica
Centrifuge (without brake)	Centrifuge 5810R	Eppendorf
Water bath	Precision CIR 35	ThermoScientific
Pipettes	Eppendorf research plus	eppendorf
Tips	ep T.I.P.S	ThermoFischer Scientific
Surgical tools	Complete set	F.S.T (Fine Science Tools)
GEMINI Cautery system	GEM5917	BRAINTREE

		SCIENTIFIC,INC.
Syringes (1ml)	LOT 1602003P LOT 16H29C8, REF 9151141	BD plastipak B|BRAUN
Needles	0.4 mm × 19 mm 0.3 mm × 12 mm	BD Microlance B|BRAUN
pH meter	inoLab® pH 7110 SET 2	WTW
Cremaster stage	Prepared in laboratory workshop	Walter Brendel Center, LMU, Munich

3.8 Software

Table 8: List of software used in this study

Software	**Version**	**Company**
ImageJ/FIJI	ImageJ-win64 (Schindelin et al. 2012)	FIJI
ImSpector	v0.1 (Schönle A. 2006)	Abberior Instruments GmbH
IMARIS	IMARIS x64 (7.6.5)	Bitplane

4. Methods

For observing CD40-CD40L dependent ULVWF multimer-platelet interaction and leukocyte extravasation, a two-photon excitation fluorescence microscopy (TriMScope by LaVision BioTec GmbH) based live cell imaging system was established by using murine cremaster microcirculation model and non-invasive murine ear model. The mice utilized for this study were either C57/BL6 wild type animals or ADAMTS13 knockout mice.

4.1 Preparation of ex vivo labeled platelets

Freshly isolated platelets from the donor mice were utilized for individual experiments. The platelets were isolated and stained by following a simple 2-step centrifugation process. The advantage of using *ex vivo* labeled platelets was that they gave better signal detection when used in conjunction with other labeled biomolecules in microvasculature.

4.1.1 Blood withdrawal from donor mouse

For taking the mice blood, a syringe was pre-filled with the anticoagulant Na-citrate to obtain a final citrate/blood ratio of 1:10. All the tools for surgical procedure were sterile. The donor C57/BL6 mouse was euthanized by an overdose of isoflurane inhalation. The mouse suffered from respiratory arrest momentarily, after which the mouse was fixed on the sterile stage and the abdomen was wiped off with 70 % ethanol. The peritoneum was cut wide open and pinned down. The intestines were carefully grabbed with blunt forceps and placed on one side. The organs were grabbed by the attached connective tissue and fat to avoid any bleeding. To have a clear view of vena cava, the mesentery attached to spleen was pinned towards right. The connective tissue around vena cava was carefully removed with the help of two sharp forceps when necessary, that also caused vena cava to dilate. The vessel was then punctured with a needle pointing up. The syringe was filled slowly while carefully watching for filling of the vessel. If the syringe was pulled too strong a vacuum was created which impeded blood sampling and activated platelets, which must be avoided. In order to get maximum blood out of

vena cava, the chest was pressed carefully without moving the needle inside vena cava. Once the vacuum was created inside vessel, blood sampling was stopped and the syringe was slightly tilted to mix anticoagulant properly. The blood was then transferred to an Eppendorf tube for platelet isolation.

4.1.2 Isolation and staining of platelets

Platelets from C57/BL6 donor animal were washed and labeled *ex vivo* with carboxyfluorescein diacetate (CFDA). For this purpose, the thrombocyte buffer (Tz-buffer) was adjusted to a pH of 7.35 and supplemented with 500 ng/ml of prostacyclin (PGI_2) before every use and placed in water bath at 37 ^oC. The equal volume of buffer was added to the collected blood and centrifuged for 5 minutes at 150 g without brake. The centrifugation gave us a clear supernatant i.e. platelet rich plasma (PRP) which was separated carefully in another Eppendorf tube. The transfer of PRP was done by using the pipette tip cut from top to reduce shear induced activation of platelets. To prepare the stain, Tz-buffer was supplemented with CFDA stain in a concentration of 1:2000 (50mg/ml stock in DMSO) and vortexed well. Later on, Tz-buffer containing PGI_2 and CFDA stain was added to an equal amount of diluted PRP with desired number of thrombocytes to be stained. The solution was incubated for 15 minutes at 37 ^oC in dark followed by centrifugation for 10 minutes at 450 g with zero brake. This left us with the pellet containing stained platelets while the clear supernatant was discarded. The pellet was resuspended in 200 µl of Tz-buffer for *in vivo* application. The stained platelets were always freshly prepared for individual experiment(s).

4.2 Labeling of endogenous platelets

In some experiments, alternatively or additionally, the animal's own platelets (endogenous platelets) were labeled by injecting PE-conjugated anti-mouse CD41 antibody intravenously (i.v., tail vein). 5-10 µl of labeled antibody always proved to be enough for labeling maximum endogenous platelets within a minute after injection. The endogenous platelets were labeled to confirm the efficacy and sensitivity of using *ex vivo* labeled platelets. The labeled endogenous platelets proved to be difficult in detection of adhered platelets in comparison to *ex vivo* labeled platelets because of

their high amount in circulation which made the vessels looked saturated. While in case of *ex vivo* labeled platelets, the injected platelet volume *in vivo* was easily controlled by adding desired number of stained platelets and they were brighter to detect.

4.3 Preparation of recipient mice cremaster

Before the start of surgery, the recipient mice were anesthetized using a combination of ketamine/xylazine in initial experiments which was replaced by a combination of medetomidin, midazolam and fentanyl in later experiments. It normally took 15 minutes for the mice to go to deep sleep. Meanwhile, all the tools for surgical procedure were sterilized. Before starting surgery, the animal was checked for its reflexes by pinching at the toe. The mice were then transferred onto the cremaster preparatory stage and an eye-ointment was applied to prevent their eyes from damage. The stage was connected with the heating platform that maintained a constant normal body temperature. The chamber was then sealed with silicone and filled with warm saline solution to keep the cremaster moist during preparation. The mice were stabilized by fixing their legs with adhesive surgical tape around the cremaster stage. A tiny cut was made on the skin of scrotum and one out of two cremasters was pulled out using blunt forceps. It was pinned to one side of chamber and the excessive connective tissue around the cremaster was carefully removed using sharp forceps. That helped to reduce the tension exerted on cremaster, which if not removed normally pulled back the cremaster in and also caused muscle movement during intravital microscopy recording.

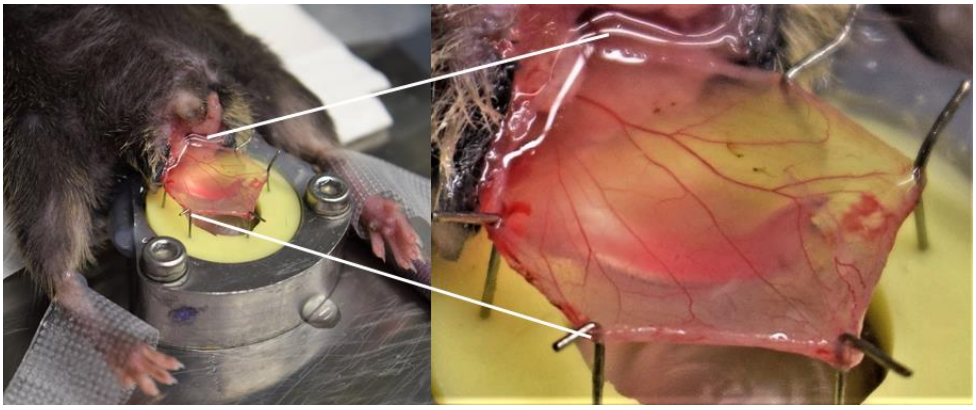

Figure 7: Murine cremaster preparation. *Prepared cremaster pinned down in a form of sheet with finely visible microvasculature to be observed under two-photon laser scanning microscope.*

The cremaster was carefully cut using small surgical scissors, avoiding to damage the big vessels. The cut opened muscle was then pinned down in the form of sheet circumventing any excess stretch (Figure 7).

4.3.1 Labeling of cremaster microvasculature

The endothelium was labeled by topical application of 50 µl of anti-mouse Alexa Flour 647-labeled-CD31 antibody to cremaster muscle for 1 hour. The chamber was covered during the incubation time to prevent the conjugated antibody from susceptible photo-bleaching. After 1 hour, the antibody was washed away and the chamber was filled again with fresh warm saline solution. The microvasculature was nicely labeled for ECs when observed under two-photon microscopy (Figure 8).

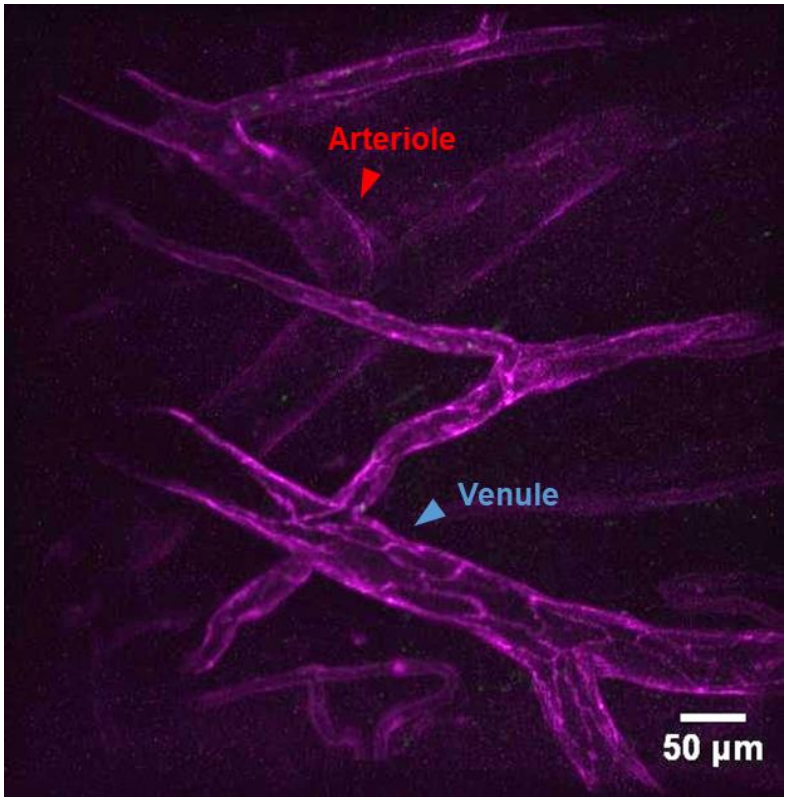

Figure 8: Endothelial cell labeling *in vivo.* *Representative image for the EC (violet) labeling of murine cremaster microcirculation showing an arteriole and a venule. The differentiation between blood vessels was made possible under bright field microscopy by observing different blood flow directions.*

4.4 Preparation of recipient mice ear pinna

In addition to murine cremaster microcirculation experiments, murine ear pinna experiments were also performed to confirm the phenomenon of platelet string formation in ADAMTS13ko mice even under non-invasive conditions (Figure 9). For this purpose the mice ear pinna was disinfected using 70 % ethanol and the endothelium of microvasculature was labeled by injecting 20 µl of anti-mouse Alexa Fluor 647-conjugated-CD31 antibody into the pinna. It labeled the microvessels within 30 minutes of its injection. This model was used only to confirm the formation of platelet strings in ADAMTS13ko mice microvasculature and not used for further studies since we were not able to differentiate between arterioles and venules under bright field microscopy. And under two-photon excitation fluorescence microscope we were able to observe only endothelial-platelet interactions.

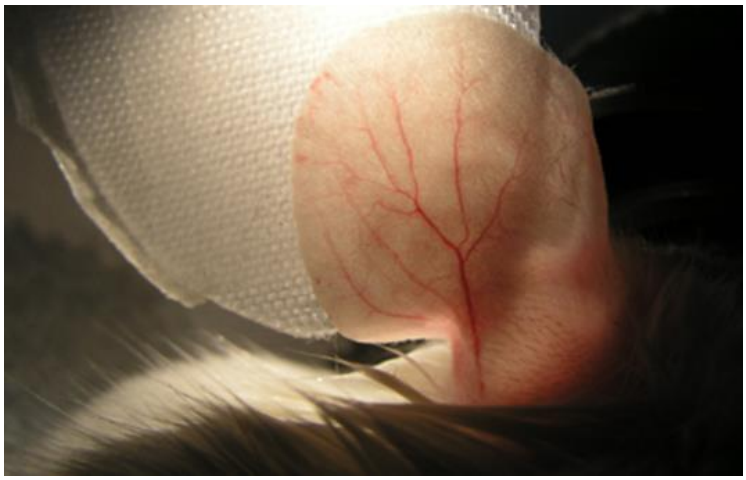

Figure 9: Murine ear pinna model. *The finely visible microvasculature of murine ear pinna for intravital microscopy (Institute of Physiology and Pathophysiology 2014).*

4.5 Preparation of femoral artery catheter

For the administration of *ex vivo* labeled platelets and labeling antibodies, the recipient mice were implanted with a femoral artery catheter. The preparation involved the formation of fine head catheter connected to a syringe. In order to prepare a thin

femoral artery catheter, a flanked tubing was prepared by burning the catheter tubing and pulling it apart from both sides. It gave us a sharp pointed catheter for easy insertion into femoral artery. The tubing was then connected to a syringe filled with heparin solution and the catheter was filled with anticoagulant to prevent blood coagulation. After that, the artery in the hind limb was spotted through the translucent skin and the area was wiped off with 70 % ethanol. A small skin incision was made and with the help of sharp forceps the tissue fats were removed from the neurovascular bundle. The artery was carefully separated from the neighboring vein and nerve bundle. During the surgery, the artery was kept moist at all times with 0.9 % saline solution. At the proximal end of the artery a loop of surgical thread was loosely placed to be closed later, while at the distal end the artery was blocked with the help of a tightened suture knot. The aneurysm clip was placed at the proximal end above the loosened thread to stop the arterial blood flow temporarily. With the help of a needle femoral artery was punctured in between proximal and distal ends and the catheter was then carefully implanted into the artery. The loosened loop of surgical thread was then tightened firmly to affix the catheter within the artery and the catheter was further secured with the artery by tying at the distal end. The surgical clip was removed and the successful catheter implantation was assured by the spontaneous inflow of blood into catheter. The skin was stitched with the help of sutures and finally the catheter together with syringe was fixed on the stage with the help of adhesive tape.

4.6 Two-photon excitation fluorescence microscope

In order to visualize inter-cellular crosstalk between platelets, ECs and leukocytes in microvasculature, multifocal two-photon excitation fluorescence microscope was selected. Similar as confocal microscopy it allows to study defined optical sections within a tissue, however it allows to study structures in a greater depth below the organ surface than confocal microscopy. Images can be obtained when two photons of infrared light arrive at an absorbing electron within 1 attosecond (1×10^{-18} s). Since this is very unlikely to happen under normal conditions, so a focused pulsed laser (TiSa-Sapphire) is used to generate a high photon density. At any given time, the incident photons generate light emission from one point which is scanned over the specimen.

The emitted photons from each point is recorded by the detectors (PMTs or HPD) and the images are re-constructed by computer. Although, this technique is complex and expensive but it also offers many advantages such as:

1. As it uses near infrared range as incident light and the scattering decreases with longer wavelengths so there is less absorption and deep tissue penetration, allowing us to image a live tissue up to a depth of 1 mm.
2. The excitation and bleaching occurs at only one focal point, not above or below it like with confocal microscopy, hence preventing the sample from phototoxicity and out of focus bleaching (Figure 10).
3. Unlike confocal microscopy, two-photon microscope does not have a pinhole, hence preventing any loss of emitted photons and enabling non-ballistic photons to contribute to the image.

Figure 10: Single and double photon excitation fluorescence at one focal point. *Notice that the single photon excitation fluorescence bleaches the sample above and below the focal point while double (white arrow) photon excitation fluorescence prevents the unwanted bleaching of sample (MRC Laboratory of Molecular Biology).*

In the two-photon excitation fluorescence microscope separation of neighboring fluorochromes are more difficult due to crosstalk of emission spectra, so at a time, a maximum of three detecting channels could be utilized for simultaneous recording.

Compromises were made for the selection of following labeled molecules for their detection depending upon the aim of experiment.

1. Platelets
2. Leukocytes
3. Endothelial cells
4. vWF
5. CD40

4.7 Experimental protocol

4.7.1 Experimental groups

With the aim of observing ULVWF multimer-platelet string formation and leukocyte extravasation in the murine cremaster microcirculation, two different experimental groups were established, namely:

1. C57/BL6 mice
    - Control
    - CD40L stimulation
2. ADAMTS13 knockout mice
    - Control
    - CD40L stimulation

The recipient mice were first checked for any further dose of anesthesia by pinching at the toe. A volume of 200 µl corresponding to about 8×10^6 labeled *ex vivo* platelets were injected into the circulation through either tail vein or femoral artery catheter and the mice were then placed on the microscopic stage inside a two-photon microscopy chamber for recordings (Figure 11).

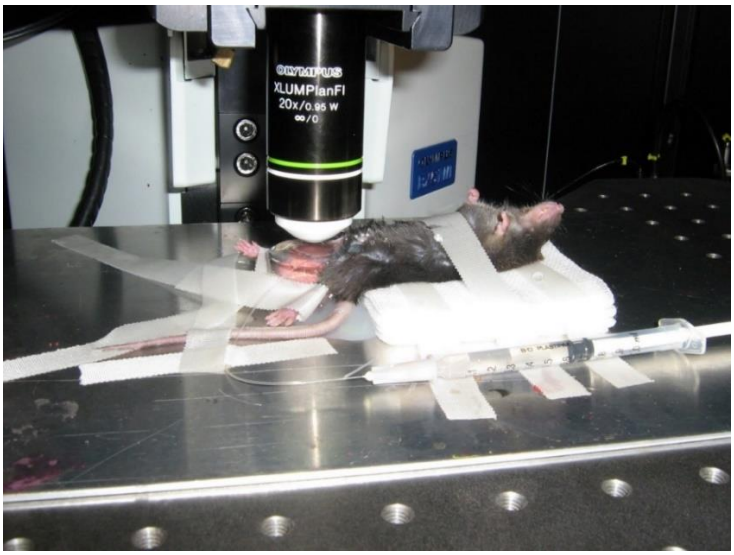

Figure 11: Experimental setup of multiphoton-based live cell imaging method. *An anaesthetized recipient mouse with prepared cremaster and femoral artery catheter placed under two-photon excitation fluorescence microscope for observing ULVWF multimer-platelet mediated leukocyte transmigration in microcirculation.*

4.7.2 CCD-camera recording

The microscope was capable of recording bright field, fluorescence and two-photon microscopy as per requirement. The cremaster microcirculation was first visualized under camera recording with a CCD-camera that allowed to gain an overview over the whole cremaster preparation and to select 3-5 areas of interest. For all microscopic recordings either 20x or 60x water immersion lenses were used. The cremaster was kept moist with warm saline solution throughout the recording phase. This on one hand prevented the tissue from drying and on the other hand facilitated the water immersion lenses in recording. The initial camera recording helped to achieve three aims:

a. To distinguish between arterioles and venules on the basis of blood flow direction.
b. To calculate platelet velocities from their traces and to perform shear rate calculations.
c. To locate platelet hotspots as we called areas with visible preferential platelet adhesion.

For the image acquisition the ImSpector® software was used. The settings used for CCD top recording were as follows (Table 9) (Figure 12):

Table 9: Functions and settings of CCD top recording

Functions	Settings
Instrument mode	CCD top
Devices	Time-time
Scanfield	300 µm × 300 µm
Frequency	1200 Hz
Scan Quality	Medium
Exposure Time	48 ms
Binning	2 × 2
Wait time	30 s
Fast mode	On
No. of steps	120
Frame time should be around 50 ms.	

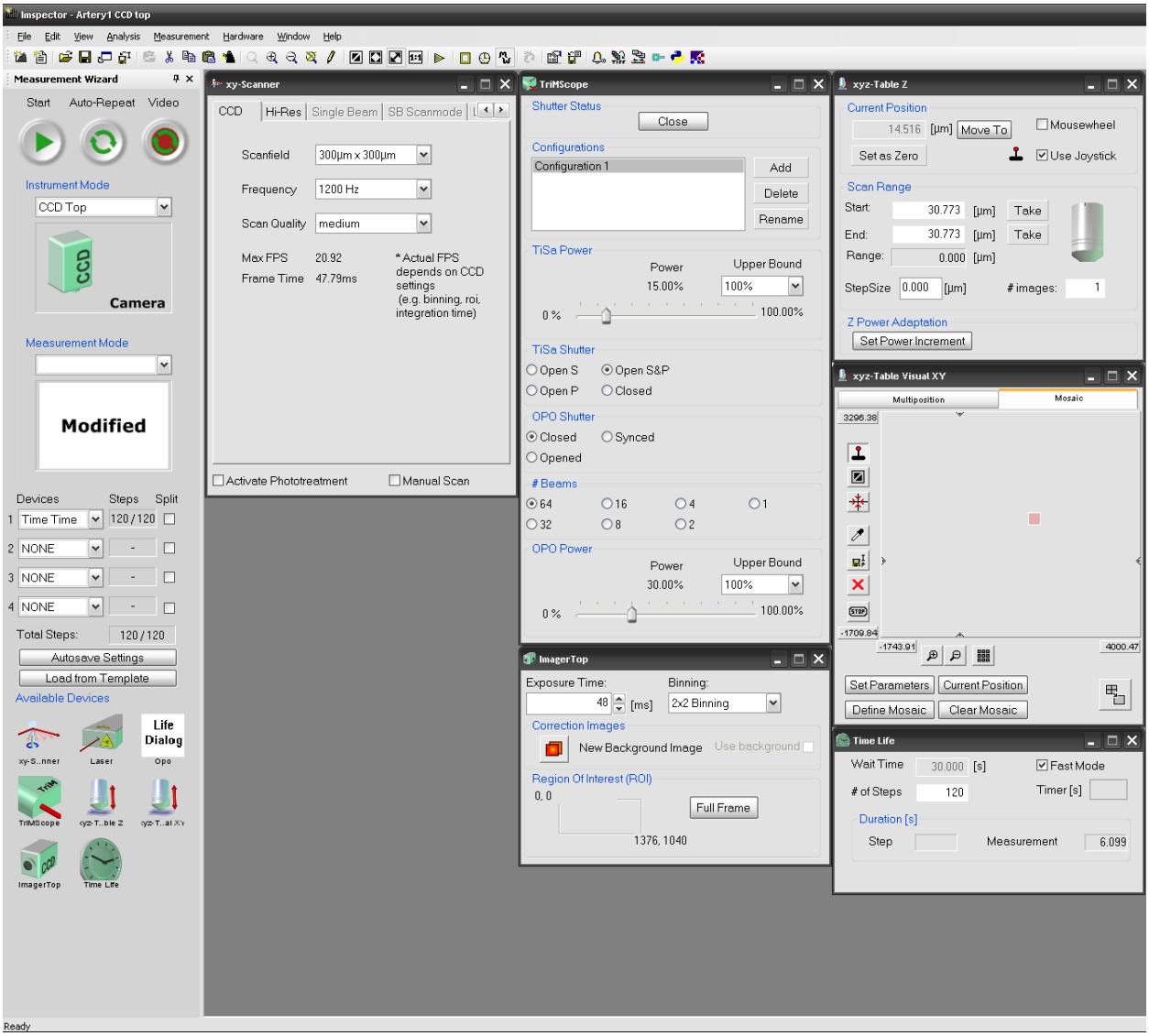

Figure 12: CCD-camera settings for bright field microscopy. *Screenshot of ImSpector software displaying settings for CCD top recording of cremaster microcirculation for platelet velocity and shear rate measurements.*

4.7.3 Single-beam TiSa recording

Soon after distinguishing between arterioles and venules, recording platelet velocities and identifying any hotspot(s), the cremaster microvasculature was observed under two-photon excitation fluorescence microscope for the selected vessels before and after stimulated conditions. The settings used for regular recording under two-photon microscope were as follows (Table 10) (Figure 13):

Table 10: Functions and their settings for two-photon excitation fluorescence microscope

Functions	Settings
Instrument mode	SingleBeam Tisa
Devices	Time-time or xyz-Table z
Size	500 µm × 500 µm (for overview)
Frequency	800 Hz
Line average	1
Wavelength	800 nm
System	On
Shutter	Open
TiSa power	10-30 %
TiSa shutter	Open S&P
OPO shutter	Closed
Xyz-Table Z	Step size 0.5 µm – 2 µm
PMTs	USP-525 (for CFDA/Qdot 525) 580-560 (for PE/Qdot 565) 665-660 (for AF647)
Wait time	30 s
Fast mode	On
No. of steps	120

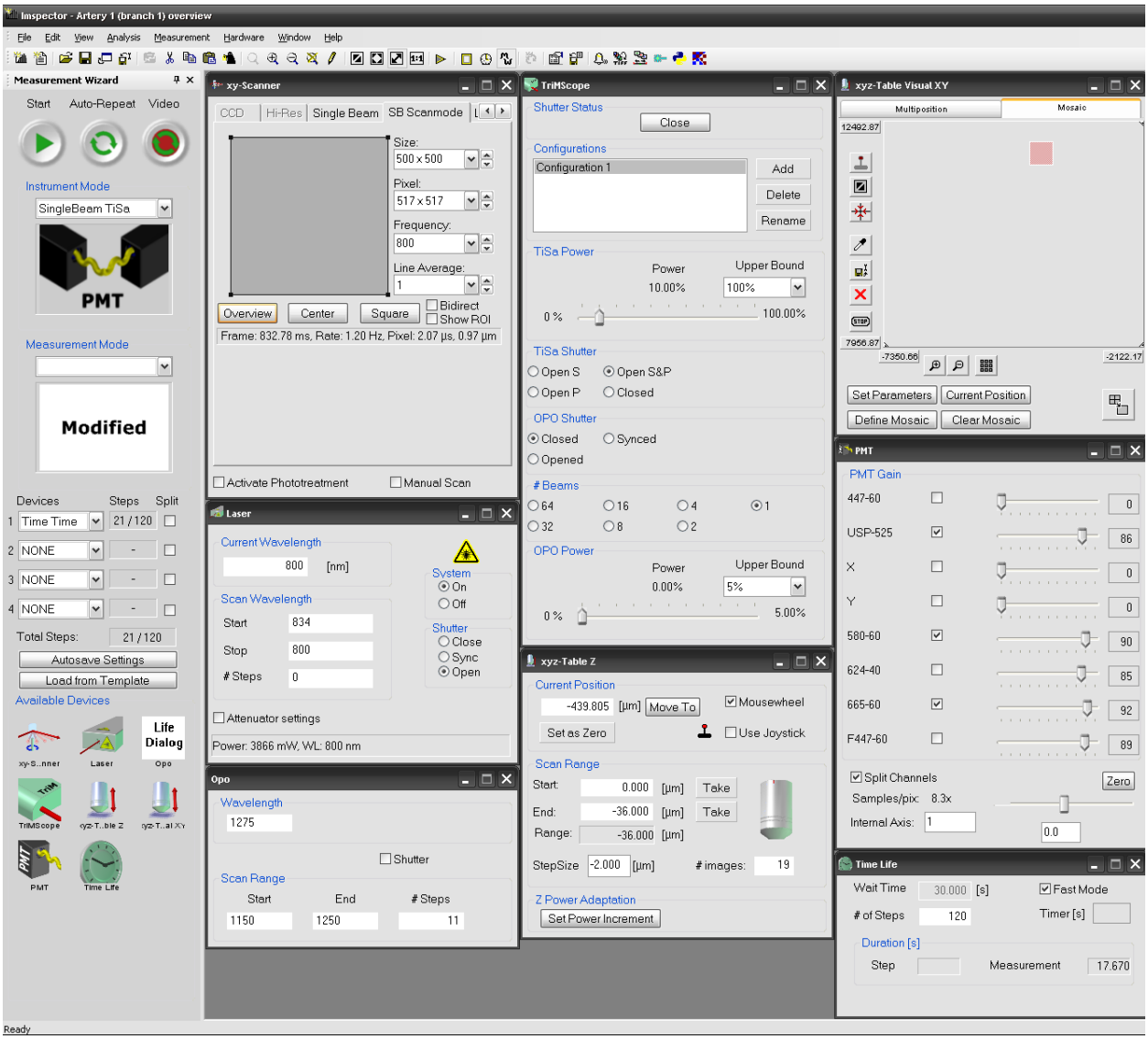

Figure 13: Single Beam TiSa laser settings for two-photon excitation fluorescence microscopy. *Screenshot of ImSpector software displaying the settings of wavelength, laser power and the desired channels for observing endothelial-platelet-leukocyte interaction under two-photon excitation fluorescence microscope. Here the PMTs used were USP-525, 580-560 and 665-660 for CFDA stained platelets, PE-labeled leukocytes and AF-647 labeled ECs respectively.*

Before the application of stimulus at least 3 arterioles and 3 venules, previously identified under CCD top recordings, were observed for any signs of adhered platelets. If the platelets were found to adhere on vessel wall and they formed pearl like structures (consisting of at least three platelets at short distance in a row), we termed them as

"platelet strings". The two experimental groups were compared in terms of amount and length of platelet strings under control and stimulated conditions. ULVWF multimers were elicited by superfusion of commercially available (ENZO) recombinant soluble CD40L called MegaCD40L for 20 minutes. It is an effective stimulator of CD40 because of its two linked trimeric CD40L molecules through their collagen domain of Adiponectin/ACRP30/AdipoQ (Figure 14). After 20 minutes of CD40L stimulation, the selected vessels were again observed for any increase in platelet strings formation. In addition to this, in a subset of experiments all circulating leukocytes were labeled by injecting 50 µl of PE-conjugated anti-mouse CD45 antibody i.v. or via femoral artery catheter. The labeled leukocytes were then observed for their interaction with the platelet strings and their extravasation in the cremaster muscle arterioles and venules.

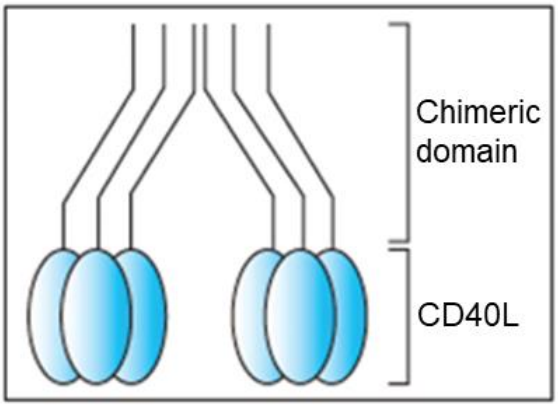

Figure 14: Graphical representation of MegaCD40L. *The cartoon showing two trimeric CD40L molecules attached to the chimeric domain for an enhanced stimulation (ENZO).*

VWF and CD40 visualization was made possible by labeling vWF and CD40 with primary antibodies coupled to Qdot-565 and Qdot-525, respectively, and injected i.v. The protocol followed for Qdot labeling was provided together with SiteClick™ Qdot® 525,565 antibody labeling kits. 5-10 µl of injected labeled antibody was sufficient for observing the distribution of CD40 and vWF in the microvasculature.

4.8 Images/video analysis by IMARIS software

The recorded images and videos from two-photon excitation fluorescence microscopy were analyzed off line using IMARIS x64 software (Figure 15A). Imaris is Bitplane's scientific software that facilitated us to analyze, visualize and interpret two photon microscopy datasets in time-time as well as 3D simulations.

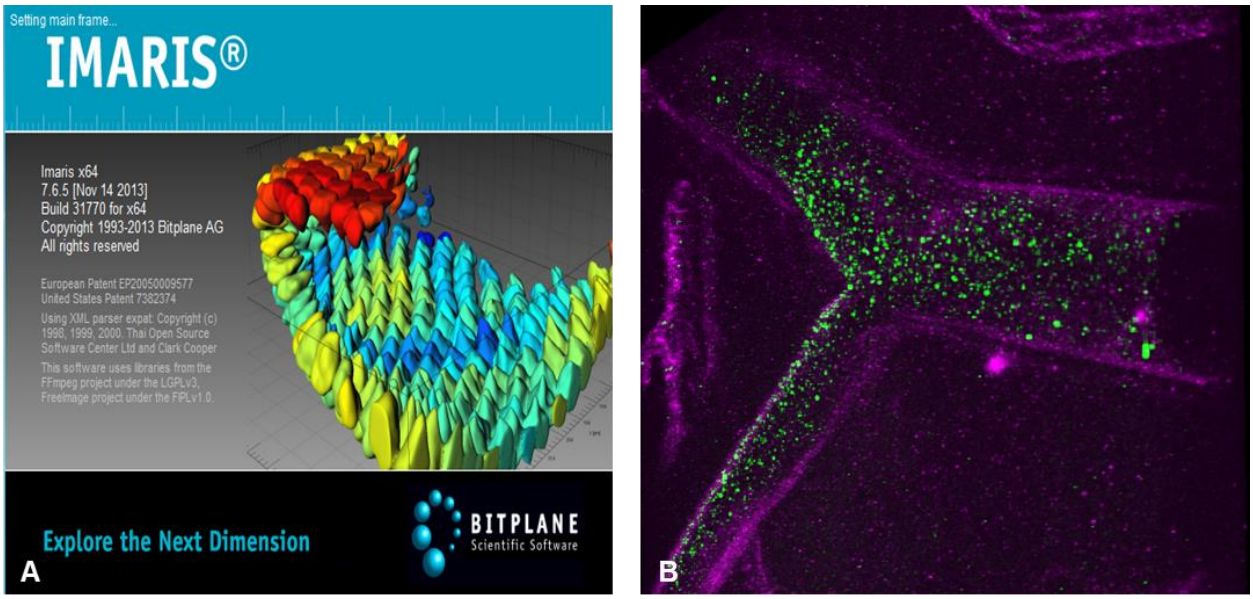

Figure 15: IMARIS software used for re-establishment of recorded images/videos. *Screenshot of IMARIS x64 version used to simulate recorded data from two-photon excitation fluorescence microscope* ***(A),*** *and 3D construction of a venule made by IMARIS showing circulating platelets (green) in the vessel, violet = endothelium* ***(B).***

4.8.1 Time-time videos and 3D z-stacks

IMARIS was very helpful in analyzing the interaction between different stained molecules by turning ON or OFF utilized channels and adjusting the brightness/contrast of recorded fluorescence at a time. In addition, by using the "Surpass view" it was possible to visualize 3D constitution of vessels by adding the original data sets (sheets) to a stack that helped to discover the otherwise hidden vascular and immune cells interactions in all dimensions (Fig. 4.9B). The "Snapshot" feature was convenient to

capture any image view during the recording, which was saved in a standard format for offline evaluation.

4.8.2 Quantification of perivascular leukocytes

IMARIS was also utilized for quantifying labeled perivascular leukocytes next to venules and arterioles for comparison. During the experiment, since only intravascular leukocytes were labeled by injecting PE-conjugated CD45 antibody into the circulation, labeled perivascular leukocytes could be identified as extravasated since the time of intravascular labeling. For quantification, 200 μm^2 areas were selected along the vessels and the number of extravasated leukocytes was manually counted for comparison (Figure 16). The 3D feature of IMARIS helped to include extravasated leukocytes in all dimensions for quantification.

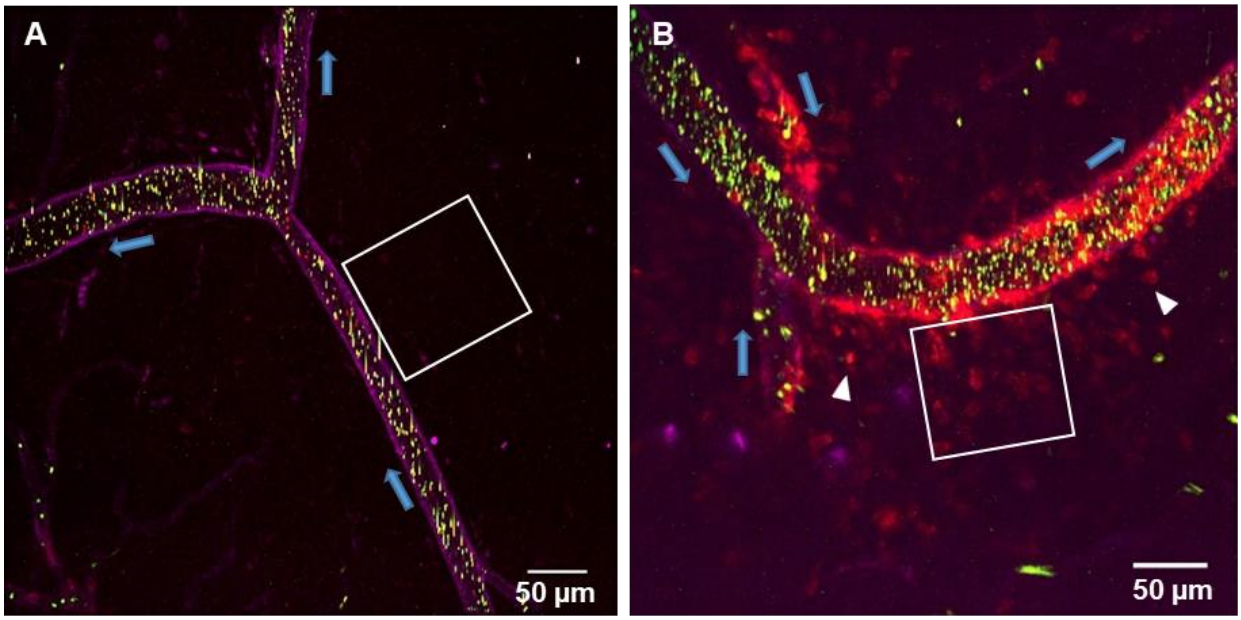

Figure 16: Representative images of perivascular leukocyte quantification. *The perivascular space of 200 μm^2 (representative white square) around arteriole **(A)** and venule **(B)** selected for manual quantification of extravasated leukocytes. Blue arrows indicate the direction of blood flow while white arrow heads are pointing towards single extravasated leukocytes (red). Violet = endothelium.*

4.9 Analysis by FIJI/ImageJ

Further analysis for velocity, shear rate measurements and confirmation of platelet strings in the vessels was performed using FIJI/ImageJ software.

4.9.1 Platelet velocity and shear rate calculations

From the CCD top recordings platelet velocity (v) was calculated first by measuring the distance traveled by platelet in one frame. It was done by taking the average of two recorded frames and tracking the trails of circulating platelets from the start of one frame till the start of second frame and dividing the distance traveled by time for one frame (Figure 17A) i.e.

$$Velocity\ (v) = \frac{\text{Distance traveled}}{Time\ for\ one\ frame}$$

The vascular diameter (d) was simply measured by measuring the distance between vessel walls perpendicularly (Figure 17B). Platelet velocity and vascular inner diameter measured by video microscopy were then used for calculating respective shear rates ($\dot{\gamma}$) in the vessels in sec^{-1} as follows:

$$\dot{\gamma} = \frac{8v}{d}$$

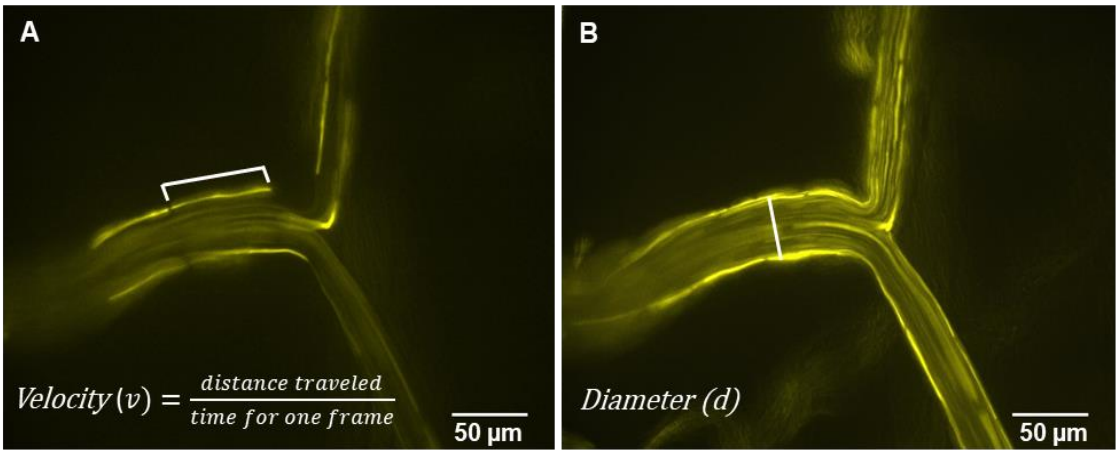

Figure 17: Measurement of platelet velocity and shear rate in the microvasculature. *CCD top recordings of ex vivo labeled platelets (yellow) in cremaster microcirculation for measuring platelet velocity (v)* ***(A)*** *and vascular inner diameter (d)* ***(B)*** *which were used for calculating shear rates ($\dot{\gamma}$) in the vessels.*

4.9.2 Confirmation of platelet strings by average and maximum intensity features of FIJI/ImageJ

The adhesion of platelets to the vascular wall in the form of platelet strings as observed under two-photon microscopy recordings were confirmed by FIJI/ImageJ. For this purpose, the average intensity of images from time-time recordings of two-photon microscopy were taken that showed all the stationary platelets adhered to the vascular wall during the time span of recording, confirming the presence of platelet strings in the microvasculature. In contrast, the maximum intensity images of time-time recordings showed all the platelets that passed through the selected region of vessel during given period of time (Figure 18). In FIJI/ImageJ this feature was done by following:

Image > Stacks > Z-project > Average/Maximum Intensity

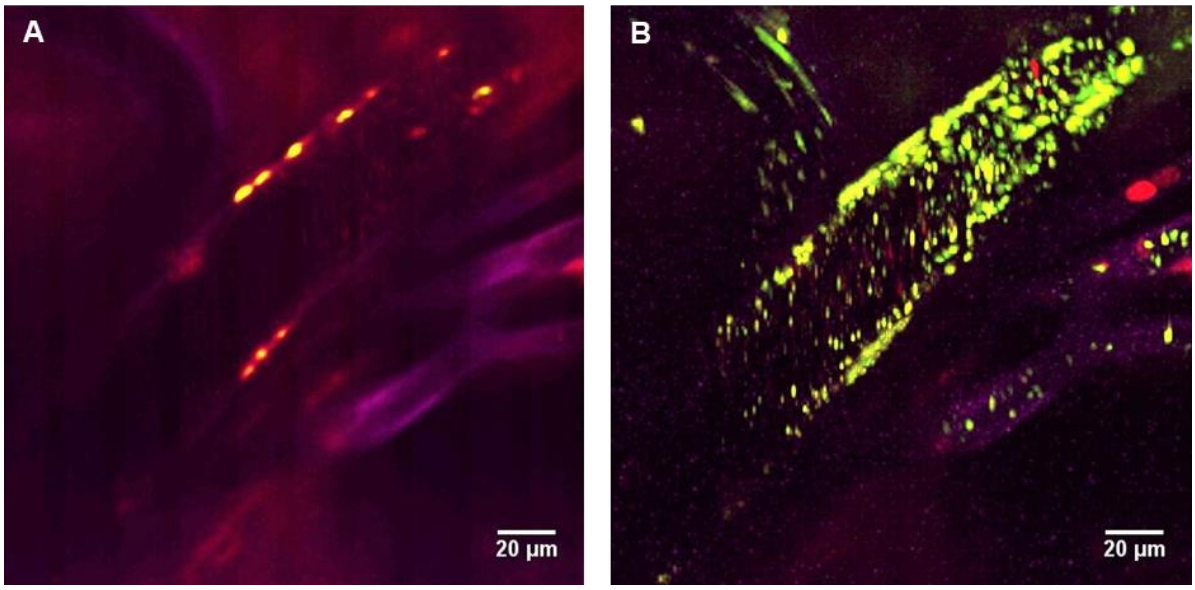

Figure 18: Confirmation of platelet strings by average and maximum intensity feature of ImageJ. *Average intensity output from ImageJ showed the stationary adherent platelets at vascular wall during the time course of recorded observation* ***(A),*** *while the maximum intensity output showed the platelets altogether passed through the vessel during the same time interval* ***(B)****, green = platelets, violet = endothelium.*

4.10 Cremaster fixation

In order to observe the expression and distribution of CD40 in microvasculature, freshly isolated cremasters were fixed and labeled for CD40 and ECs. For this purpose zinc fixative (Zn-fixative) buffer was used since zinc based fixatives preserve protein structures well and they are better for observing protein expression (Wester et al. 2003). Freshly isolated cremasters were pinned down in a lab-designed silicone rubber based petri-plates. Here it was important to stretch the cremasters in a form of sheet and then pin them down for proper EC and CD40 labeling. The cremasters were washed well with PBS for any blood removal and fixed for 15 minutes in Zn-fixative buffer. After fixation, the cremasters were washed well 3X with PBS. The cremasters were then blocked and permeabilized together with 2 % BSA and 0.1 % Triton X-100 respectively for 1 hour at room temperature. The tissues were washed again thoroughly 3X with PBS. CD40 receptor was then labeled by using AF-488 labeled anti-mouse CD40 antibody in a concentration of 1:250 for 1 hour in dark at room temperature. After 1 hour the unbound antibody was washed 3X with PBS for 10 minutes each. The cremasters were finally labeled for ECs with AF-647 conjugated anti-mouse CD31 antibody in a concentration of 1:250 for 1 hour in dark at room temperature. Then the final washing was done with PBS 3X for 10 minutes each to remove the unbound antibody. The cremasters were placed on glass slides and left for 5 minutes for drying. They were mounted in 1-2 drops of confocal-UV-matrix and covered with 18×18 mm coverslips. The coverslips were placed on top very carefully avoiding any trapping of air bubbles which can oxidize the fluorophores. The coverslips were then sealed with a quick dry top coat of transparent nail polish and stored in dark at 4 ^{o}C for further observations under two-photon excitation fluorescence microscope.

4.11 Statistical analysis

Data analysis was performed using Sigma Plot 13.0. Statistical tests were chosen where appropriate and comprised student’s t-test for unpaired data, Mann-Whitney Rank Sum Test, One Way Analysis of Variance followed by post-hoc tests (Holm-Sidak method) or Kruskal-Wallis One Way Analysis of Variance on Ranks followed by Dunn's

Method post-hoc test, and the differences were considered statistically significant with an error probability of <0.05. The individual statistical method used is indicated in all figure legends. All results shown here are presented as means ± SEM even when non parametric testing was applied. A total of 3-10 blood vessels were observed in each experimental group with the total number of animals varying from 3 to 13.

5. Results

5.1 *Ex vivo* labeled platelets form pearl like strings preferentially in venules *in vivo*

In order to establish a working model for live cell imaging with two-photon excitation fluorescence microscopy to investigate ULVWF multimer-platelet string formation *in vivo*, the first step was labeling of the endothelium and detection of platelets in the microcirculation *in vivo*. The endothelium of the cremaster microcirculation was labeled successfully by fluorescently labeled CD31 antibody throughout all tissue layers studied. When the e*x vivo* labeled platelets from the donor mice were injected intravenously into anesthetized C57/BL6 (n=4) recipient mice, they could be observed flowing through all vessels within less than one minute after injection. With time, some of the platelets were found to become stationary at the vessel wall where they formed pearl necklace like “platelet strings” (Figure 19A, B). In addition, single sticky platelets were observed but the vast majority was part of strings. The strings were initially spotted with conventional CCD recording that helped to more easily distinguish whether they were located in arterioles or in venules, evaluating the different flow characteristics of these vessels which was more difficult with two-photon microscopy recording.

Platelet strings under control conditions were found preferentially in venules while they were only occasionally present in arterioles (Figure 19C). In more than 70 % of the cases we observed the strings at the same place over an observation period of 60 mins. In the remaining cases, the platelet strings vanished again within this period of time. It was not possible to determine the exact time since always several vessels had to be observed in a strict order. So, to study the development of strings under comparable conditions during control and subsequent treatment conditions, *ex vivo* labeled platelets were injected twice (each dose containing 8×10^6 platelets), one before and the other after treatment, e.g. application of CD40L, with a mean time difference of 48 ± 9 min. While observing these strings, there were always fine spaces between adjacent adhered platelets, suggesting the possible contribution of unlabeled endogenous

platelets in making up these strings. The average length of platelet strings observed in all experimental groups was 14 ± 2 µm (n=29).

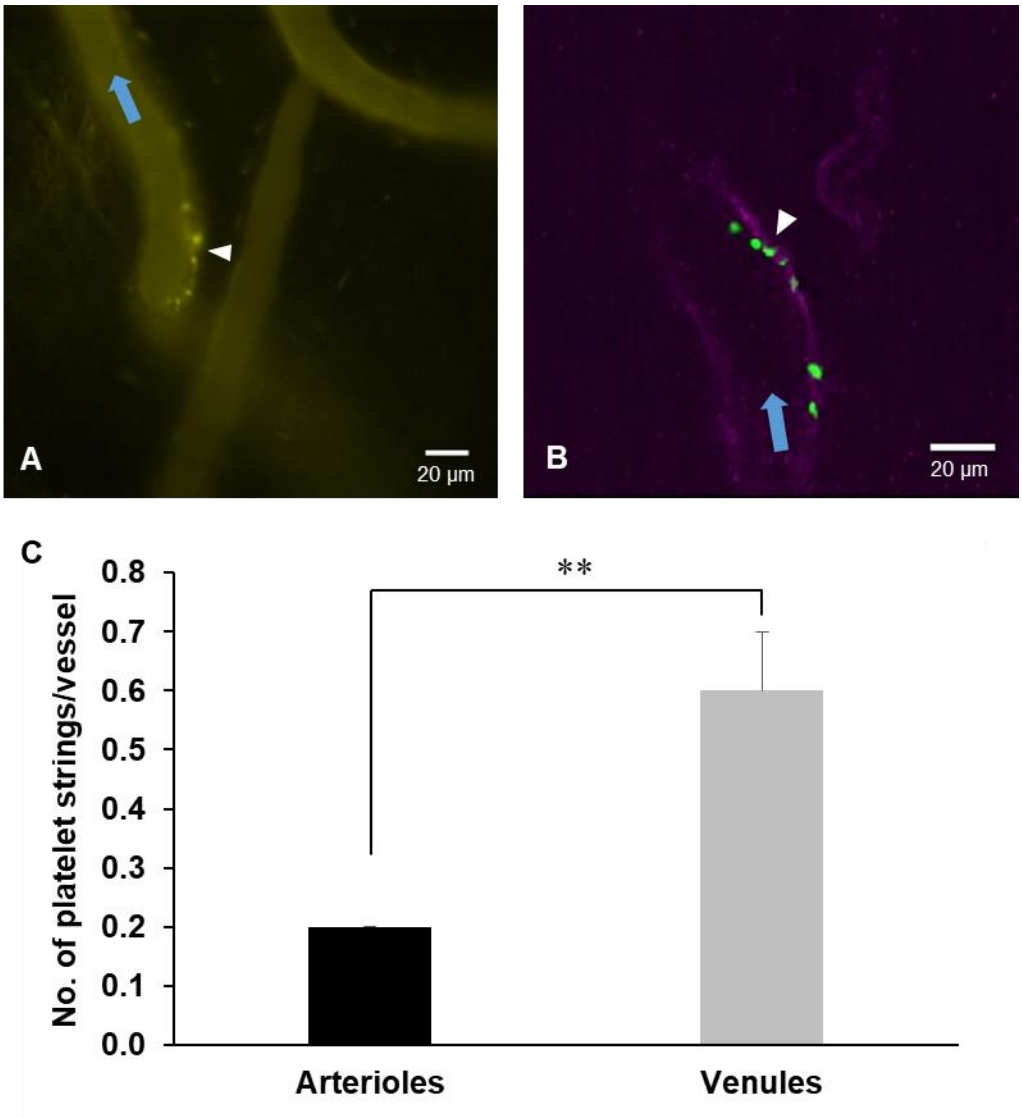

Figure 19: ULVWF multimer-platelet string formation and its quantification *in vivo.* *Representative images of pearl like platelet string formation (white arrow heads) under CCD top recording **(A)** and two-photon laser scanning microscopy **(B)** in the murine cremaster microcirculation. Blue arrows indicate the direction of blood flow. The phenomenon of platelet string formation preferentially occurred in venules **(C)**, n=4 mice, **p≤0.01, Mann-Whitney Rank Sum Test.*

The threshold length was set to 6 µm (consisting of at least three platelets at short distance in a row) to be included in the definition of a platelet string. These strings were observed with a predisposition of 2:1 in bifurcations to linear segments of the vessels.

5.1.1 ADAMTS13ko mice show platelet adhesion in the microcirculation even under non-invasive conditions in ear pinna

Since the cremaster preparation involved an invasive surgery that could lead to a pro-inflammatory condition, promoting platelet adhesion to the vessel wall. In order to validate the working model of ADAMTS13ko mice under non-invasive control conditions, the behavior of circulating *ex vivo* labeled platelets in the microcirculation of the ear pinna was observed. The mouse ear pinna is a natural thin tissue with fine visible blood vessels that were easily detectable with two-photon excitation fluorescence microscopy. The microvascular ECs in the ADAMTS13ko mice were labeled by firstly disinfecting the ear with 70 % ethanol and then injecting AF647-labeled anti-CD31 antibody into the ear pinna. The ear preparation did not involve any invasive surgery. After 20 min of endothelial labeling, *ex vivo* labeled platelets were injected i.v. The dorsal ear was then observed with two-photon excitation fluorescence microscopy that revealed occasional adhesion of labeled platelets to the vessel wall (Figure 20), thus providing evidence for platelet adhesion without trauma in the ear pinna of the knockout mice at baseline.

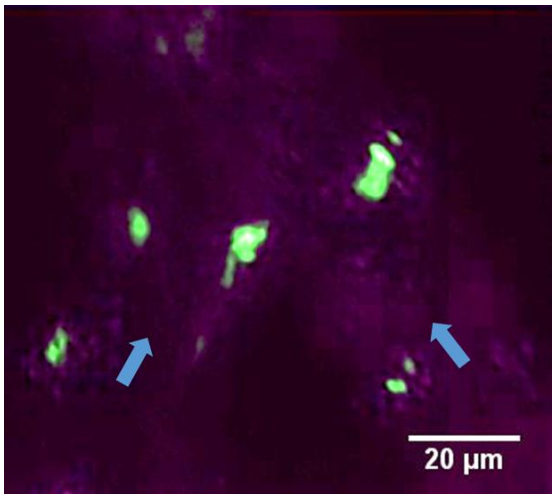

Figure 20: Representative image of ULVWF multimer-platelet strings formation in ADAMTS13ko mice at baseline. *Average intensified image of ADAMTS13ko mice ear microcirculation under non-invasive control conditions showed prolonged adhesion of platelets (green) to the ECs (violet). Blue arrows indicate the direction of blood flow.*

Despite of the usefulness of the ear model, it was not easy to distinguish between arterioles and venules, as blood flow in the microvasculature was not visible under bright field microscopy. So, all the forthcoming experiments were performed in the murine cremaster microcirculation.

5.1.2 By use of ex vivo labeled platelets the total number of platelet strings is underestimated but facilitates signal detection

In some experiments, the endogenous platelets were labeled (using a different fluorescence dye) in addition to the injected *ex vivo* labeled platelets to investigate efficiency and sensitivity of detection of ULVWF multimer-platelet strings comprised of mixed endogenous and exogenous platelets. In fact, both kinds of platelets participated in string formation (Figure 21A) which contained exogenous (yellow) and endogenous (red) platelets. However, exogenous platelets did either not participate in all strings, or appeared as “single” platelets and as such were not recognisable due to a too weak fluorescence signal. Quantification revealed that strings containing exogenously labeled platelets were significantly fewer in number than all strings (Figure 21C). In spite of its limitations, the use of only *ex vivo* labeled platelets proved to be helpful as it provided a brighter fluorescence signal (Figure 21B) which was particularly helped when other labeled immune cells like leukocytes were monitored in parallel. Therefore all further observations are based on the quantification of strings containing exogenous platelets-only.

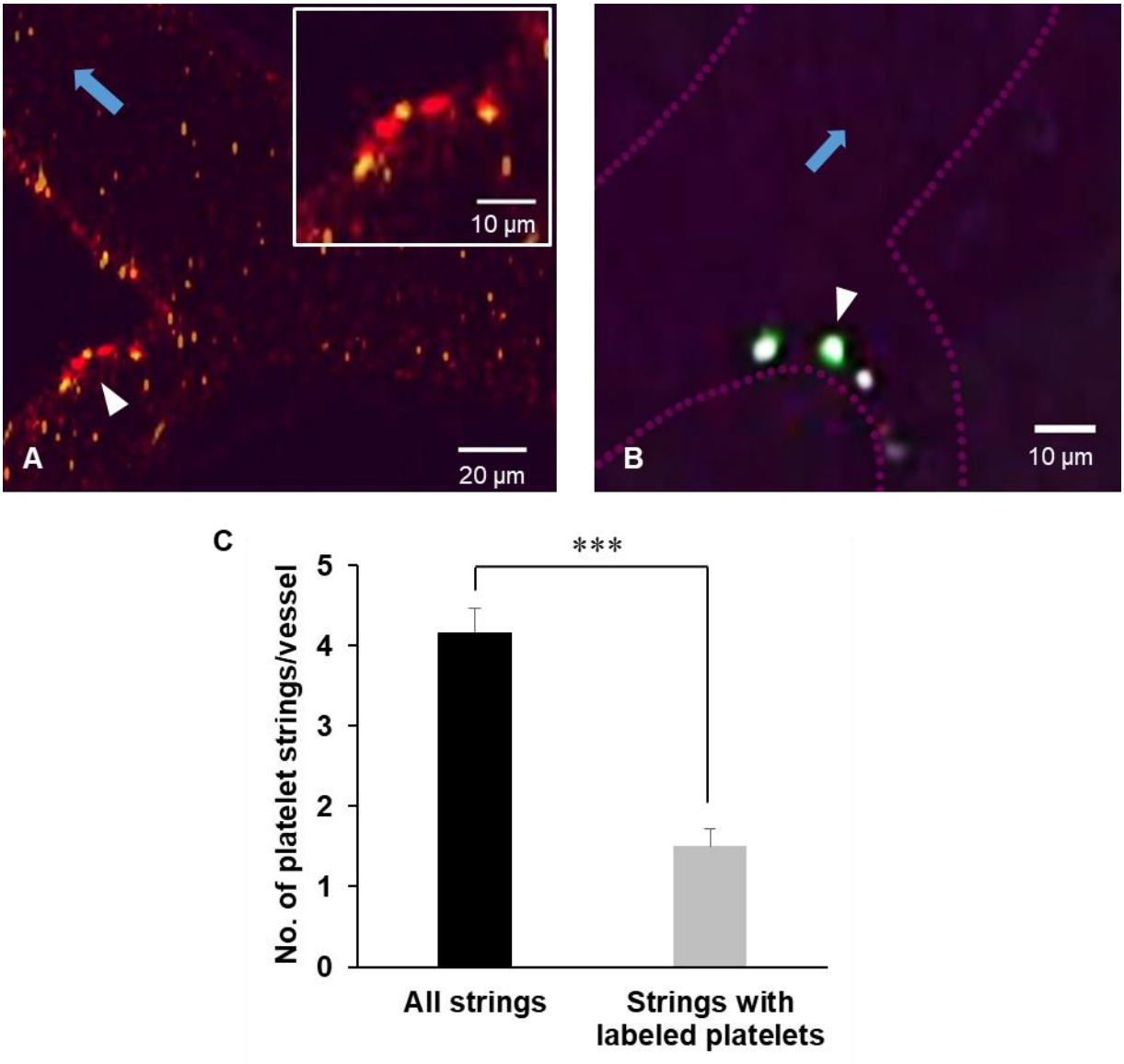

Figure 21: Confirmation of effective ULVWF multimer-platelet string detection using *ex vivo* labeled platelets. *Platelet strings (white arrow head) containing both exogenous (yellow) and endogenous (red) platelets confirmed effective string detection using ex vivo labeled platelets **(A)**. Top right box in A shows higher magnification of a string. Ex vivo labeled platelets gave brighter fluorescence signals **(B)**. Bar graph showing that ~3 times more strings/vessel were detected when labeling endogenous platelets **(C)**. n=3 mice, ***p ≤ 0.001, t-test.*

5.2 CD40L enhances ULVWF multimer-platelet string formation preferentially in venules

The cremaster microcirculation of C57/BL6 mice was exposed to CD40L for at least 20 min prior to observing ULVWF multimer-platelet string formation. No change was detected in arterioles in terms of string formation following application of CD40L. By contrast, in venules CD40L was found to significantly enhance string formation by ~2 fold (Figure 22).

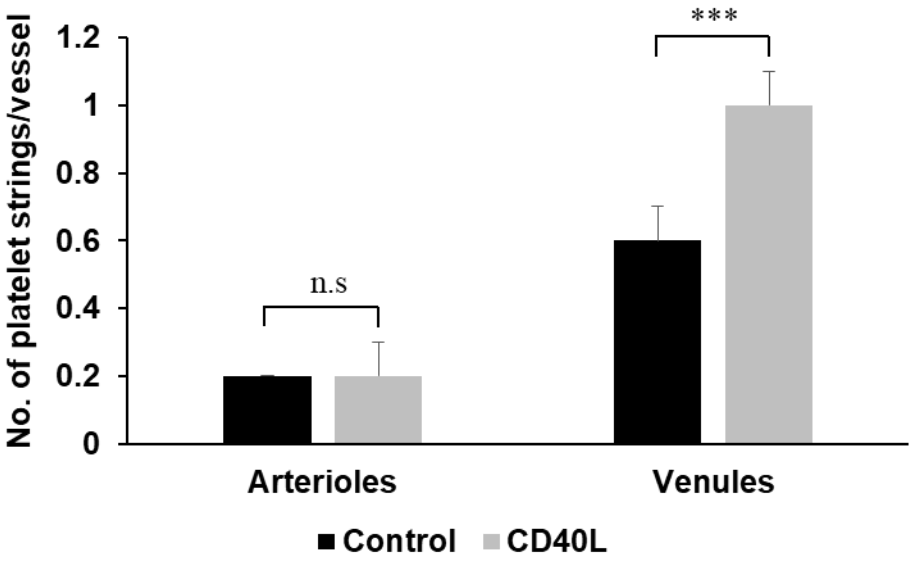

Figure 22: Increase in ULVWF multimer-platelet string formation in venules in response to CD40L stimulation. *n = 4-7, ***p≤0.001, n.s=non-significant, Mann-Whitney Rank Sum Test.*

5.3 ADAMTS13 deficiency significantly raises the number of ULVWF multimer-platelet strings in venules

In the presence of ADAMTS13, the number of ULVWF multimer-platelet strings observed was rather low in arterioles as compared to venules. In the absence of ADAMTS13, string formation in the venules increased even further by about 2-fold. In

contrast, the arterioles showed no significant difference with regard to the number of strings either in the presence or in the absence of ADAMTS13 (Figure 23).

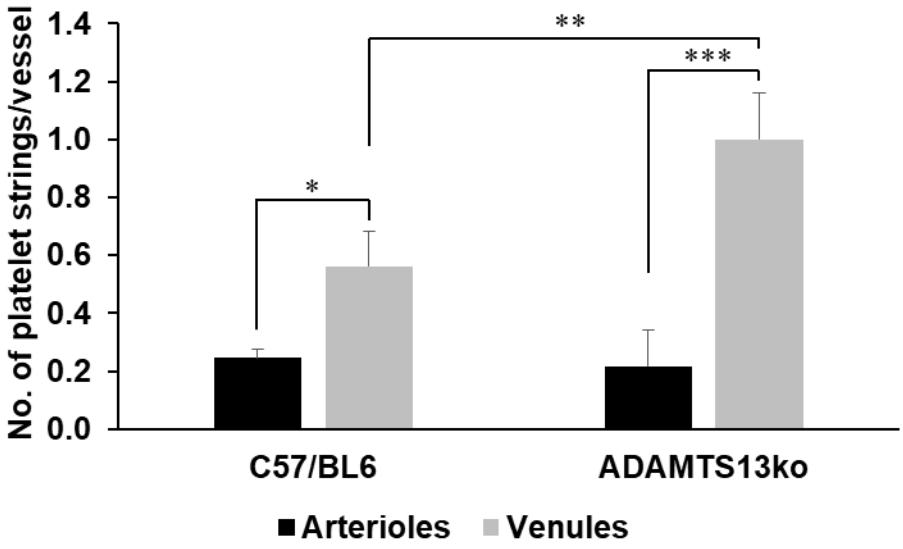

Figure 23: Absence of ADAMTS13 augments baseline ULVWF multimer-platelet string formation in venules but not in arterioles. *n=4-5, *p≤0.05, **p≤0.01 ***p≤0.001, One Way Analysis of Variance followed by Holm-Sidak post-hoc test.*

5.4 CD40L exacerbates string formation in venules in the absence of ADAMTS13

The deficiency of ADAMTS13 exerted its effect mainly in venules through enhanced ULVWF multimer-platelet string formation which was significantly enhanced further in response to CD40L stimulation. Both baseline and CD40L-stimulated string formation in venules was enhanced further in ADAMTS13ko mice while string formation in the arterioles of these animals was not different at baseline or following exposure to CD40L (Figure 24).

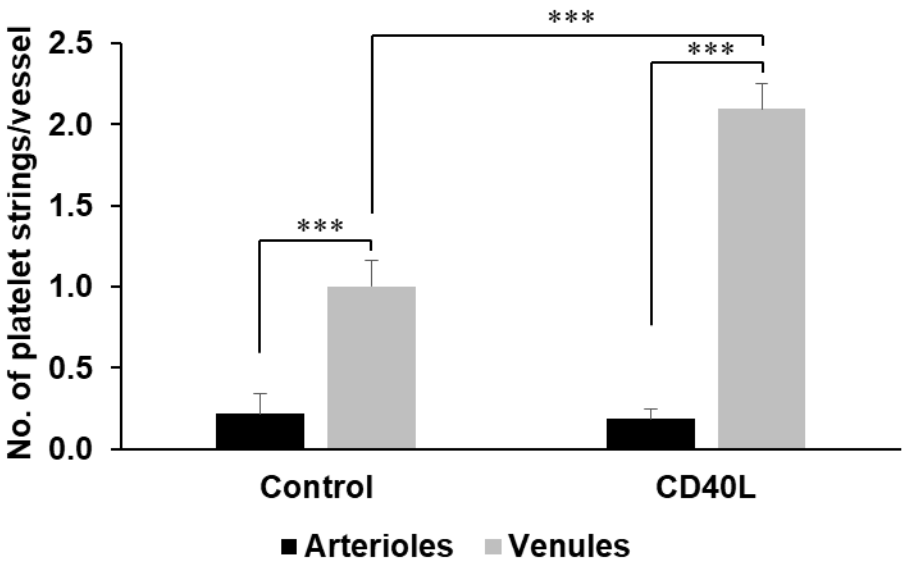

Figure 24: ADAMTS13ko mice are more responsive to CD40L stimulation than C57/BL6 mice. *ULVWF multimer-platelet string formation in arterioles and venules of ADAMTS13ko mice in the absence and presence of CD40L. n=4-13, ***p≤0.001, One Way Analysis of Variance followed by Holm-Sidak post-hoc test.*

5.5 Shear rate does not affect the number of platelet strings

According to *in vitro* studies, higher unidirectional shear rate supports the phenomenon of ULVWF multimer-platelet string formation by unfolding vWF concatamers and exposing their binding sites for platelets to adhere. To validate this finding *in vivo*, the effect of the shear rate, which under conditions of constant viscosity is inversely related to shear stress, on string formation was studied. As anticipated, arterioles on average revealed higher shear rates than venules (Figure 25).

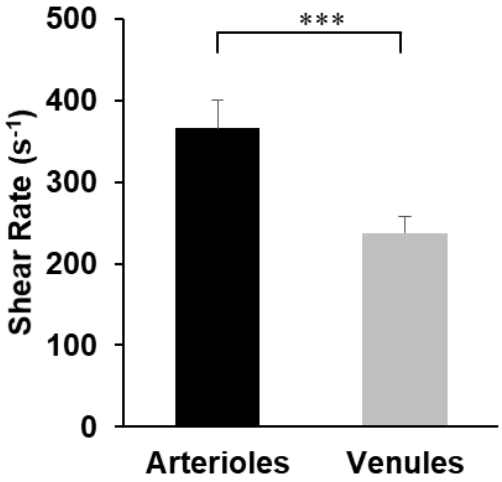

Figure 25: Arterioles have higher shear rates than venules. *n=21, ***p≤0.001, Mann-Whitney Rank Sum Test.*

In order to study a potential effect of the shear rate on the number of ULVWF multimer-platelet strings in response to CD40L stimulation, venules and arterioles of ADAMTS13ko mice were selected on the basis of comparable shear rates ranging from 240 to 440 s^{-1} (Table 11).

Table 11: ADAMTS13ko vessels with comparable shear rates selected for comparison of platelet string formation. *Random selection of arterioles and venules having comparable shear rates from 6 different ADAMTS13ko mice which were later compared for ULVWF multimer-platelet string formation in response to CD40L stimulation.*

Animal	Shear Rate (s^{-1})	
	Arteriole	Venule
1	311	349
2	311	327
3	242	249
4	310	290
5	415	428
6	415	436
Mean ± SEM (n=6)	**334**	**347**

These vessels were then matched and compared with regard to the number of strings. Despite having similar shear rates, again venules revealed significantly higher number of platelets strings than arterioles (Figure 26).

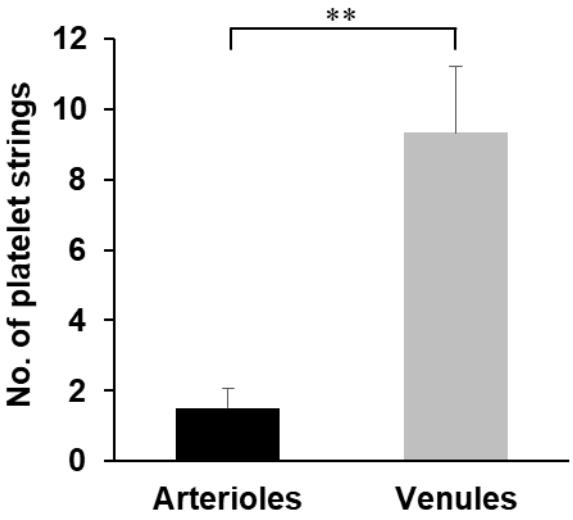

Figure 26: At comparable shear rates ULVWF multimer-platelet string formation is still more prevalent in venules of ADAMTS13ko mice in response to CD40L stimulation than in arterioles. *The individual shear rates are listed in Table 11. n=6, **p≤0.01, t-test.*

5.6 High shear rate increases the length of ULVWF multimer-platelet strings in the absence of ADAMTS13

Since high shear rate was found to show no effect on the number of ULVWF multimer-platelet strings, one step ahead was taken and the length of strings in individual arterioles and venules was measured both in wild type and ADAMTS13ko mice.

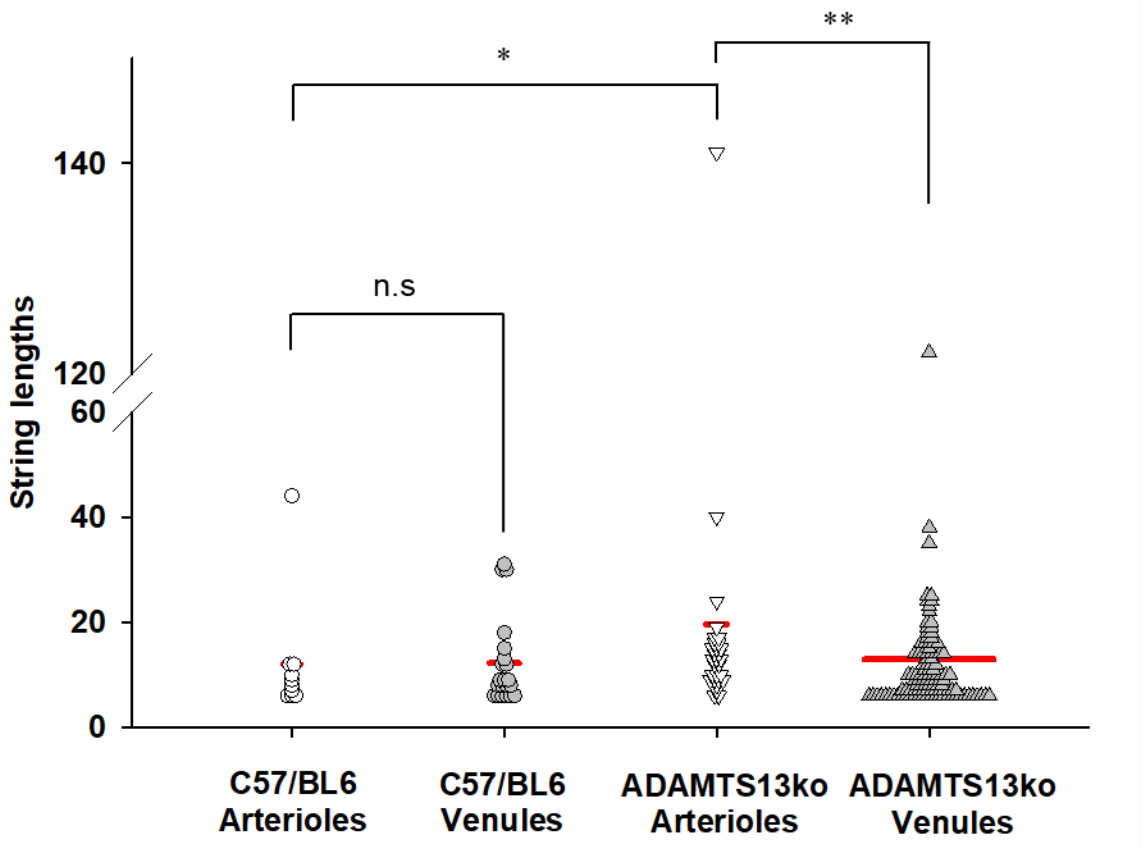

Figure 27: Higher shear rate in arterioles enhances the length of ULVWF multimer-platelet strings as compared to venules only in the absence of ADAMTS13. *n=6-14, mean (red horizontal line) ± SEM, *p≤0.05, One Way Analysis of Variance on Ranks followed by Dunn's method.*

Arterioles and venules in C57/BL6 (control) mice did not show any difference in length of the ULVWF multimer-platelet strings, suggesting that ADAMTS13 present in plasma is cleaving the released ULVWF multimers thus limiting the length of the strings. In the absence of ADAMTS13, although there was a greater number of strings in venules, they were not longer. In contrast, in the arterioles string length increased by about 50 % in the ADAMTS13ko mice (Figure 27) consistent with an unfolding of ULVWF multimers at higher shear rates in arterioles when not cleaved by ADAMSTS13.

5.7 VWF is abundant in venules

The finding that ULVWF multimer-platelet string formation was predominant in venules as compared to arterioles raised the question whether vWF is differentially expressed in the microcirculatory blood vessels of the two mouse lines studied. To this end, vWF distribution in the microvasculature was analyzed by labeling it *in vivo* using a Qdot-coupled anti-vWF antibody and then subjecting the cremaster preparation to CD40L to elicit endothelial cell vWF release. VWF was detected in arterioles (20-50 µm diameter) and venules (10-50 µm diameter) before and after CD40L stimulation. Before stimulation with CD40L there was nearly no vWF detectable whereas after exposure to CD40L abundance of vWF increased in the venules but not in the arterioles (Figure 28A). Upon quantification nearly 40 % of the length of the venules was positive for vWF following CD40 stimulation (Figure 28B).

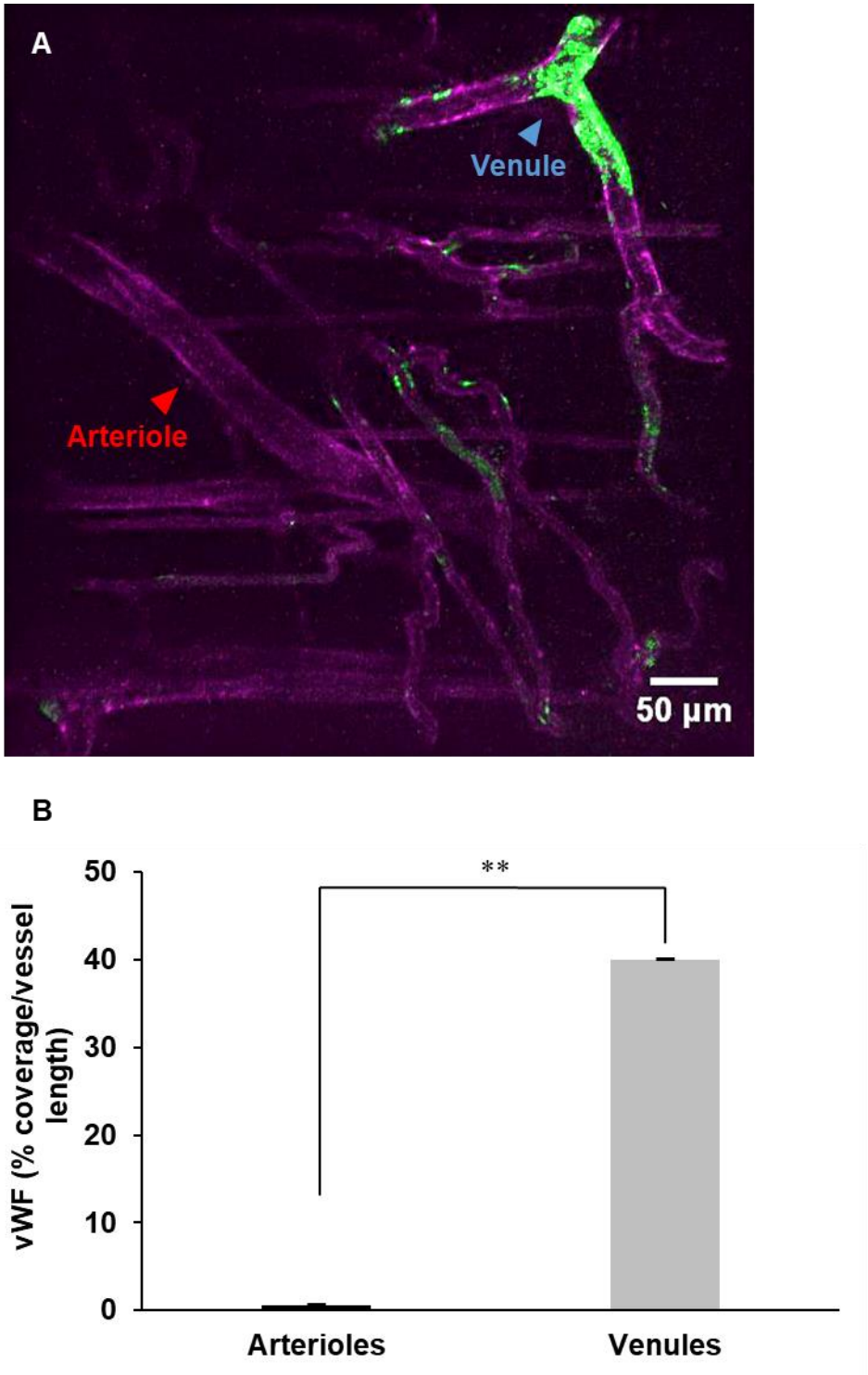

Figure 28: VWF is preferentially expressed in venules. *Representative image where vWF (green) was primarily found in a branching venule in comparison to an unbranched arteriole after CD40L stimulation* ***(A),*** *violet = endothelium. Quantification indicated that in venules 40 % of their vessel length is covered by vWF* ***(B),*** *n=4-7, **p≤0.01, t-test.*

5.8 VWF deposition in venules stimulated by CD40L is time-dependent

By following the occurrence of vWF in venules and capillaries after CD40L stimulation, it was found that CD40L triggered a gradual increase in venular vWF abundance in both wild type and ADAMTS13ko mice. The buildup of vWF on the EC surface initiated within 20 min of CD40L application kept on increasing with time. Localization of these changes in vWF disposition was not limited to bifurcations but extended to straight regions of the venules (Figure 29).

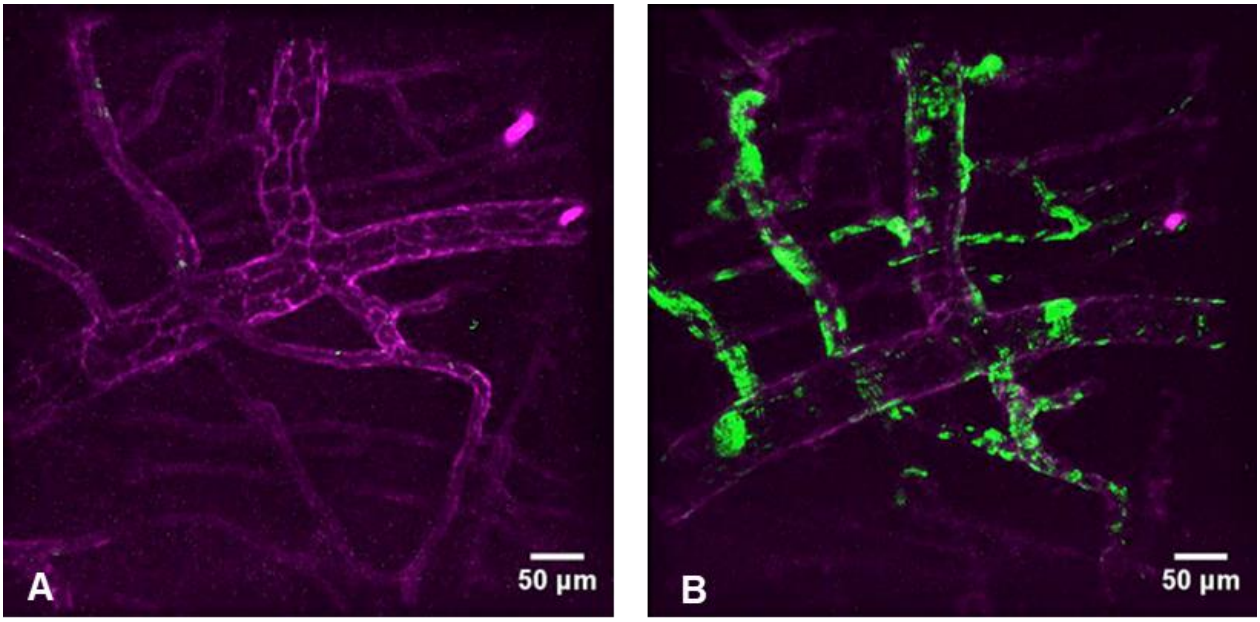

Figure 29: Inhomogeneous distribution of vWF in the cremaster microvasculature. *Representative images of venules in the cremaster of ADAMTS13ko show a time-dependent release of vWF (green) before **(A)** and after 60 min of CD40L stimulation **(B)**. Notice that vWF buildup in the venules is not limited to bifurcations.*

5.9 VWF co-localizes with platelet strings

When e*x vivo* labeled platelets were injected together with Qdot-labeled anti-vWF antibody to study their interaction, platelets were found to associate with extracellular vWF resulting in the formation of ULVWF multimer-platelet strings both in wild type and

ADAMTS13ko mice (Figure 30). Localization of strings was somewhat unpredictable although there was a preference of bifurcations over inter-segment regions of 2:1.

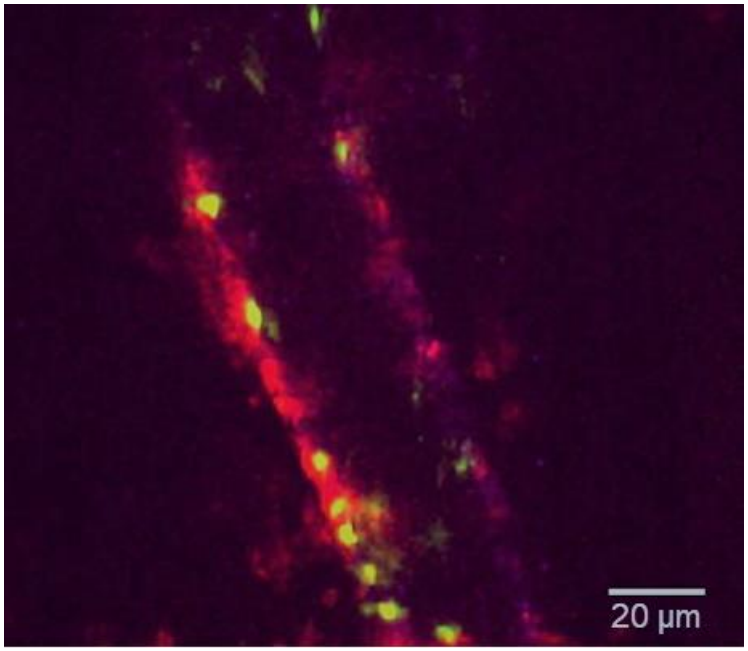

Figure 30: Co-localization of extracellular vWF with platelet strings *in vivo*. *Screenshot where vWF (red) is co-localized with adherent platelets (yellow) in a venule of an ADAMTS13ko mouse following CD40L stimulation, violet = endothelium.*

5.10 Leukocyte extravasation focuses on regions with visible ULVWF multimer-platelet strings

According to our hypothesis, ULVWF multimer-platelet strings serve as a recruiting mechanism for circulating leukocytes at the site of the atherosclerotic lesion, helping in their adhesion and transmigration through the EC monolayer. Soon after recognition of the platelet strings and their co-localization with vWF, the next step was to examine their interaction with circulating leukocytes and their role in leukocyte extravasation. Herein, platelet adhesion and string formation were found to be random inside the vasculature with a clear preference for venules. Even inside the same venule there were certain regions with high susceptibility to ULVWF multimer-platelet string formation which were termed “hotspots” as compared to platelet-free regions (Figure 31A).

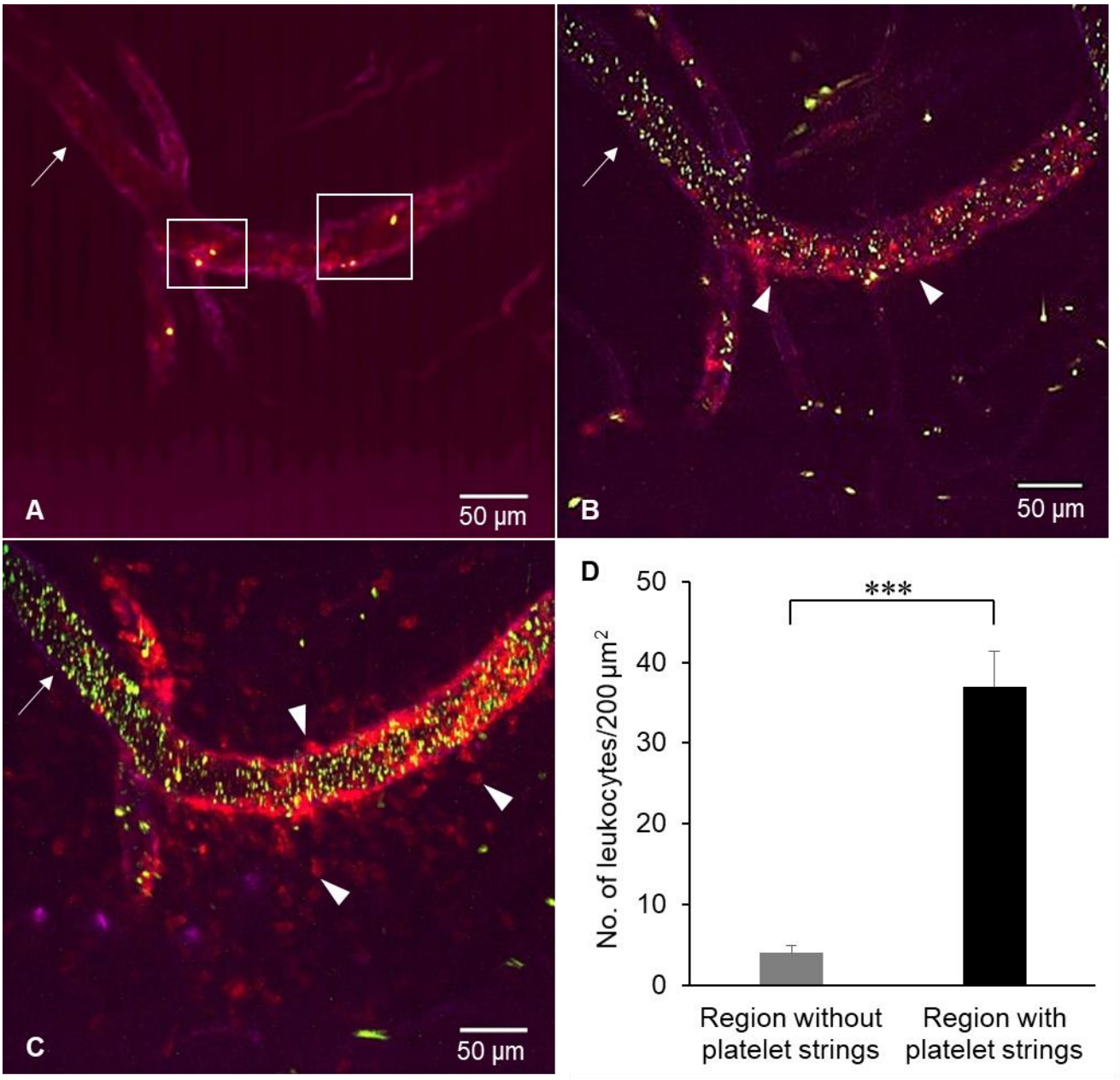

Figure 31: Leukocytes transmigrate preferentially in hotspot regions with visible platelet strings. *White squares specifying hotspot regions in a venule of a … mouse following exposure to CD40L showing ULVWF multimer-platelet (yellow) strings in an otherwise empty vessel (white arrow)* ***(A)****. Subsequent to leukocyte labeling hotspots show leukocyte (red) adhesion (white arrow heads) in contrast to the upstream leukocyte-free region of the same vessel (white arrow)* ***(B)****. The same venule observed 150 min later reveals prominent extravasation of leukocytes (white arrow heads) at hotspots only, while leukocyte-free regions (white arrow) remain as such* ***(C)****, violet=endothelium. The statistical summary of this phenomenon is shown in* ***(D)****. n=6, ***p≤0.001, t-test.*

Distinction between these regions was confirmed by observing the average intensified images of time-time recordings of the two-photon microscope in ImageJ. This feature allowed to detect regions within a vessel where platelets were tethered to the luminal EC surface throughout the time period of recording by taking the average of the recorded intensities in xyz projection. Venules with such hotspots were then followed for 150 min post CD40L stimulation. Directly after labeling of the leukocytes, the hotspot region(s) displayed increased leukocyte rolling and adhesion while the clear region(s) showed no sign of either platelet or leukocyte adhesion according to several screenshots (Figure 31B). During the 150-min follow-up hotspots were found not only to be more crowded with adherent leukocytes but there was also a very prominent leukocyte extravasation in comparison to the clear regions that could be followed easily (Figure 31C). Quantification of the perivascular leukocytes in the same venule suggested that regions with ULVWF multimer-platelet strings show a marked increase in the number of extravasated leukocytes in comparison to regions without any platelet adhesion during the follow-up period (Figure 31D).

5.11 ADAMTS13 deficiency increases the number of perivascular leukocytes in venules in response to CD40L stimulation

The number of perivascular leukocytes was quantified in arterioles and venules of ADAMTS13ko mice both at baseline and following CD40L exposure. The number of emigrated perivascular leukocytes (which originally had been labeled intravascularly) was very low in arterioles as compared to venules in ADAMTS13ko mice under both conditions. CD40L stimulation reinforced leukocyte extravasation only in venules. Quantification revealed a ~3-fold rise in the number of perivascular leukocytes along in venules of ADAMTS13ko mice after exposure to CD40L (Figure 32).

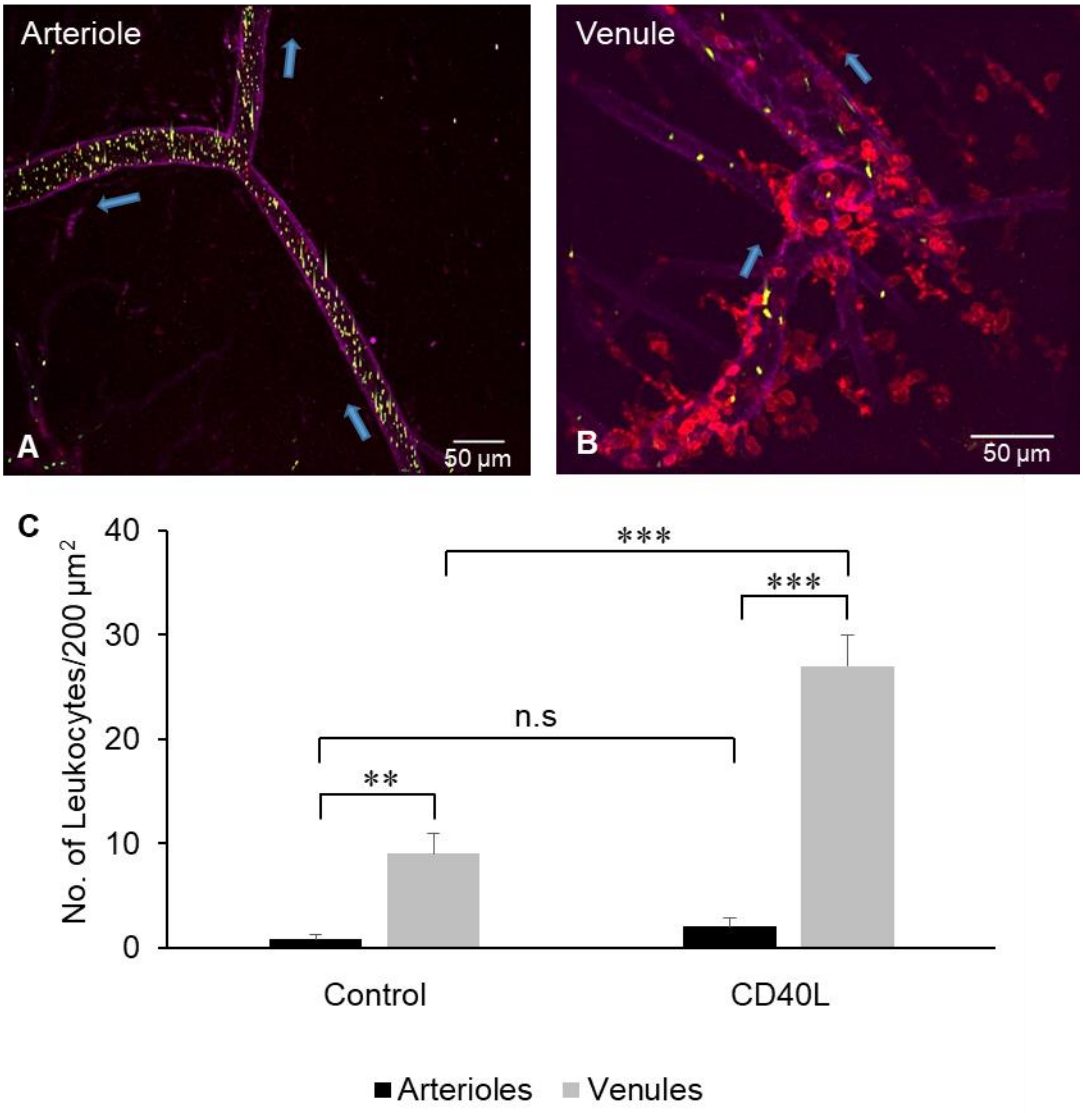

Figure 32: Preferential leukocyte extravasation in venules of ADAMTS13ko mice is significantly enhanced following CD40L stimulation. *Representative images of perivascular leukocytes (red) in an arteriole **(A)** and venule **(B)** of a ADAMTS13ko mouse, violet=endothelium, green=platelets. Statistical summary **(C)**, n=6, ***p≤0.001, **p≤0.01, Two Way ANOVA followed by Holm-Sidak post-hoc test.*

5.12 CD40 receptor expression is triggered by inflammation

So far there is very limited information on the distribution of endothelial cell CD40 in microvessels. At baseline, there was no constitutive CD40 expression at all in freshly isolated cremaster preparations from both wild type and ADAMTS13ko mice (Figure

33A and B). Once inflammation had been induced in the C57/BL6 cremaster muscle by TNF-α injection into the scrotum 2 hours prior to isolation of the cremaster, there was a striking increase in CD40 abundance on the luminal EC surface. It was difficult though to differentiate between arterioles and venules in the fixed cremaster due to the no-flow conditions. Perivascular leukocyte(s) could also be observed due to the presence of CD40 on the surface of the leukocytes (Figure 33C).

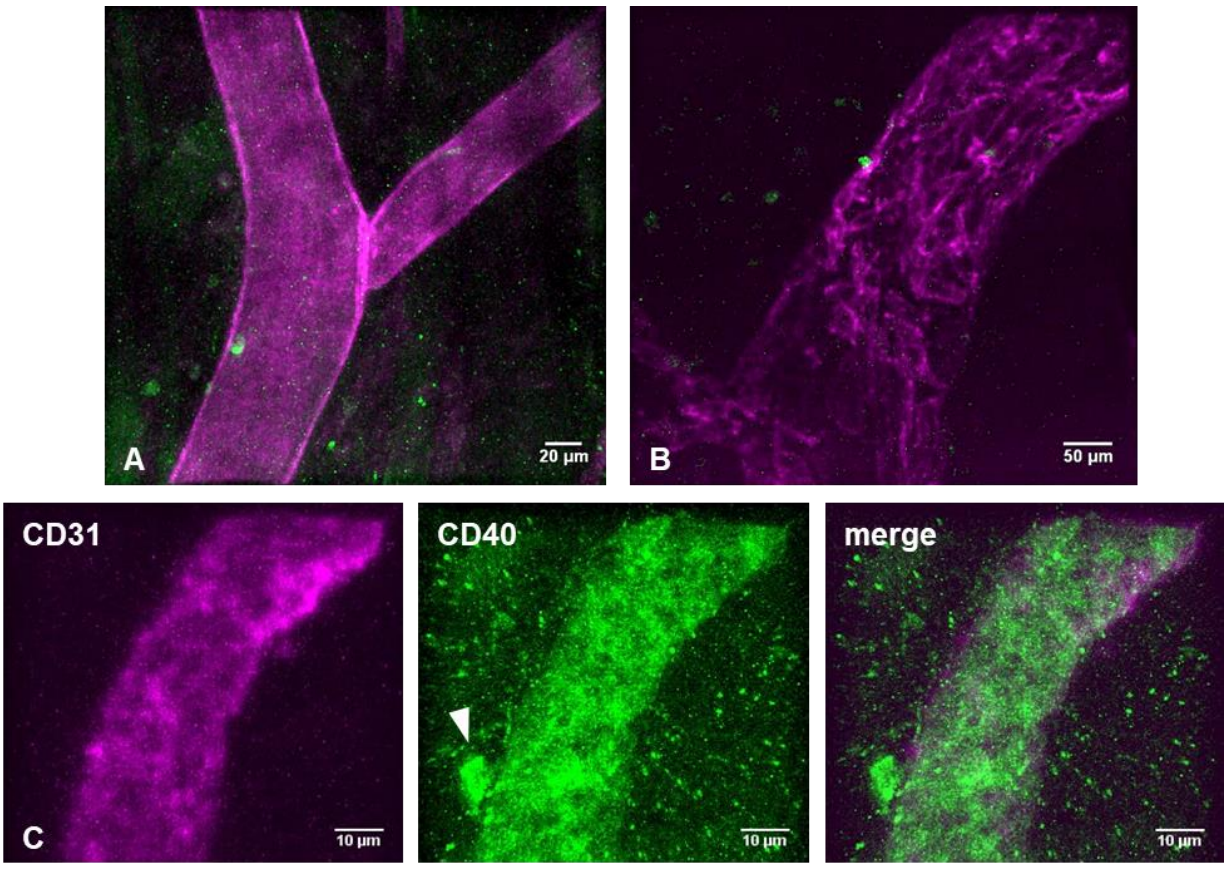

Figure 33: Inflamation induces CD40 receptor expression in the cremaster microcirculation. *No constitutive CD40 receptor expression was observed at baseline in the isolated cremaster of C57/BL6* ***(A)*** *or ADAMTS13ko* ***(B)*** *mice. CD40 (green) abundance was markedly increased following stimulation with TNF-α in C57/BL6 cremaster microcirculation. Due to their expression of CD40, perivascular leukocytes also became visible (white arrow head)* ***(C)****, violet=endothelium.*

5.13 Post-surgery trauma also upregulates CD40 expression in control and ADAMTS13 knockout mice

Since there was no use of TNF-α in our experimental groups for inducing endothelial cell CD40expression, it was important to check the “spontaneous” abundance following isolation of the cremaster muscle. For this purpose, we recorded the amount of CD40 on the luminal EC surface without any CD40L stimulation in the isolated cremaster of both wild type and ADAMTS13ko mice over the same 5-hour time period as in the experiments with CD40L stimulation.

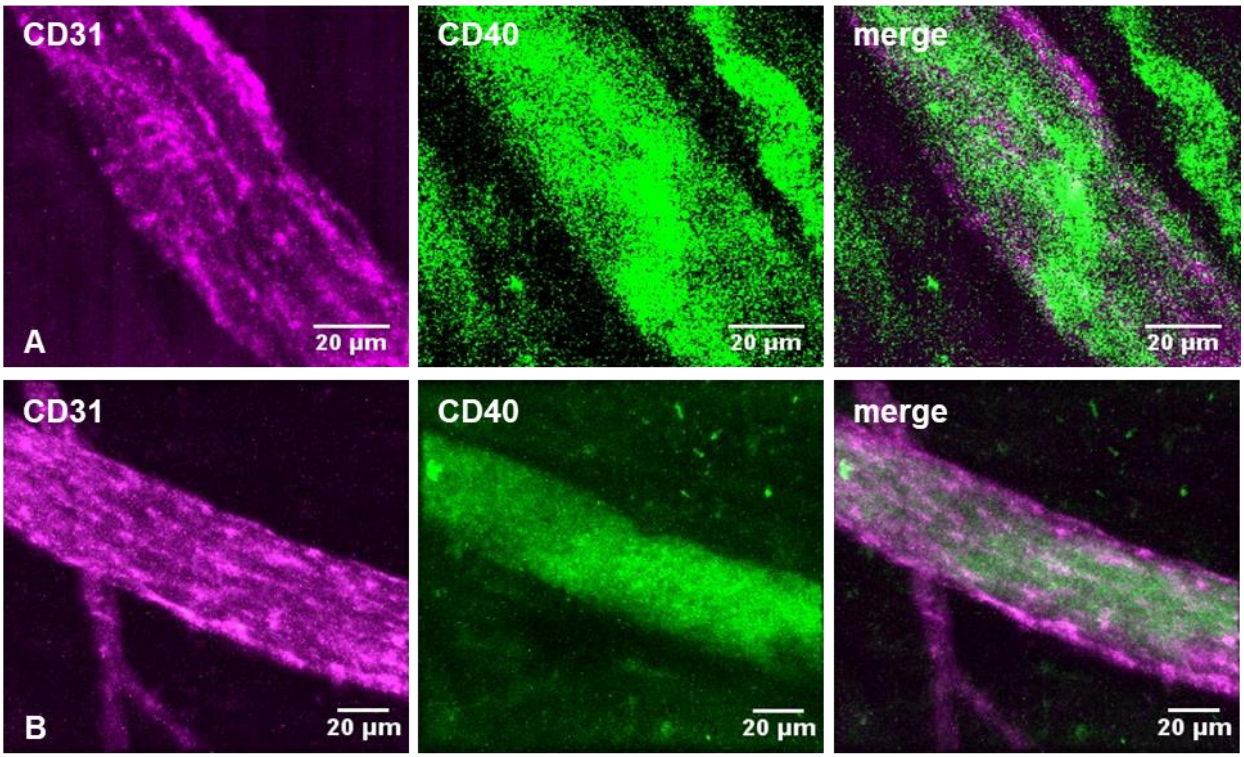

Figure 34: Post-surgery trauma also enhances endothelial cell CD40 (green) abundance in the isolated cremaster of *C57/BL6 (A) and ADAMTS13ko (B) mice*. *Representative images, violet=endothelium.*

Post-surgery trauma proved to be sufficient for inducing tissue inflammation and, as a consequence, a marked rise in endothelial cell CD40 abundance both in C57/BL6 and ADAMTS13ko mice (Figure 34). Yet again, no differentiation between arterioles and venules was possible in the fixed cremaster. About 73 % of the microvessels after 5

hours stained positive for endothelial cell CD40 (n=3, 30 observed vessels). In addition, the smooth muscle cells also stained positive for CD40 in some recordings.

5.14 CD40 and vWF partially co-localize in the microcirculation

So far, there was no evidence for the co-localization of CD40 and vWF in microvessels. To address this question, CD40 and vWF were labeled simultaneously by injecting the corresponding Qdot-labeled primary antibodies into the C57/BL6 mice followed by CD40L stimulation. This *in situ* labeling yielded a partial co-localization of CD40 and vWF in the microvessels. Interestingly, only the venules showed a labeling for both biomolecules although it was not homogenous, while the arterioles essentially remained unstained (Figure 35). This finding is in agreement with the preferential ULVWF multimer-platelet string formation and leukocyte extravasation in venules observed herein.

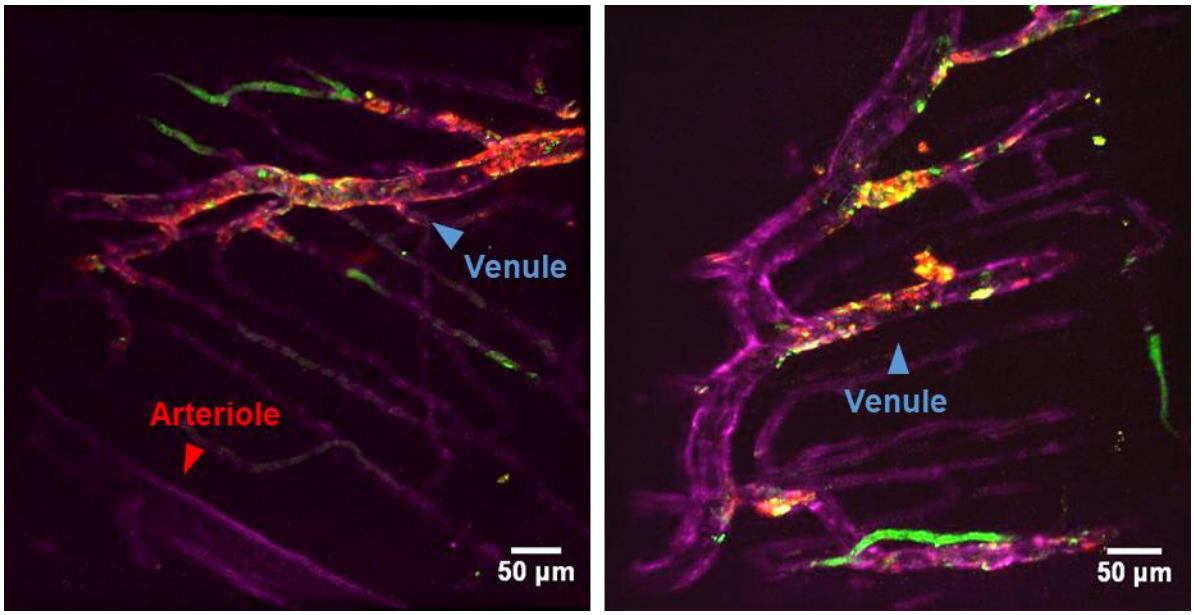

Figure 35: Partial co-localization of CD40 and vWF in venules. *Representative images of the simultaneous in situ staining of CD40 (green) and vWF (red) in the microcirculation of the cremaster of a C57/BL6 mouse, violet=endothelium.*

6. Discussion

Vascular remodeling processes involve the innate immune responses that can be linked to primary hemostasis. On the one hand, platelets maintain hemostasis by thrombus formation and prevent blood loss in case of tissue injury, but on the other hand the same mechanism can either lead to a life-threatening situation in advanced atherosclerosis (Lievens and von Hundelshausen 2011; Huo and Ley 2004) by causing acute thrombotic occlusion or result in a potentially life-saving mechanism of remodeling collateral arterioles during arteriogenesis (Van Hinsbergh and Tasev 2015; Deindl et al. 2011). Endothelial dysfunction serves as an early marker of vascular diseases and provides the platform for interaction of platelets with immune cells leading to inflammation. Both inflammation and coagulation are mutually dependent processes that can reinforce each other, however the underlying mechanism that links inflammation and coagulation to thrombosis and vascular remodeling still remains poorly understood. One of the important pathways that is implicated in the maintenance of blood vessel integrity is CD40-CD40L co-stimulation. The ligation of CD40L on numerous cell types has been found to play an essential role in inflammation leading to vascular remodeling (Mach et al. 1998; Henn et al. 1998). In this regard, particular emphasis herein was placed on investigating the interaction of platelets with endothelial and immune cells in a CD40-CD40L dependent manner particularly in the less well studied microcirculation.

During inflammatory reactions, resident cells of the innate immune system secrete cytokines and pro-inflammatory mediators that activate ECs. The activated endothelium expresses cell adhesion molecules including selectins on their surface which are recognized by the respective ligands on circulating leukocytes, initiating a cascade of events (Muller 2014). Leukocytes are then captured followed by their slow rolling, firm adhesion, adhesion strengthening, intraluminal crawling and transmigration (Vestweber 2015) (Figure 36). Leukocytes adhere and transmigrate mainly after direct interaction with EC adhesion molecules and leukocyte crawling seems not to be affected by ULVWF multimer-platelets strings. But it is well known that the intercellular crosstalk

between ECs and platelets serves as an additional gateway for leukocyte recruitment and eventually their transmigration into the vessel wall. The mechanism by which platelets link primary hemostasis to vascular remodeling by facilitating leukocyte recruitment to the vessel wall is still elusive. Inflammation-driven release and deposition of vWF on the luminal EC surfaces followed by the adherence and activation of platelets is such a likely link and can be described as an additional effect, perhaps especially when inflammation conditions occur which reinforce the expression of CD40 by the ECs.

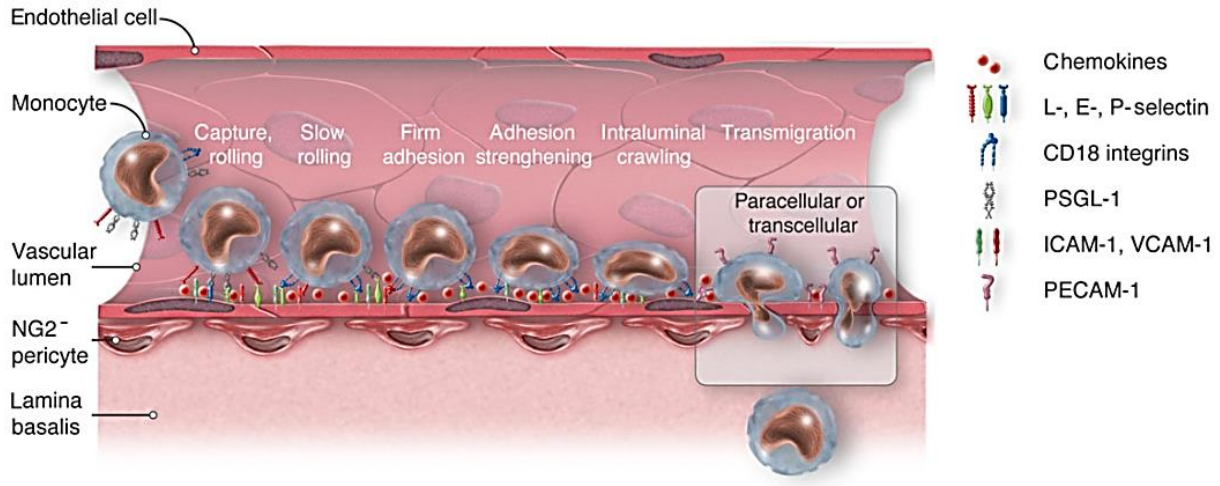

Figure 36: Schematic diagram of leukocyte trafficking across the vessel wall. *Leukocytes interact with the activated endothelium expressing adhesion molecules and chemokines, leading to a series of events comprising leukocyte capture, rolling, slow rolling, firm adhesion, adhesion strengthening, intraluminal crawling and subsequent transmigration that can be either paracellular or transcellular (Gerhardt and Ley 2015).*

Herein, we have shown that CD40L acts as a potent stimulus for ULVWF multimer-platelet recruitment also fostering recruitment of leukocytes and their extravasation in the murine microcirculation *in vivo.* Using the cremaster muscle preparation as a model, we have shown that EC CD40-(platelet) CD40L interaction induces release from and deposition of ULVWF multimers on the luminal surface of the ECs that is followed by platelet binding to vWF in a pearl necklace-like conformation leading to their activation. This in turn leads to the recruitment of leukocytes distal to the site of formation of these ULVWF multimer-platelet strings and their transmigration, namely in venules. This

mechanism may thus be an important player in inflammation-enhanced vascular remodeling though it can hardly explain arteriolar remodeling by direct interaction.

6.1 CD40L: a potent vWF secretagogue in vascular ECs

Elevated plasma levels of CD40L have been observed in patients suffering from cardiovascular diseases including coronary artery disease, hypercholesterolemia, unstable angina and acute myocardial infarction (Antoniades et al. 2009; Tousoulis et al. 2010). Another study has shown that CD40-CD40L interaction on ECs increases their generation of ROS which is regarded as an initial symptom of endothelial dysfunction (Chakrabarti et al. 2007). The impaired endothelium serves as an anchoring site for surveilling platelets that lead to their activation. Recently, it has been shown by our group that human platelet-bound or soluble CD40L induces the calcium-dependent release of vWF from WPB stores of human ECs in the presence of shear stress *in vitro* (Moller et al. 2015) thus potentially further enhancing platelet adhesion and activation. In our study, we used the commercially available MegaCD40L to stimulate ECs and we also observed CD40L to be a potent stimulus for vWF-mediated platelet adhesion in the murine microcirculation *in vivo.*

The predilection sites for vWF accumulation on the EC surface were found to be venules where also platelet adhesion and leukocyte extravasation were preferentially. Interestingly, ULVWF multimer deposits were not limited to bifurcations which are believed to be especially prone for initiating vascular inflammation. The straight regions were also partly covered by ULVWF multimer-platelet strings albeit to a lesser extent. ULVWF multimer buildup in response to CD40L stimulation was found to be a time-dependent process with a linear increase in vWF concatamer formation within the microvessels which probably reflects the time-dependent expression of CD40 on the luminal EC surface as observed after surgical preparation of the cremaster.

Though we have directly demonstrated the presence of extracellular vWF in venules, we cannot exclude that part of this signal came also from the trapped platelets releasing vWF from their α-granules at the site of adhesion. Therefore, it is difficult to

quantitatively evaluate the role of endothelial vWF as compared to platelet vWF in our setting. However, other studies have clearly identified the endothelium as a source of ULVWF multimers *in vivo* (Chauhan et al. 2007). Moreover, *in vitro* data suggest that vWF concatamers normally are stored in the WPBs as a globular molecule which upon release can stretch up to a length of 100 µm (Schneider et al. 2007). CD40-CD40L interaction also induces the expression of CD40L on the EC surface *in vitro* which can be seen at both the mRNA and protein level after CD40L stimulation (Wagner et al. 2004). It appeared to influence the inflammatory response by activation of transmigrating CD40-expressing monocytes.

In addition, platelets are also known to become activated by the constitutively expressed CD40 on their surface. The ligation of platelet CD40L to platelet CD40 induces the expression of CD62P, release of platelet α and dense granules together with the morphological changes linked to activated platelets (Inwald et al. 2003). Since vWF is stored in platelet α-granules, platelet activation causes its release at sites of platelet adhesion that recruit more platelets and circulating leukocytes, hence exacerbating the inflammatory response. In another study platelet CD40 was found to play an essential role in inflammation by transcellular activation of ECs and leukocytes (Gerdes et al. 2016). Therefore, CD40-CD40L interactions may play a central role in boosting the ensuing pro-inflammatory response through the simultaneous two-way activation of ECs platelets and leukocytes. In our experiments, it cannot be excluded therefore that part of the superligand we used for EC stimulation may also have reached platelets directly and activated them. However, we consider this not likely since the streaming blood may have rapidly dissolved any superficially applied CD40L eventually permeating the internal elastic lamina and the endothelial barrier.

6.2 Formation of ULVWF multimer-platelet strings in response to CD40L stimulation

ECs and platelets tightly regulate expression of the CD40 receptor and its ligand (CD40L) on their surfaces. We have observed that the endothelium did not express CD40 at all under resting conditions, unlike the endothelium of atherosclerotic large

arteries (Korff et al. 2007). Only upon TNF-α stimulation or inflammation due to surgical trauma, ECs started to express CD40 on their surface preferentially in venules. The CD40-dependent release of vWF from WPBs in ECs results in the deposition of ULVWF multimers on their luminal surface that provide the binding sites for platelet adhesion. Platelet-vWF interaction is initiated by the weak reversible binding of platelet GPIbα to theA1 domain of vWF (Madabhushi et al. 2014) that permits platelet rolling and adhesion on the EC surface which is reinforced by platelet GPIIb-IIIα (also called integrin αIIbβ3) interaction with the C1 domain of vWF (Bryckaert et al. 2015; Savage et al. 1996). As a consequence, in our experimental model, the murine cremaster microcirculation, pearl necklace-like ULVWF multimer-platelet string formation was observed. The co-localization of platelet strings with the released vWF shows their direct interaction on the EC surface, but it is still not clear whether this co-localization was only with endothelium-derived or additionally with platelet-derived vWF, since we were not able to differently label them.

ULVWF multimer-platelet strings formed both in arterioles and venules after CD40L treatment *in vivo* but were clearly more prevalent in venules in spite of the lower shear rate there. Whether the sparse formation in arterioles can support a possible role in arterial thrombosis remains to be studied in more detail. Moreover, arteriolar remodeling seems not to be induced directly by enhanced ULWF multimer-platelet string formation and platelet activation in the arterioles themselves, though higher numbers of perivascular monocytes have been observed in arterioles undergoing arteriogenesis (Deindl and Schaper 2005). Whether venous platelet adhesion supports emigration of monocytes which secondarily migrate towards arterioles has not yet been studied. Bifurcations having disturbed flow conditions are considered in the macrocirculation to be the regions with high predisposition towards thrombus formation and atherosclerosis (Spanos et al. 2016; Chiu and Chien 2011). In the microcirculation, the occurrence of ULVWF multimer-platelet strings was not strictly limited to bifurcations as many were observed in linear regions as well. The length of the platelet strings observed in our experimental studies in the microvasculature ranged from 10 to 140 µm, though this only incompletely can indicate the true length of the vWF concatamers. Moreover, we have shown that our labeling with exogenous platelets underestimates the number and

length of the platelet strings. Therefore it is difficult to compare our results with the ones of others reported for the microcirculation. However, within these constraints our findings are in agreement with results reported before by others. In mesenteric vessels *in vivo* platelet strings in the range between 30 and 100 µm length have been reported (Chauhan et al. 2007). However, much longer platelet strings have been observed *in vitro* in response to CD40L stimulation, ranging from 100 to 300 µm (Moller et al. 2015). Under *in vitro* conditions, the length of fully stretched vWF was found to be around 100 µm (Schneider et al. 2007). Of note, one study has shown extraordinarily long platelet-decorated ULVWF strings on the EC surface with a maximum length of 3 mm at a shear stress of 2.5 dyn/cm^2 (Dong 2005). Surprisingly, the lack of the ULVWF multimer-cleaving enzyme ADAMTS13 had not generally increased the length of platelet strings herein, indicating that other mechanisms may also be involved in the control of string length.

The platelet strings were anchored to the endothelium for a comparatively long time period of approximately 30 min in comparison to previously observed periods of 45 s on average (Chauhan et al. 2007). The contribution of platelets in thrombus development is dependent on their adhesive properties and the longer they adhere the more likely is the buildup of a thrombus. Upon activation by platelet agonists, like ADP or thromboxane A_2, adherent platelets transition into a highly active state that enables them to recruit additional platelets to the site of injury, which is mediated by their GPIbα receptors. This whole platelet buildup can then result in a progression towards thrombosis, which could be explained herein by the detection of blocked vessels with minor to no flow in ADAMTS13ko blood vessels. Nonetheless, the degree of thrombosis also in these animals appeared to be rather low following stimulation with CD40L.

6.3 Effect of ADAMTS13 on the number of ULVWF multimer-platelet strings

VWF defines a fine line between carrying out normal hemostasis and causing potential life-threatening thrombotic events. It is therefore very important to maintain regular

levels of this protein in plasma which is taken care of by ADAMTS13. In the context of its proteolytic action, it has long been believed that ADAMTS13 is a constitutively active enzyme in plasma efficiently cleaving ULVWF multimers upon encounter, but recently it has been shown that ADAMTS13 is itself activated by conformational changes after vWF-ADAMTS13 inter-domain interactions (South et al. 2017). ADAMTS13 plays an important role in maintaining vascular integrity by preventing thrombus formation whereas its deficiency has been related to various microangiopathies including the life-threatening microangiopathy TTP (Zheng et al. 2001). Recently, low plasma ADAMTS13 activity has also been associated with an increased risk of ischemic stroke. Moreover, it has been reported in many studies that the high plasma levels of vWF are directly linked to an increase risk of cardiovascular diseases including myocardial infarction and ischemic stroke (Wieberdink et al. 2010; Wannamethee et al. 2012; Bongers et al. 2006). The link between low levels of ADAMTS13 and the increased risk of ischemic stroke can be explained by the reduced cleavage of ULVWF multimers, which by nature are highly pro-thrombotic, on the EC surface. As a result, there is an increased incidence of ULVWF multimers which may be further aggravated by enhanced CD40 expression, providing even more binding sites for platelet adhesion at the damaged site thus leading to thrombus progression. Therefore, low ADAMTS13 plasma levels as observed in patients with coronary heart disease may contribute to the pro-thrombotic and pro-inflammatory state of the vessel wall.

In our study we also observed a similar role of ADAMTS13 in platelet adhesion on the EC surface. In C57/BL6 control mice, platelet adhesion to the vessel wall was rather low in venules and particularly in arterioles because of the presence of ADAMTS13 in the plasma (and on the ECs). However, in spite of this the balance can be shifted towards a higher number of ULVWF multimer-platelet strings upon exposure to CD40L. This possibly could be due to more release of vWF (which was profound in venules) from the endothelial cell WPBs in response to CD40L stimulation while the abundance and activity of ADAMTS13 did not change. In contrast, deficiency of ADAMTS13 significantly augmented the number of platelet strings at the luminal EC surface *in vivo* in the absence and presence of CD40L. Moreover, this effect was restricted to venules. Therefore, the (relative) lack of ADAMTS13 might become most important under pro-

inflammatory conditions where endothelial cell CD40 expression is upregulated. The difference in platelet string formation in arterioles and venules (of the same animal) despite identical ADAMTS13 plasma levels and exposure to CD40L stimulation supports the idea that the preferential ULVWF multimer-platelet string formation in venules is closely related to the abundance of endothelial cell CD40 in these microvessels.

6.4 Is shear stress a regulator of endothelial cell vWF release and platelet string formation?

Shear stress, which is a product of shear rate and plasma viscosity, is an important parameter for controlling EC function and is known to play a significant role in every stage of vascular remodeling. With regard to ULVWF multimers, shear stress facilitates uncoiling of the vWF concatamer, so that more binding sites become available for platelet adhesion leading to their activation and subsequently an augmentation of the ensuing pro-inflammatory response (Casa and Ku 2017). According to *in vitro* studies, shear stress has received much attention in this regard and is believed to be directly involved in controlling vascular integrity by regulating both vWF-platelet and vWF-ADAMTS13 interactions (Reininger 2015; Bonazza et al. 2015). Several groups have shown that non-physiologically high shear stress causes activation of platelets in the absence of any agonist (Kroll et al. 1996) via GPIbα and GPIIb/IIIα-mediated interactions with vWF (Goto et al. 2000; Tamura et al. 2002). Shear stress regulates the length of ULVWF multimers. Once vWF is stretched upon encountering a critical level of shear stress they expose their cleavage sites for ADAMTS13 (Huisman et al. 2017) and serve as a preferential substrate for ADAMTS13 cleavage in the presence of shear stress (Shim et al. 2008).

Arterioles should always have a higher shear rate in comparison to venules (Papaioannou and Stefanadis 2005). It has been shown in older humans that exercise-induced shear stress raises the plasma level of vWF through EC activation (Gonzales et al. 2009). As pointed out before, shear stress dynamically regulates ULVWF multimers

by not only exposing their binding sites for platelets but also their faster cleavage by increasingly exposing cleavage sites ADAMTS13. These opposing effects are probably the reason why we did not observe any elongation of platelet strings in arterioles as compared to venules under control conditions. We did also not find that shear stress could affect the number of platelet strings, since in arterioles and venules with comparable shear stress (shear rate) the arteriolar/venular distribution of ULVWF multimer-platelet strings was not altered compared to the overall situation.

To take a step further, the lengths of platelet strings was measured and compared between the experimental groups. Although the higher shear rate in arterioles should have facilitated multimerization and unfolding of vWF units, this was not observed in control mice. However, it was very interesting to find that shear rate was in fact playing some role in arterioles in the absence of ADAMTS13 where the string length was significantly higher than in venules, suggesting that ADAMTS13 may cleave the unfolded ULVWF multimer-platelet strings in arterioles more effectively as shown *in vitro* (Gogia and Neelamegham 2015).

6.5 Preferential leukocyte extravasation in venules

Even though there are many cells contributing to vascular remodeling including ECs, vascular SMCs, granular and agranular leukocytes, the major cell type mediating the pro-inflammatory response are monocyte-derived macrophages (Bobryshev 2006). CD40L stimulation of ECs induces their expression of CD40L and their release of MCP-1 enabling the enhanced recruitment of CD40-positive immune cells (Wagner et al. 2004; Chakrabarti et al. 2007). Leukocyte recruitment to the vessel wall has been the hallmark of pathophysiologic remodeling processes in large vessels (Braunersreuther and Mach 2006). Therefore, understanding the mechanism by which these leukocytes arrive at the vessel wall is essential, as it might give us therapeutic targets for driving the vascular remodeling processes and preventing disease onset and/or progression.

In our *in vivo* studies we labeled leukocytes intravascularly to ensure that the leukocytes which we observed in perivascular tissue are derived from the circulating blood. It was

interesting to note that despite the formation of ULVWF multimer-platelet strings in both arterioles and venules, leukocyte extravasation was observed only in venules. By carefully following the labeled leukocytes, there was preferential leukocyte adherence and transmigration towards regions with visible ULVWF multimer-platelet strings. This is in accordance with the findings of others (Zuchtriegel et al. 2016). Of note is that regions devoid of platelet strings even in the same vessel behaved normally with circulating platelets and leukocytes, showing no apparent sign of either adhesion or transmigration, though the endothelium there probably constitutively expressed adhesion molecules for integrin-dependent leukocyte adhesion (Bevilacqua 1993; Cybulsky and Gimbrone 1991; Dustin et al. 1986). Consequently, it provides direct evidence that ULVWF-tethered platelets (Andre et al. 2000) serve as a preferential docking site for circulating leukocytes (van Gils et al. 2009; Brill et al. 2011; Bernardo et al. 2005). Moreover, leukocyte transmigration was enhanced in the absence of ADAMTS13, namely following CD40L stimulation. Impaired ADAMTS13 activity is expected to reduce ULVWF multimer degradation on the EC surface, thus reinforcing platelet adhesion and in turn leukocyte transmigration.

Since we observed leukocytes to extravasate from venules only, it is partly due to the preferential ULVWF multimer deposition in venules which was also in line with our *in situ* staining data. It was interesting that leukocyte extravasation which initially started from the ULVWF multimer-platelet string hotspots spread to the vicinity of such regions. It suggests that the adhered platelets therein initiated leukocyte transmigration which then signals to nearby ECs in a paracrine fashion leading to increased permeability and massive leukocyte transmigration. As we were unable to visualize individual ECs with distinct cell borders at such sites, we could not distinguish between paracellular and transcellular leukocyte transmigration.

6.6 CD40 receptor expression

The CD40 receptor is an important co-stimulatory molecule for both humoral and cell-mediated immune responses (Grewal and Flavell 1998; van Kooten and Banchereau

2000). It was initially characterized in lymphomas and carcinomas (Paulie et al. 1985; O'Grady et al. 1994) but later on its presence on non-immune cells (like ECs) opened a new era of investigation. Since long CD40 expression has been studied on ECs in culture as well in tissues which upregulate CD40 expression in response to inflammatory mediators such as TNF-α, IL-1, IFN-β and IFN-γ, and also in inflamed tissues (Karmann et al. 1995; Pammer et al. 1996). Because of its detection on ECs in inflammatory responses, it is believed that CD40 actively participates in inflammation. The interaction of CD40 receptor on ECs with its ligand leads to EC activation which is mediated by the expression of E-selectin, ICAM-1 and VCAM-1 on the EC surface (Hollenbaugh et al. 1995). The upregulation of these adhesion molecules then aids in the recruitment and activation of leukocytes at the sites of inflammation. Small interfering RNA silencing of endothelial CD40 receptor expression has shown to prevent CD40L-mediated leukocyte adhesion (Pluvinet et al. 2004). This shows the importance of endothelial CD40 expression in pro-inflammatory responses.

However, little is known about the distribution of CD40 on microvascular ECs *in vivo*. Herein, we show that CD40 expression on normal microvascular ECs is minimal but that its expression is responsive to inflammation as was observed by a prominent increase in its expression in response to TNF-α stimulation. The time period of only two hours for this effect to occur suggests that CD40 may not be synthesized *de novo*, but is transported from intracellular EC stores to the surface, which warrants further investigation regarding the molecular mechanism involved therein. To verify that CD40 expression is upregulated in our model, surgically prepared cremasters were kept untreated for 5 hours. This post-surgery trauma proved to be sufficient for raising endothelial cell CD40 abundance primarily in the venules. However, this was not a general phenomenon throughout these microcirculatory blood vessels.

Previously, endothelial cell CD40 distribution in bigger vessels has been studied *ex vivo* in mice and was shown to be mainly expressed in veins (mesenteric and femoral vein) but not in arteries (mesenteric and femoral artery) (Korff et al. 2007). But its distribution in the microvessels was not clear. We therefore studied CD40 receptor distribution in the murine cremaster microcirculation both under fixed and living conditions. During *in vivo* experiments, we tracked CD40 by using very bright Qdot-labeled anti-CD40

antibodies that enabled us to visualize surface CD40 in conjunction with other labeled cells. Here, we also report that CD40 is distributed mainly in the venules and capillaries but usually not in arterioles *in vivo*, which suggests that its distribution is governed by the microenvironment. Arteriolar specific determinants seem to prevent the expression of CD40 on ECs while venular and capillary specific determinants enhance its expression, the latter being involved in the inflammatory processes by the recruitment and adhesion of leukocytes.

In addition, the co-localization of CD40 with vWF concatamers on the luminal EC surface of only venules and small capillaries *in vivo* suggests a heterogeneous expression pattern the reason for which is still unknown. Part of the inhomogeneous distribution could be attributed to the possibility that the detected CD40 was not solely derived from ECs, but also from leukocytes and platelets gathered at the prototypic site of leukocyte diapedesis in inflammation, i.e. the post-capillary venules. Similarly, the detected vWF could have been platelet-derived as well, released from the vWF-bound activated platelets at these sites.

6.7 General Discussion

There is strong evidence that platelet-mediated EC-leukocyte interactions increase significantly during cardiovascular events (Totani and Evangelista 2010; Sarma et al. 2002) or in the presence of prototypic cardiovascular risk factors like hypertension or dyslipidemia on blood vessels in such diseases (Kossmann et al. 2017). It is still not clear though whether these interactions are the cause or consequence of such events. Animal models of vascular diseases like atherosclerosis have shown platelets to be an important regulator of disease progression (Massberg et al. 2004). Moreover, both the *in vivo* and *in vitro* data support that platelets play a role in vascular remodeling (physiologic or pathophysiologic response) by recruiting leukocytes to the vessel wall (Gawaz et al. 2005). It is still an open question whether interfering with this platelet-mediated leukocyte recruitment will have any beneficial effect in controlling cardiovascular diseases especially in the microcirculation.

Since vWF concatamers were preferentially deposited on the venular endothelium where they co-localized with platelet strings and CD40 we suggest that pro-inflammatory leukocyte extravasation preferentially takes place at such hotspots presumably following platelet activation due to binding to vWF multimers that had been released from the ECs, at least in part, through platelet-CD40L stimulation. A similar mechanism may reinforce leukocyte diapedesis at macrovascular atherosclerosis predilection sites where endothelial cell CD40 is upregulated (Korff et al. 2007). Leukocyte transmigration in venules and capillaries but not arterioles suggests that vascular remodeling processes which take place in arterioles and arteries might be facilitated by these transmigrated leukocytes that somehow line up alongside the arteriolar vessel wall and release chemotactic mediators or migrate themselves into the arteriolar vessel wall from “behind” to maintain the pro-inflammatory process.

ADAMTS13 controls the interaction between ECs and platelet by cleaving released ULVWF multimers into smaller inactive fragments (Crawley et al. 2011). The absence of ADAMTS13 enhances platelet adhesion and leukocyte transmigration especially in conditions of CD40L stimulation. Because of the co-expression of CD40 and CD40L on platelets and ECs alike during such an inflammatory episode, it may greatly augment the immune response during cardiovascular events (Figure 37). Therefore both molecules might provide a suitable therapeutic target for intervening in unwanted interactions between immune and non-immune cells during the onset or progression of vascular diseases.

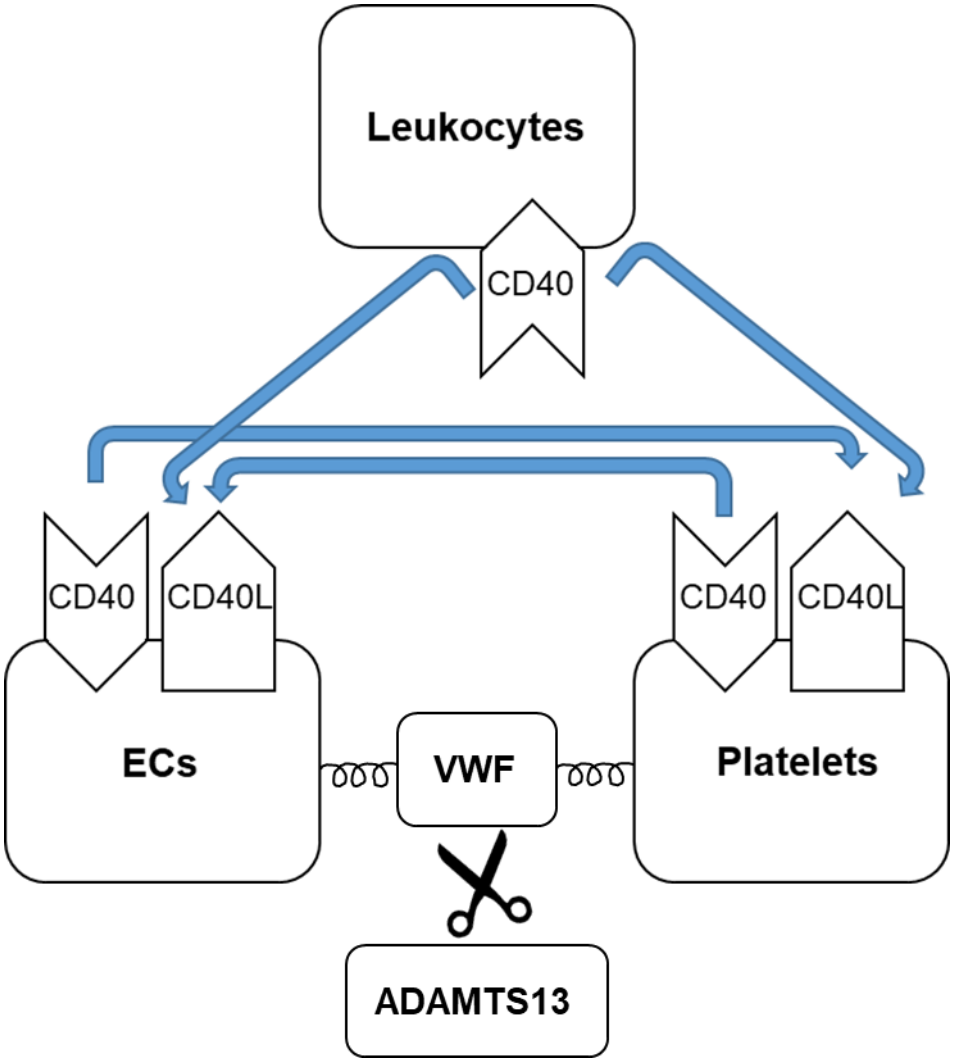

Figure 37: Possible CD40-CD40L mediated interactions between immune and non-immune cells. *Schematic diagram showing the potential CD40-CD40L mediated interactions between ECs, platelets and leukocytes. ADAMTS13 can regulate these interactions by cleaving vWF concatamers into smaller monomers thus limiting platelet-EC interaction.*

7. Outcome

Taken together, our study revealed the following:

1. CD40L induces vWF-platelet string formation on the surface of microvascular EC preferentially in venules *in vivo*.
2. ADAMTS13 deficiency augments the number of vWF-platelet strings formed following CD40L stimulation.
3. Shear stress plays no obvious role for the number of vWF-platelet strings but enhances vWF-platelet string length in arterioles in the absence of ADAMTS13.
4. Leukocyte extravasation prevails in areas with high density of vWF-tethered platelets.
5. In the microvasculature, CD40 expression on EC appears to be highly dependent on the microenvironment with preferential localization in venules and capillaries.
6. CD40-positive EC partially co-localize with vWF in venules and capillaries *in vivo.*

Bibliography

Akyol O, Akyol S, Chen CH (2016) Update on ADAMTS13 and VWF in cardiovascular and hematological disorders. Clin Chim Acta 463:109-118. doi:10.1016/j.cca.2016.10.017

Amano H, Ito Y, Eshima K, Kato S, Ogawa F, Hosono K, Oba K, Tamaki H, Sakagami H, Shibuya M, Narumiya S, Majima M (2015) Thromboxane A2 induces blood flow recovery via platelet adhesion to ischaemic regions. Cardiovasc Res 107 (4):509-521. doi:10.1093/cvr/cvv139

Andre P, Denis CV, Ware J, Saffaripour S, Hynes RO, Ruggeri ZM, Wagner DD (2000) Platelets adhere to and translocate on von Willebrand factor presented by endothelium in stimulated veins. Blood 96 (10):3322-3328

Antoniades C, Bakogiannis C, Tousoulis D, Antonopoulos AS, Stefanadis C (2009) The CD40/CD40 ligand system: linking inflammation with atherothrombosis. J Am Coll Cardiol 54 (8):669-677. doi:10.1016/j.jacc.2009.03.076

Aponte-Santamaria C, Huck V, Posch S, Bronowska AK, Grassle S, Brehm MA, Obser T, Schneppenheim R, Hinterdorfer P, Schneider SW, Baldauf C, Grater F (2015) Force-sensitive autoinhibition of the von Willebrand factor is mediated by interdomain interactions. Biophys J 108 (9):2312-2321. doi:10.1016/j.bpj.2015.03.041

Bernardo A, Ball C, Nolasco L, Choi H, Moake JL, Dong JF (2005) Platelets adhered to endothelial cell-bound ultra-large von Willebrand factor strings support leukocyte tethering and rolling under high shear stress. J Thromb Haemost 3 (3):562-570. doi:10.1111/j.1538-7836.2005.01122.x

Bevilacqua MP (1993) Endothelial-leukocyte adhesion molecules. Annu Rev Immunol 11:767-804. doi:10.1146/annurev.iy.11.040193.004003

Bobryshev YV (2006) Monocyte recruitment and foam cell formation in atherosclerosis. Micron 37 (3):208-222. doi:10.1016/j.micron.2005.10.007

Bonazza K, Rottensteiner H, Schrenk G, Frank J, Allmaier G, Turecek PL, Scheiflinger F, Friedbacher G (2015) Shear-Dependent Interactions of von Willebrand Factor with Factor VIII and Protease ADAMTS 13 Demonstrated at a Single Molecule Level by Atomic Force Microscopy. Anal Chem 87 (20):10299-10305. doi:10.1021/acs.analchem.5b02078

Bongers TN, de Bruijne EL, Dippel DW, de Jong AJ, Deckers JW, Poldermans D, de Maat MP, Leebeek FW (2009) Lower levels of ADAMTS13 are associated with cardiovascular disease in young patients. Atherosclerosis 207 (1):250-254. doi:10.1016/j.atherosclerosis.2009.04.013

Bongers TN, de Maat MP, van Goor ML, Bhagwanbali V, van Vliet HH, Gomez Garcia EB, Dippel DW, Leebeek FW (2006) High von Willebrand factor levels increase the risk of first ischemic stroke: influence of ADAMTS13, inflammation, and

genetic variability. Stroke 37 (11):2672-2677. doi:10.1161/01.STR.0000244767.39962.f7

Braunersreuther V, Mach F (2006) Leukocyte recruitment in atherosclerosis: potential targets for therapeutic approaches? Cell Mol Life Sci 63 (18):2079-2088. doi:10.1007/s00018-006-6127-2

Brill A, Fuchs TA, Chauhan AK, Yang JJ, De Meyer SF, Kollnberger M, Wakefield TW, Lammle B, Massberg S, Wagner DD (2011) von Willebrand factor-mediated platelet adhesion is critical for deep vein thrombosis in mouse models. Blood 117 (4):1400-1407. doi:10.1182/blood-2010-05-287623

Bruce AC, Kelly-Goss MR, Heuslein JL, Meisner JK, Price RJ, Peirce SM (2014) Monocytes are recruited from venules during arteriogenesis in the murine spinotrapezius ligation model. Arterioscler Thromb Vasc Biol 34 (9):2012-2022. doi:10.1161/ATVBAHA.114.303399

Bryckaert M, Rosa JP, Denis CV, Lenting PJ (2015) Of von Willebrand factor and platelets. Cell Mol Life Sci 72 (2):307-326. doi:10.1007/s00018-014-1743-8

Cai H, Griendling KK, Harrison DG (2003) The vascular NAD(P)H oxidases as therapeutic targets in cardiovascular diseases. Trends Pharmacol Sci 24 (9):471-478. doi:10.1016/S0165-6147(03)00233-5

Cai H, Harrison DG (2000) Endothelial dysfunction in cardiovascular diseases: the role of oxidant stress. Circ Res 87 (10):840-844

Casa LDC, Ku DN (2017) Thrombus Formation at High Shear Rates. Annu Rev Biomed Eng 19:415-433. doi:10.1146/annurev-bioeng-071516-044539

Chaabane C, Coen M, Bochaton-Piallat ML (2014) Smooth muscle cell phenotypic switch: implications for foam cell formation. Curr Opin Lipidol 25 (5):374-379. doi:10.1097/MOL.0000000000000113

Chakrabarti S, Blair P, Freedman JE (2007) CD40-40L signaling in vascular inflammation. J Biol Chem 282 (25):18307-18317. doi:10.1074/jbc.M700211200

Chandraratne S, von Bruehl ML, Pagel JI, Stark K, Kleinert E, Konrad I, Farschtschi S, Coletti R, Gartner F, Chillo O, Legate KR, Lorenz M, Rutkowski S, Caballero-Martinez A, Starke R, Tirniceriu A, Pauleikhoff L, Fischer S, Assmann G, Mueller-Hoecker J, Ware J, Nieswandt B, Schaper W, Schulz C, Deindl E, Massberg S (2015) Critical role of platelet glycoprotein ibalpha in arterial remodeling. Arterioscler Thromb Vasc Biol 35 (3):589-597. doi:10.1161/ATVBAHA.114.304447

Chauhan AK, Goerge T, Schneider SW, Wagner DD (2007) Formation of platelet strings and microthrombi in the presence of ADAMTS-13 inhibitor does not require P-selectin or beta3 integrin. J Thromb Haemost 5 (3):583-589. doi:10.1111/j.1538-7836.2006.02361.x

Chiu JJ, Chien S (2011) Effects of disturbed flow on vascular endothelium: pathophysiological basis and clinical perspectives. Physiol Rev 91 (1):327-387. doi:10.1152/physrev.00047.2009

Choi WS, Jeon OH, Kim DS (2010) CD40 ligand shedding is regulated by interaction between matrix metalloproteinase-2 and platelet integrin alpha(IIb)beta(3). J Thromb Haemost 8 (6):1364-1371. doi:10.1111/j.1538-7836.2010.03837.x

Crawley JT, de Groot R, Xiang Y, Luken BM, Lane DA (2011) Unraveling the scissile bond: how ADAMTS13 recognizes and cleaves von Willebrand factor. Blood 118 (12):3212-3221. doi:10.1182/blood-2011-02-306597

Crawley JT, Scully MA (2013) Thrombotic thrombocytopenic purpura: basic pathophysiology and therapeutic strategies. Hematology Am Soc Hematol Educ Program 2013:292-299. doi:10.1182/asheducation-2013.1.292

Cybulsky MI, Gimbrone MA, Jr. (1991) Endothelial expression of a mononuclear leukocyte adhesion molecule during atherogenesis. Science 251 (4995):788-791

Danese S, Scaldaferri F, Papa A, Pola R, Gasbarrini A, Sgambato A, Cittadini A (2004) CD40L-positive platelets induce CD40L expression de novo in endothelial cells: adding a loop to microvascular inflammation. Arterioscler Thromb Vasc Biol 24 (9):e162. doi:10.1161/01.ATV.0000138073.91195.70

De Ceunynck K, De Meyer SF, Vanhoorelbeke K (2013) Unwinding the von Willebrand factor strings puzzle. Blood 121 (2):270-277. doi:10.1182/blood-2012-07-442285

De Maeyer B, De Meyer SF, Feys HB, Pareyn I, Vandeputte N, Deckmyn H, Vanhoorelbeke K (2010) The distal carboxyterminal domains of murine ADAMTS13 influence proteolysis of platelet-decorated VWF strings in vivo. J Thromb Haemost 8 (10):2305-2312. doi:10.1111/j.1538-7836.2010.04008.x

De Marco L, Girolami A, Zimmerman TS, Ruggeri ZM (1986) von Willebrand factor interaction with the glycoprotein IIb/IIa complex. Its role in platelet function as demonstrated in patients with congenital afibrinogenemia. J Clin Invest 77 (4):1272-1277. doi:10.1172/JCI112430

De Meyer SF, Stoll G, Wagner DD, Kleinschnitz C (2012) von Willebrand factor: an emerging target in stroke therapy. Stroke 43 (2):599-606. doi:10.1161/STROKEAHA.111.628867

de Vries MR, Peters EA, Quax PH, Nossent AY (2017) von Willebrand factor deficiency leads to impaired blood flow recovery after ischaemia in mice. Thromb Haemost. doi:10.1160/TH16-12-0957

Deindl E, Pagel JI, von Bruehl ML, Schaper W, Massberg S (2011) Functional role of the platelet glycopeptide receptor type GPIbα in arteriogenesis. The FASEB Journal 25 (1 Supplement):1092.1014

Deindl E, Schaper W (2005) The art of arteriogenesis. Cell Biochem Biophys 43 (1):1-15. doi:10.1385/CBB:43:1:001

Dhanesha N, Prakash P, Doddapattar P, Khanna I, Pollpeter MJ, Nayak MK, Staber JM, Chauhan AK (2016) Endothelial Cell-Derived von Willebrand Factor Is the Major Determinant That Mediates von Willebrand Factor-Dependent Acute Ischemic Stroke by Promoting Postischemic Thrombo-Inflammation. Arterioscler Thromb Vasc Biol 36 (9):1829-1837. doi:10.1161/ATVBAHA.116.307660

Dong JF (2005) Cleavage of ultra-large von Willebrand factor by ADAMTS-13 under flow conditions. J Thromb Haemost 3 (8):1710-1716. doi:10.1111/j.1538-7836.2005.01360.x

Dong JF, Moake JL, Bernardo A, Fujikawa K, Ball C, Nolasco L, Lopez JA, Cruz MA (2003) ADAMTS-13 metalloprotease interacts with the endothelial cell-derived ultra-large von Willebrand factor. J Biol Chem 278 (32):29633-29639. doi:10.1074/jbc.M301385200

Dong JF, Moake JL, Nolasco L, Bernardo A, Arceneaux W, Shrimpton CN, Schade AJ, McIntire LV, Fujikawa K, Lopez JA (2002) ADAMTS-13 rapidly cleaves newly secreted ultralarge von Willebrand factor multimers on the endothelial surface under flowing conditions. Blood 100 (12):4033-4039. doi:10.1182/blood-2002-05-1401

Drexler H, Hornig B (1999) Endothelial dysfunction in human disease. J Mol Cell Cardiol 31 (1):51-60. doi:10.1006/jmcc.1998.0843

Dustin ML, Rothlein R, Bhan AK, Dinarello CA, Springer TA (1986) Induction by IL 1 and interferon-gamma: tissue distribution, biochemistry, and function of a natural adherence molecule (ICAM-1). J Immunol 137 (1):245-254

Dzau VJ, Braun-Dullaeus RC, Sedding DG (2002) Vascular proliferation and atherosclerosis: new perspectives and therapeutic strategies. Nat Med 8 (11):1249-1256. doi:10.1038/nm1102-1249

Eyries M, Collins T, Khachigian LM (2004) Modulation of growth factor gene expression in vascular cells by oxidative stress. Endothelium 11 (2):133-139. doi:10.1080/10623320490482691

Federici AB (2003) The factor VIII/von Willebrand factor complex: basic and clinical issues. Haematologica 88 (6):EREP02

Feletou M, Huang Y, Vanhoutte PM (2011) Endothelium-mediated control of vascular tone: COX-1 and COX-2 products. Br J Pharmacol 164 (3):894-912. doi:10.1111/j.1476-5381.2011.01276.x

Feng W, Madajka M, Kerr BA, Mahabeleshwar GH, Whiteheart SW, Byzova TV (2011) A novel role for platelet secretion in angiogenesis: mediating bone marrow-derived cell mobilization and homing. Blood 117 (14):3893-3902. doi:10.1182/blood-2010-08-304808

Foy TM, Aruffo A, Bajorath J, Buhlmann JE, Noelle RJ (1996) Immune regulation by CD40 and its ligand GP39. Annu Rev Immunol 14:591-617. doi:10.1146/annurev.immunol.14.1.591

Fuentes QE, Fuentes QF, Andres V, Pello OM, Font de Mora J, Palomo GI (2013) Role of platelets as mediators that link inflammation and thrombosis in atherosclerosis. Platelets 24 (4):255-262. doi:10.3109/09537104.2012.690113

Galkina E, Ley K (2009) Immune and inflammatory mechanisms of atherosclerosis (*). Annu Rev Immunol 27:165-197. doi:10.1146/annurev.immunol.021908.132620

Garlichs CD, John S, Schmeisser A, Eskafi S, Stumpf C, Karl M, Goppelt-Struebe M, Schmieder R, Daniel WG (2001) Upregulation of CD40 and CD40 ligand (CD154) in patients with moderate hypercholesterolemia. Circulation 104 (20):2395-2400

Gauchat JF, Henchoz S, Fattah D, Mazzei G, Aubry JP, Jomotte T, Dash L, Page K, Solari R, Aldebert D, et al. (1995) CD40 ligand is functionally expressed on human eosinophils. Eur J Immunol 25 (3):863-865. doi:10.1002/eji.1830250335

Gauchat JF, Henchoz S, Mazzei G, Aubry JP, Brunner T, Blasey H, Life P, Talabot D, Flores-Romo L, Thompson J, et al. (1993) Induction of human IgE synthesis in B cells by mast cells and basophils. Nature 365 (6444):340-343. doi:10.1038/365340a0

Gawaz M, Langer H, May AE (2005) Platelets in inflammation and atherogenesis. J Clin Invest 115 (12):3378-3384. doi:10.1172/JCI27196

Gerdes N, Seijkens T, Lievens D, Kuijpers MJ, Winkels H, Projahn D, Hartwig H, Beckers L, Megens RT, Boon L, Noelle RJ, Soehnlein O, Heemskerk JW, Weber C, Lutgens E (2016) Platelet CD40 Exacerbates Atherosclerosis by Transcellular Activation of Endothelial Cells and Leukocytes. Arterioscler Thromb Vasc Biol 36 (3):482-490. doi:10.1161/ATVBAHA.115.307074

Gerhardt T, Ley K (2015) Monocyte trafficking across the vessel wall. Cardiovasc Res 107 (3):321-330. doi:10.1093/cvr/cvv147

Gibbons GH, Dzau VJ (1994) The emerging concept of vascular remodeling. N Engl J Med 330 (20):1431-1438. doi:10.1056/NEJM199405193302008

Gogia S, Neelamegham S (2015) Role of fluid shear stress in regulating VWF structure, function and related blood disorders. Biorheology 52 (5-6):319-335. doi:10.3233/BIR-15061

Gonzales JU, Thistlethwaite JR, Thompson BC, Scheuermann BW (2009) Exercise-induced shear stress is associated with changes in plasma von Willebrand factor in older humans. Eur J Appl Physiol 106 (5):779-784. doi:10.1007/s00421-009-1074-x

Goto S, Ichikawa N, Lee M, Goto M, Sakai H, Kim JJ, Yoshida M, Handa M, Ikeda Y, Handa S (2000) Platelet surface P-selectin molecules increased after exposing platelet to a high shear flow. Int Angiol 19 (2):147-151

Grewal IS, Flavell RA (1998) CD40 and CD154 in cell-mediated immunity. Annu Rev Immunol 16:111-135. doi:10.1146/annurev.immunol.16.1.111

Hansson GK, Robertson AK, Soderberg-Naucler C (2006) Inflammation and atherosclerosis. Annu Rev Pathol 1:297-329. doi:10.1146/annurev.pathol.1.110304.100100

Hayward CP, Furmaniak-Kazmierczak E, Cieutat AM, Moore JC, Bainton DF, Nesheim ME, Kelton JG, Cote G (1995) Factor V is complexed with multimerin in resting platelet lysates and colocalizes with multimerin in platelet alpha-granules. J Biol Chem 270 (33):19217-19224

Henn V, Slupsky JR, Grafe M, Anagnostopoulos I, Forster R, Muller-Berghaus G, Kroczek RA (1998) CD40 ligand on activated platelets triggers an inflammatory reaction of endothelial cells. Nature 391 (6667):591-594. doi:10.1038/35393

Henn V, Steinbach S, Buchner K, Presek P, Kroczek RA (2001) The inflammatory action of CD40 ligand (CD154) expressed on activated human platelets is temporally limited by coexpressed CD40. Blood 98 (4):1047-1054

Ho-Tin-Noe B, Demers M, Wagner DD (2011) How platelets safeguard vascular integrity. J Thromb Haemost 9 Suppl 1:56-65. doi:10.1111/j.1538-7836.2011.04317.x

Hollenbaugh D, Mischel-Petty N, Edwards CP, Simon JC, Denfeld RW, Kiener PA, Aruffo A (1995) Expression of functional CD40 by vascular endothelial cells. J Exp Med 182 (1):33-40

Huisman B, Hoore M, Gompper G, Fedosov DA (2017) Modeling the cleavage of von Willebrand factor by ADAMTS13 protease in shear flow. Med Eng Phys. doi:10.1016/j.medengphy.2017.06.044

Huo Y, Ley KF (2004) Role of platelets in the development of atherosclerosis. Trends Cardiovasc Med 14 (1):18-22

Institute of Physiology and Pathophysiology (2014) The vascular system of the mouse ear resembles arms of a river on a map. In transmitted light even smallest blood vessels are apparentb. http://www.medizinische-fakultaet-hd.uni-heidelberg.de/index.php?id=110793&L=en. Accessed 24.08.2017

Inwald DP, McDowall A, Peters MJ, Callard RE, Klein NJ (2003) CD40 is constitutively expressed on platelets and provides a novel mechanism for platelet activation. Circ Res 92 (9):1041-1048. doi:10.1161/01.RES.0000070111.98158.6C

Jaffe EA, Hoyer LW, Nachman RL (1974) Synthesis of von Willebrand factor by cultured human endothelial cells. Proc Natl Acad Sci U S A 71 (5):1906-1909

Junt T, Schulze H, Chen Z, Massberg S, Goerge T, Krueger A, Wagner DD, Graf T, Italiano JE, Jr., Shivdasani RA, von Andrian UH (2007) Dynamic visualization of thrombopoiesis within bone marrow. Science 317 (5845):1767-1770. doi:10.1126/science.1146304

Kahn ML (2015) A critical role of platelet glycoprotein Ibalpha in arterial remodeling. Arterioscler Thromb Vasc Biol 35 (3):498-499. doi:10.1161/ATVBAHA.115.305213

Karmann K, Hughes CC, Schechner J, Fanslow WC, Pober JS (1995) CD40 on human endothelial cells: inducibility by cytokines and functional regulation of adhesion molecule expression. Proc Natl Acad Sci U S A 92 (10):4342-4346

Karshovska E, Weber C, von Hundelshausen P (2013) Platelet chemokines in health and disease. Thromb Haemost 110 (5):894-902. doi:10.1160/TH13-04-0341

Kisucka J, Butterfield CE, Duda DG, Eichenberger SC, Saffaripour S, Ware J, Ruggeri ZM, Jain RK, Folkman J, Wagner DD (2006) Platelets and platelet adhesion

support angiogenesis while preventing excessive hemorrhage. Proc Natl Acad Sci U S A 103 (4):855-860. doi:10.1073/pnas.0510412103

Korff T, Aufgebauer K, Hecker M (2007) Cyclic stretch controls the expression of CD40 in endothelial cells by changing their transforming growth factor-beta1 response. Circulation 116 (20):2288-2297. doi:10.1161/CIRCULATIONAHA.107.730309

Kossmann S, Lagrange J, Jackel S, Jurk K, Ehlken M, Schonfelder T, Weihert Y, Knorr M, Brandt M, Xia N, Li H, Daiber A, Oelze M, Reinhardt C, Lackner K, Gruber A, Monia B, Karbach SH, Walter U, Ruggeri ZM, Renne T, Ruf W, Munzel T, Wenzel P (2017) Platelet-localized FXI promotes a vascular coagulation-inflammatory circuit in arterial hypertension. Sci Transl Med 9 (375). doi:10.1126/scitranslmed.aah4923

Kragh T, Napoleone M, Fallah MA, Gritsch H, Schneider MF, Reininger AJ (2014) High shear dependent von Willebrand factor self-assembly fostered by platelet interaction and controlled by ADAMTS13. Thromb Res 133 (6):1079-1087. doi:10.1016/j.thromres.2014.03.024

Kroll MH, Hellums JD, McIntire LV, Schafer AI, Moake JL (1996) Platelets and shear stress. Blood 88 (5):1525-1541

Kupinski JM, Miller JL (1985) Multimeric analysis of von Willebrand factor in megakaryocytes. Thromb Res 38 (6):603-610

Lam FW, Vijayan KV, Rumbaut RE (2015) Platelets and Their Interactions with Other Immune Cells. Compr Physiol 5 (3):1265-1280. doi:10.1002/cphy.c140074

Lancellotti S, Basso M, De Cristofaro R (2013) Proteolytic processing of von Willebrand factor by adamts13 and leukocyte proteases. Mediterr J Hematol Infect Dis 5 (1):e2013058. doi:10.4084/MJHID.2013.058

Langille BL (1996) Arterial remodeling: relation to hemodynamics. Can J Physiol Pharmacol 74 (7):834-841

Ley K (1996) Molecular mechanisms of leukocyte recruitment in the inflammatory process. Cardiovasc Res 32 (4):733-742

Libby P (2002) Inflammation in atherosclerosis. Nature 420 (6917):868-874. doi:10.1038/nature01323

Libby P, Aikawa M (2002) Stabilization of atherosclerotic plaques: new mechanisms and clinical targets. Nat Med 8 (11):1257-1262. doi:10.1038/nm1102-1257

Lievens D, von Hundelshausen P (2011) Platelets in atherosclerosis. Thromb Haemost 106 (5):827-838. doi:10.1160/TH11-08-0592

Liu J, Wang Y, Akamatsu Y, Lee CC, Stetler RA, Lawton MT, Yang GY (2014) Vascular remodeling after ischemic stroke: mechanisms and therapeutic potentials. Prog Neurobiol 115:138-156. doi:10.1016/j.pneurobio.2013.11.004

Mach F, Schonbeck U, Sukhova GK, Atkinson E, Libby P (1998) Reduction of atherosclerosis in mice by inhibition of CD40 signalling. Nature 394 (6689):200-203. doi:10.1038/28204

Mach F, Schonbeck U, Sukhova GK, Bourcier T, Bonnefoy JY, Pober JS, Libby P (1997) Functional CD40 ligand is expressed on human vascular endothelial cells, smooth muscle cells, and macrophages: implications for CD40-CD40 ligand signaling in atherosclerosis. Proc Natl Acad Sci U S A 94 (5):1931-1936

Madabhushi SR, Zhang C, Kelkar A, Dayananda KM, Neelamegham S (2014) Platelet GpIba binding to von Willebrand Factor under fluid shear:contributions of the D'D3-domain, A1-domain flanking peptide and O-linked glycans. J Am Heart Assoc 3 (5):e001420. doi:10.1161/JAHA.114.001420

Massberg S, Brand K, Gruner S, Page S, Muller E, Muller I, Bergmeier W, Richter T, Lorenz M, Konrad I, Nieswandt B, Gawaz M (2002) A critical role of platelet adhesion in the initiation of atherosclerotic lesion formation. J Exp Med 196 (7):887-896

Massberg S, Gruner S, Konrad I, Garcia Arguinzonis MI, Eigenthaler M, Hemler K, Kersting J, Schulz C, Muller I, Besta F, Nieswandt B, Heinzmann U, Walter U, Gawaz M (2004) Enhanced in vivo platelet adhesion in vasodilator-stimulated phosphoprotein (VASP)-deficient mice. Blood 103 (1):136-142. doi:10.1182/blood-2002-11-3417

McEver RP (2001) Adhesive Interactions of Leukocytes, Platelets, and the Vessel Wall during Hemostasis and Inflammation. Thrombosis and Haemostasis 86 (9):746-756

McGrath RT, van den Biggelaar M, Byrne B, O'Sullivan JM, Rawley O, O'Kennedy R, Voorberg J, Preston RJ, O'Donnell JS (2013) Altered glycosylation of platelet-derived von Willebrand factor confers resistance to ADAMTS13 proteolysis. Blood 122 (25):4107-4110. doi:10.1182/blood-2013-04-496851

McKusick VA, Amberger JS (1993) The morbid anatomy of the human genome: chromosomal location of mutations causing disease. J Med Genet 30 (1):1-26

Megens RT, Vijayan S, Lievens D, Doring Y, van Zandvoort MA, Grommes J, Weber C, Soehnlein O (2012) Presence of luminal neutrophil extracellular traps in atherosclerosis. Thromb Haemost 107 (3):597-598. doi:10.1160/TH11-09-0650

Moller K, Adolph O, Grunow J, Elrod J, Popa M, Ghosh S, Schwarz M, Schwale C, Grassle S, Huck V, Bruehl C, Wieland T, Schneider SW, Nobiling R, Wagner AH, Hecker M (2015) Mechanism and functional impact of CD40 ligand-induced von Willebrand factor release from endothelial cells. Thromb Haemost 113 (5):1095-1108. doi:10.1160/TH14-04-0336

Montezano AC, Touyz RM (2014) Reactive oxygen species, vascular Noxs, and hypertension: focus on translational and clinical research. Antioxid Redox Signal 20 (1):164-182. doi:10.1089/ars.2013.5302

Mourik MJ, Valentijn JA, Voorberg J, Koster AJ, Valentijn KM, Eikenboom J (2013) von Willebrand factor remodeling during exocytosis from vascular endothelial cells. J Thromb Haemost 11 (11):2009-2019. doi:10.1111/jth.12401

MRC Laboratory of Molecular Biology Single and double photon excitation of fluorescence.

Muller WA (2014) How endothelial cells regulate transmigration of leukocytes in the inflammatory response. Am J Pathol 184 (4):886-896. doi:10.1016/j.ajpath.2013.12.033

Mulvany MJ (2002) Small artery remodeling and significance in the development of hypertension. News Physiol Sci 17:105-109

O'Grady JT, Stewart S, Lowrey J, Howie SE, Krajewski AS (1994) CD40 expression in Hodgkin's disease. Am J Pathol 144 (1):21-26

Owens GK (1989) Control of hypertrophic versus hyperplastic growth of vascular smooth muscle cells. Am J Physiol 257 (6 Pt 2):H1755-1765

Pammer J, Weninger W, Mazal PR, Horvat R, Tschachler E (1996) Expression of the CD40 antigen on normal endothelial cells and in benign and malignant tumours of vascular origin. Histopathology 29 (6):517-524

Papaioannou TG, Stefanadis C (2005) Vascular wall shear stress: basic principles and methods. Hellenic J Cardiol 46 (1):9-15

Paulie S, Ehlin-Henriksson B, Mellstedt H, Koho H, Ben-Aissa H, Perlmann P (1985) A p50 surface antigen restricted to human urinary bladder carcinomas and B lymphocytes. Cancer Immunol Immunother 20 (1):23-28

Petri B, Broermann A, Li H, Khandoga AG, Zarbock A, Krombach F, Goerge T, Schneider SW, Jones C, Nieswandt B, Wild MK, Vestweber D (2010) von Willebrand factor promotes leukocyte extravasation. Blood 116 (22):4712-4719. doi:10.1182/blood-2010-03-276311

Pluvinet R, Petriz J, Torras J, Herrero-Fresneda I, Cruzado JM, Grinyo JM, Aran JM (2004) RNAi-mediated silencing of CD40 prevents leukocyte adhesion on CD154-activated endothelial cells. Blood 104 (12):3642-3646. doi:10.1182/blood-2004-03-0817

Postea O, Vasina EM, Cauwenberghs S, Projahn D, Liehn EA, Lievens D, Theelen W, Kramp BK, Butoi ED, Soehnlein O, Heemskerk JW, Ludwig A, Weber C, Koenen RR (2012) Contribution of platelet CX(3)CR1 to platelet-monocyte complex formation and vascular recruitment during hyperlipidemia. Arterioscler Thromb Vasc Biol 32 (5):1186-1193. doi:10.1161/ATVBAHA.111.243485

Quyyumi AA (1998) Endothelial function in health and disease: new insights into the genesis of cardiovascular disease. Am J Med 105 (1A):32S-39S

Raife TJ, Cao W, Atkinson BS, Bedell B, Montgomery RR, Lentz SR, Johnson GF, Zheng XL (2009) Leukocyte proteases cleave von Willebrand factor at or near the ADAMTS13 cleavage site. Blood 114 (8):1666-1674. doi:10.1182/blood-2009-01-195461

Reininger AJ (2015) The function of ultra-large von Willebrand factor multimers in high shear flow controlled by ADAMTS13. Hamostaseologie 35 (3):225-233. doi:10.5482/HAMO-14-12-0077

Rendu F, Brohard-Bohn B (2001) The platelet release reaction: granules' constituents, secretion and functions. Platelets 12 (5):261-273. doi:10.1080/09537100120068170

Ribatti D, Crivellato E (2012) "Sprouting angiogenesis", a reappraisal. Dev Biol 372 (2):157-165. doi:10.1016/j.ydbio.2012.09.018

Roquer J, Segura T, Serena J, Castillo J (2009) Endothelial dysfunction, vascular disease and stroke: the ARTICO study. Cerebrovasc Dis 27 Suppl 1:25-37. doi:10.1159/000200439

Roy M, Waldschmidt T, Aruffo A, Ledbetter JA, Noelle RJ (1993) The regulation of the expression of gp39, the CD40 ligand, on normal and cloned CD4+ T cells. J Immunol 151 (5):2497-2510

Sarma J, Laan CA, Alam S, Jha A, Fox KA, Dransfield I (2002) Increased platelet binding to circulating monocytes in acute coronary syndromes. Circulation 105 (18):2166-2171

Savage B, Saldívar E, Ruggeri ZM (1996) Initiation of Platelet Adhesion by Arrest onto Fibrinogen or Translocation on von Willebrand Factor. Cell 84 (2):289-297. doi:https://doi.org/10.1016/S0092-8674(00)80983-6

Savoia C, Schiffrin EL (2007) Vascular inflammation in hypertension and diabetes: molecular mechanisms and therapeutic interventions. Clin Sci (Lond) 112 (7):375-384. doi:10.1042/CS20060247

Schiffrin EL (2015) Mechanisms of remodelling of small arteries, antihypertensive therapy and the immune system in hypertension. Clin Invest Med 38 (6):E394-402

Schindelin J, Arganda-Carreras I, Frise E, Kaynig V, Longair M, Pietzsch T, Preibisch S, Rueden C, Saalfeld S, Schmid B, Tinevez JY, White DJ, Hartenstein V, Eliceiri K, Tomancak P, Cardona A (2012) Fiji: an open-source platform for biological-image analysis. Nat Methods 9 (7):676-682. doi:10.1038/nmeth.2019

Schneider SW, Nuschele S, Wixforth A, Gorzelanny C, Alexander-Katz A, Netz RR, Schneider MF (2007) Shear-induced unfolding triggers adhesion of von Willebrand factor fibers. Proc Natl Acad Sci U S A 104 (19):7899-7903. doi:10.1073/pnas.0608422104

Schönle A. (2006) Imspector Image Acquisition and Analysis Software, v0.1.

Shahidi M (2017) Thrombosis and von Willebrand Factor. Adv Exp Med Biol 906:285-306. doi:10.1007/5584_2016_122

Shim K, Anderson PJ, Tuley EA, Wiswall E, Sadler JE (2008) Platelet-VWF complexes are preferred substrates of ADAMTS13 under fluid shear stress. Blood 111 (2):651-657. doi:10.1182/blood-2007-05-093021

South K, Freitas MO, Lane DA (2017) A Model for the Conformational Activation of the Structurally Quiescent Metalloprotease ADAMTS13 by Von Willebrand Factor. J Biol Chem. doi:10.1074/jbc.M117.776732

Spanos K, Petrocheilou G, Karathanos C, Labropoulos N, Mikhailidis D, Giannoukas A (2016) Carotid Bifurcation Geometry and Atherosclerosis. Angiology:3319716678741. doi:10.1177/0003319716678741

Tamura N, Yoshida M, Ichikawa N, Handa M, Ikeda Y, Tanabe T, Handa S, Goto S (2002) Shear-induced von Willebrand factor-mediated platelet surface translocation of the CD40 ligand. Thromb Res 108 (5-6):311-315

Tan J, Town T, Mori T, Obregon D, Wu Y, DelleDonne A, Rojiani A, Crawford F, Flavell RA, Mullan M (2002) CD40 is expressed and functional on neuronal cells. EMBO J 21 (4):643-652

Tati R, Kristoffersson AC, Manea Hedstrom M, Morgelin M, Wieslander J, van Kooten C, Karpman D (2017) Neutrophil Protease Cleavage of Von Willebrand Factor in Glomeruli - An Anti-thrombotic Mechanism in the Kidney. EBioMedicine 16:302-311. doi:10.1016/j.ebiom.2017.01.032

Tati R, Kristoffersson AC, Stahl AL, Morgelin M, Motto D, Satchell S, Mathieson P, Manea-Hedstrom M, Karpman D (2011) Phenotypic expression of ADAMTS13 in glomerular endothelial cells. PLoS One 6 (6):e21587. doi:10.1371/journal.pone.0021587

Totani L, Evangelista V (2010) Platelet-leukocyte interactions in cardiovascular disease and beyond. Arterioscler Thromb Vasc Biol 30 (12):2357-2361. doi:10.1161/ATVBAHA.110.207480

Tousoulis D, Androulakis E, Papageorgiou N, Briasoulis A, Siasos G, Antoniades C, Stefanadis C (2010) From atherosclerosis to acute coronary syndromes: the role of soluble CD40 ligand. Trends Cardiovasc Med 20 (5):153-164. doi:10.1016/j.tcm.2010.12.004

Tousoulis D, Kampoli AM, Tentolouris C, Papageorgiou N, Stefanadis C (2012) The role of nitric oxide on endothelial function. Curr Vasc Pharmacol 10 (1):4-18

Turner N, Nolasco L, Tao Z, Dong JF, Moake J (2006) Human endothelial cells synthesize and release ADAMTS-13. J Thromb Haemost 4 (6):1396-1404. doi:10.1111/j.1538-7836.2006.01959.x

van Gils JM, Zwaginga JJ, Hordijk PL (2009) Molecular and functional interactions among monocytes, platelets, and endothelial cells and their relevance for cardiovascular diseases. J Leukoc Biol 85 (2):195-204. doi:10.1189/jlb.0708400

Van Hinsbergh VW, Tasev D (2015) Platelets and thromboxane receptors: pivotal players in arteriogenesis. Cardiovasc Res 107 (4):400-402. doi:10.1093/cvr/cvv194

van Kooten C, Banchereau J (2000) CD40-CD40 ligand. J Leukoc Biol 67 (1):2-17

Varo N, de Lemos JA, Libby P, Morrow DA, Murphy SA, Nuzzo R, Gibson CM, Cannon CP, Braunwald E, Schonbeck U (2003) Soluble CD40L: risk prediction after acute coronary syndromes. Circulation 108 (9):1049-1052. doi:10.1161/01.CIR.0000088521.04017.13

Vestweber D (2015) How leukocytes cross the vascular endothelium. Nat Rev Immunol 15 (11):692-704. doi:10.1038/nri3908

Vogel LA, Noelle RJ (1998) CD40 and its crucial role as a member of the TNFR family. Semin Immunol 10 (6):435-442. doi:10.1006/smim.1998.0145

von Bruhl ML, Stark K, Steinhart A, Chandraratne S, Konrad I, Lorenz M, Khandoga A, Tirniceriu A, Coletti R, Kollnberger M, Byrne RA, Laitinen I, Walch A, Brill A, Pfeiler S, Manukyan D, Braun S, Lange P, Riegger J, Ware J, Eckart A, Haidari S, Rudelius M, Schulz C, Echtler K, Brinkmann V, Schwaiger M, Preissner KT, Wagner DD, Mackman N, Engelmann B, Massberg S (2012) Monocytes, neutrophils, and platelets cooperate to initiate and propagate venous thrombosis in mice in vivo. J Exp Med 209 (4):819-835. doi:10.1084/jem.20112322

von Hundelshausen P, Weber KS, Huo Y, Proudfoot AE, Nelson PJ, Ley K, Weber C (2001) RANTES deposition by platelets triggers monocyte arrest on inflamed and atherosclerotic endothelium. Circulation 103 (13):1772-1777

Wagner AH, Guldenzoph B, Lienenluke B, Hecker M (2004) CD154/CD40-mediated expression of CD154 in endothelial cells: consequences for endothelial cell-monocyte interaction. Arterioscler Thromb Vasc Biol 24 (4):715-720. doi:10.1161/01.ATV.0000122853.99978.b1

Wagner AH, Hildebrandt A, Baumgarten S, Jungmann A, Muller OJ, Sharov VS, Schoneich C, Hecker M (2011) Tyrosine nitration limits stretch-induced CD40 expression and disconnects CD40 signaling in human endothelial cells. Blood 118 (13):3734-3742. doi:10.1182/blood-2010-11-320259

Wagner DD (1990) Cell biology of von Willebrand factor. Annu Rev Cell Biol 6:217-246. doi:10.1146/annurev.cb.06.110190.001245

Walsh K, Smith RC, Kim HS (2000) Vascular cell apoptosis in remodeling, restenosis, and plaque rupture. Circ Res 87 (3):184-188

Wannamethee SG, Whincup PH, Lennon L, Rumley A, Lowe GD (2012) Fibrin D-dimer, tissue-type plasminogen activator, von Willebrand factor, and risk of incident stroke in older men. Stroke 43 (5):1206-1211. doi:10.1161/STROKEAHA.111.636373

Warhol MJ, Sweet JM (1984) The ultrastructural localization of von Willebrand factor in endothelial cells. Am J Pathol 117 (2):310-315

Weber C, Zernecke A, Libby P (2008) The multifaceted contributions of leukocyte subsets to atherosclerosis: lessons from mouse models. Nat Rev Immunol 8 (10):802-815. doi:10.1038/nri2415

Wester K, Asplund A, Backvall H, Micke P, Derveniece A, Hartmane I, Malmstrom PU, Ponten F (2003) Zinc-based fixative improves preservation of genomic DNA and proteins in histoprocessing of human tissues. Lab Invest 83 (6):889-899

Wieberdink RG, van Schie MC, Koudstaal PJ, Hofman A, Witteman JC, de Maat MP, Leebeek FW, Breteler MM (2010) High von Willebrand factor levels increase the

risk of stroke: the Rotterdam study. Stroke 41 (10):2151-2156. doi:10.1161/STROKEAHA.110.586289

Xu H, Cao Y, Yang X, Cai P, Kang L, Zhu X, Luo H, Lu L, Wei L, Bai X, Zhu Y, Zhao BQ, Fan W (2017) ADAMTS13 controls vascular remodeling by modifying VWF reactivity during stroke recovery. Blood. doi:10.1182/blood-2016-10-747089

Zarbock A, Polanowska-Grabowska RK, Ley K (2007) Platelet-neutrophil-interactions: linking hemostasis and inflammation. Blood Rev 21 (2):99-111. doi:10.1016/j.blre.2006.06.001

Zheng X, Chung D, Takayama TK, Majerus EM, Sadler JE, Fujikawa K (2001) Structure of von Willebrand factor-cleaving protease (ADAMTS13), a metalloprotease involved in thrombotic thrombocytopenic purpura. J Biol Chem 276 (44):41059-41063. doi:10.1074/jbc.C100515200

Zhou W, Inada M, Lee TP, Benten D, Lyubsky S, Bouhassira EE, Gupta S, Tsai HM (2005) ADAMTS13 is expressed in hepatic stellate cells. Lab Invest 85 (6):780-788. doi:10.1038/labinvest.3700275

Zimmerman TS, Ruggeri ZM, Fulcher CA (1983) Factor VIII/von Willebrand factor. Prog Hematol 13:279-309

Zuchtriegel G, Uhl B, Puhr-Westerheide D, Pornbacher M, Lauber K, Krombach F, Reichel CA (2016) Platelets Guide Leukocytes to Their Sites of Extravasation. PLoS Biol 14 (5):e1002459. doi:10.1371/journal.pbio.1002459

Acknowledgements

All praise is to ALLAH who has enabled me to put some successful effort in the fulfillment of this research work. The faith of my parents in me and the affectionate co-operation of my husband made it possible for me to work abroad and achieve my goals.

I would like to pay sincere thanks to my supervisor Prof. Markus Hecker for giving me this golden opportunity to work on this interesting project. I express my appreciation to my co-supervisor Andreas Wagner for his valuable suggestions throughout the research. I would like to thank SmArteR and team for polishing my skills as the new comer scientist and supporting my thesis with grant agreement No. 606998.

My deepest gratitude goes to my mentor Prof. Ulrich Pohl for his kind supervision that was full of unconditional support, guidance and advice. He has always been a source of knowledge and inspiration to me. His passion for research and critical thinking always helped me to motivate and groom myself as a scientist from a superficial learner. I would also like to thank Mrs. Pohl for taking care of me in critical times. I pray to Allah that He always bless them both. Ameen!

I am grateful to Steffen Dietzel for introducing me to the colorful world of fluorescence imaging and microscopy. Without his guidance I would not have been able to play with the fancy two-photon excitation fluorescence microscope. My gratitude goes to Hanna Mannell and Yvonn Stampnik for teaching me the basics of platelet isolation. Thank you to Prof. Sperandio's work group for their assistance in introducing the cremaster preparation to me. My special thanks to Alba de Juan for guiding me in preparation of the femoral artery catheter. I would also like to thank Ludwig Weckbach for providing me his experimental animals for studying CD40 distribution.

Besides my supervisors I would like to thank my Thesis Advisory Committee (TAC) members: Prof. Peter Angel and Prof. Karin Müller-Decker for their encouragement and insightful comments during our annual meetings.

I would like to thank Jiehua Qiu who as a good friend was always willing to help me out and especially for all his support for dealing with my aggressive knockout mice. The lab would have been lonely without him. Thanks to Anke Lübeck, Holger Schneider and Kai Michael Schubert for their help during everyday lab problems. My special thanks to Taslima Nahar, Hanna Kuk and Anca Remes who always cared for me during my visits to Heidelberg.

Last but not the least, I would like to pay my deepest gratitude to Ms. Barbara Richards for her motherly love and comfort which made all the difficulties go smoothly for me. Her guidance and timely presence was a great support during the time course of my collaboration with Munich.

List of own publications and conference papers

Publications

1 von Willebrand factor-mediated endothelial cell-platelet-monocyte interaction in atherosclerosis – role of ADAMTS13
Miruna Popa, Sibgha Tahir, Florian Leuschner, Ulrich Pohl, Andreas H. Wagner and Markus Hecker
(Submitted) Science Translational Medicine

2 CD40L-dependent von Willebrand factor-platelet string formation in the mouse microcirculation in vivo
Sibgha Tahir, Andreas H. Wagner, Steffen Dietzel, Hanna Mannell, Ludwig Weckbach, Ulrich Pohl and Markus Hecker
(In writing)

Conference Papers

1 CD40L dependent platelet string formation in the mouse microcirculation *in vivo*
Conference: 39th Annual Meeting of the German Society for Microcirculation and Vascular Biology (GfmVB), at Grainau/Garmisch- Patenkirchen, Germany October 2017.
Authors: Sibgha Tahir, Andreas H. Wager, Steffen Dietzel, Ulrich Pohl, Markus Hecker

2 CD40L dependent platelet string formation in the mouse microcirculation *in vivo*
Conference: ESM-EVBO 2017, at Geneva, Switzerland May 2017.
Authors: Sibgha Tahir, Andreas H. Wager, Steffen Dietzel, Ulrich Pohl, Markus Hecker

3 sCD154 dependent platelet string formation in veins and arterioles *in vivo*
Conference: 82 Jahrestatung Deutsche Gesellschaft für Kardiologie, at Lübeck, Germany March 2016.

Authors: Sibgha Tahir, Andreas H. Wager, Steffen Dietzel, Ulrich Pohl, Markus Hecker

4 Von Willebrand factor-mediated platelet string formation and leukocyte extravasation in the microcirculation *in vivo*

Conference: Deutsche Physiologische Gesellschaft, at Mannheim, Germany March 2016.

Authors: Sibgha Tahir, Andreas H. Wager, Steffen Dietzel, Ulrich Pohl, Markus Hecker